



CASE STUDY

# Atacama Large Aperture Submillimeter Telescope (AtLAST) science: Resolving the hot and ionized Universe through the Sunyaev-Zeldovich effect [version 1; peer review: 1 approved with reservations]

Luca Di Mascolo<sup>1-4</sup>, Yvette Perrott <sup>5</sup>, Tony Mroczkowski <sup>6</sup>, Stefano Andreon<sup>7</sup>,  
Stefano Etori <sup>8,9</sup>, Aurora Simionescu <sup>10-12</sup>, Srinivasan Raghunathan<sup>13</sup>,  
Joshiwa van Marrewijk <sup>6</sup>, Claudia Cicone <sup>14</sup>, Minju Lee <sup>15,16</sup>, Dylan Nelson<sup>17</sup>,  
Laura Sommovigo<sup>18,19</sup>, Mark Booth <sup>20</sup>, Pamela Klaassen<sup>20</sup>, Paola Andreani <sup>6</sup>,  
Martin A. Cordiner<sup>21</sup>, Doug Johnstone <sup>22,23</sup>, Eelco van Kampen <sup>6</sup>,  
Daizhong Liu <sup>24,25</sup>, Thomas J. Maccarone<sup>26</sup>, Thomas W. Morris<sup>27,28</sup>,  
Amélie Saintonge <sup>29,30</sup>, Matthew Smith <sup>31</sup>, Alexander E. Thelen<sup>32</sup>,  
Sven Wedemeyer<sup>14,33</sup>

<sup>1</sup>Laboratoire Lagrange, Observatoire de la Côte d'Azur, University of Côte d'Azur, Nice, Provence-Alpes-Côte d'Azur, 06304, France

<sup>2</sup>Astronomy Unit, Department of Physics, University of Trieste, Trieste, Friuli-Venezia Giulia, 34131, Italy

<sup>3</sup>INAF – Osservatorio Astronomico di Trieste, Trieste, 34014, Italy

<sup>4</sup>IFPU – Institute for Fundamental Physics of the Universe, Trieste, 34014, Italy

<sup>5</sup>Victoria University of Wellington, Wellington, New Zealand

<sup>6</sup>European Southern Observatory, Garching, 85748, Germany

<sup>7</sup>INAF – Osservatorio Astronomico di Brera, Milano, 20121, Italy

<sup>8</sup>INAF – Osservatorio di Astrofisica e Scienza dello Spazio, Bologna, 40129, Italy

<sup>9</sup>INFN – Sezione di Bologna, Bologna, 40127, Italy

<sup>10</sup>SRON Netherlands Institute for Space Research, Niels Bohrweg 4, Leiden, 2333 CA, The Netherlands

<sup>11</sup>Leiden Observatory, Niels Bohrweg 2, Leiden University, Leiden, 2333 CA, The Netherlands

<sup>12</sup>Kavli Institute for the Physics and Mathematics of the Universe, University of Tokyo, Kashiwa, Chiba, 277-8583, Japan

<sup>13</sup>Center for AstroPhysical Surveys, National Center for Supercomputing Applications, Urbana, Illinois, 61801, USA

<sup>14</sup>Institute of Theoretical Astrophysics, University of Oslo, Oslo, 0315, Norway

<sup>15</sup>Cosmic Dawn Center, Copenhagen, Denmark

<sup>16</sup>DTU-Space, Technical University of Denmark, Kongens Lyngby, 2800, Denmark

<sup>17</sup>Zentrum für Astronomie, Institut für Theoretische Astrophysik, Heidelberg University, Heidelberg, Baden-Württemberg, 69120, Germany

<sup>18</sup>Center for Computational Astrophysics, Flatiron Institute, New York, New York, 10010, USA

<sup>19</sup>Scuola Normale Superiore, Pisa, Tuscany, 56126, Italy

<sup>20</sup>UK Astronomy Technology Centre, Royal Observatory Edinburgh, Edinburgh, EH9 3HJ, UK

<sup>21</sup>Astrochemistry Laboratory, Code 691, NASA Goddard Space Flight Center, Greenbelt, Maryland, 20771, USA

<sup>22</sup>NRC Herzberg Astronomy and Astrophysics, Victoria, British Columbia, V9E 2E7, Canada

<sup>23</sup>Department of Physics and Astronomy, University of Victoria, Victoria, British Columbia, V8P 5C2, Canada

<sup>24</sup>Max-Planck-Institut für extraterrestrische Physik, Garching, Bayern, 85748, Germany

<sup>25</sup>Purple Mountain Observatory, Chinese Academy of Sciences, Nanjing, 210023, China

<sup>26</sup>Department of Physics & Astronomy, Texas Tech University, Lubbock, Texas, 79409-1051, USA

<sup>27</sup>Brookhaven National Laboratory, Upton, New York, 11973, USA

<sup>28</sup>Lawrence Berkeley National Laboratory, Berkeley, California, 94720, USA

<sup>29</sup>Department of Physics and Astronomy, University College London, London, England, WC1E 6BT, UK

<sup>30</sup>Max-Planck-Institut für Radioastronomie, Bonn, 53121, Germany

<sup>31</sup>School of Physics & Astronomy, Cardiff University, Cardiff, Wales, CF24 3AA, UK

<sup>32</sup>Division of Geological and Planetary Sciences, California Institute of Technology, Pasadena, California, 91125, USA

<sup>33</sup>Roseland Centre for Solar Physics, University of Oslo, Oslo, 0315, Norway

**V1** First published: 10 Jun 2024, 4:113  
<https://doi.org/10.12688/openreseurope.17449.1>

Latest published: 10 Jun 2024, 4:113  
<https://doi.org/10.12688/openreseurope.17449.1>

## Abstract

An omnipresent feature of the multi-phase “cosmic web” — the large-scale filamentary backbone of the Universe — is that warm/hot ( $\gtrsim 10^5$  K) ionized gas pervades it. This gas constitutes a relevant contribution to the overall universal matter budget across multiple scales, from the several tens of Mpc-scale intergalactic filaments, to the Mpc intracluster medium (ICM), all the way down to the circumgalactic medium (CGM) surrounding individual galaxies, on scales from  $\sim 1$  kpc up to their respective virial radii ( $\sim 100$  kpc). The study of the hot baryonic component of cosmic matter density represents a powerful means for constraining the intertwined evolution of galactic populations and large-scale cosmological structures, for tracing the matter assembly in the Universe and its thermal history. To this end, the Sunyaev-Zeldovich (SZ) effect provides the ideal observational tool for measurements out to the beginnings of structure formation. The SZ effect is caused by the scattering of the photons from the cosmic microwave background off the hot electrons embedded within cosmic structures, and provides a redshift-independent perspective on the thermal and kinematic properties of the warm/hot gas. Still, current and next-generation (sub)millimeter facilities have been providing only a partial view of the SZ Universe due to any combination of: limited angular resolution, spectral coverage, field of view, spatial dynamic range, sensitivity, or all of the above. In this paper, we motivate the development of a wide-field, broad-band, multi-chroic continuum instrument for the Atacama Large Aperture Submillimeter Telescope (AtLAST) by identifying the scientific drivers that will deepen our understanding of the complex thermal evolution of cosmic structures. On a technical side, this will necessarily require efficient multi-wavelength mapping of the SZ signal with an unprecedented spatial dynamic range (from arcsecond to degree scales) and we employ detailed theoretical forecasts to determine the key instrumental constraints for achieving our goals.

## Plain language summary

The matter content of the Universe is organized along a large-scale filamentary “cosmic web” of galaxies, gas, and an unseen “dark matter” component. Most of the ordinary matter exists as a diffuse plasma, with temperatures of 10–100 million degrees. The largest

## Open Peer Review

### Approval Status ?


1

#### version 1

10 Jun 2024

?

[view](#)

1. **François-Xavier Désert** , Univ. Grenoble Alpes, CNRS, IPAG, Grenoble, France

Any reports and responses or comments on the article can be found at the end of the article.

concentrations of such gas are found within gigantic galaxy clusters at the intersections of the cosmic web, weighing as much as 100 trillion Suns. As such, their masses, number and distribution across cosmic time probe the evolution and composition of the Universe itself. Also, the thermodynamics of the warm/hot gas provides an archeological record of those mechanisms that, over time, influence the large-scale structures — from the energy deposition by super-massive black holes to the collisions of massive clusters.

The best option for studying the cosmic warm/hot gas, especially at the beginnings of their formation, is provided by the so-called Sunyaev-Zeldovich (SZ) effect — a faint distortion of the Cosmic Microwave Background (CMB) observable at (sub)millimeter wavelengths. Using the SZ effect to study cosmic thermal history however requires technical advances not met by state-of-the-art (sub)millimeter telescopes. In fact, many key questions on the co-evolution of the warm/hot gas, the embedded galaxies, and the cosmic web remain unanswered.

With these motivations in mind, we discuss the development of the Atacama Large Aperture Submillimeter Telescope (AtLAST). Thanks to its unprecedented combination of a 50-meter aperture and wide 2° field of view (4× wider than the full Moon), AtLAST will map vast sky areas and detect extremely faint signals across multiple wavelengths. Overall, AtLAST will push these studies beyond the legacy of the many (sub)millimeter facilities that, during the 50 years since the theoretical foundations of the SZ effect, have pioneered the exploration of the warm/hot Universe through the SZ effect.

### Keywords

galaxy clusters, intracluster medium, intergalactic medium, galaxy halos, cosmic background radiation, submillimeter facility

The logo for Horizon 2020, featuring the text "H2020" in white on a blue square background.

This article is included in the [Horizon 2020](#) gateway.



This article is included in the [European Research Council \(ERC\)](#) gateway.



This article is included in the [Marie-Sklodowska-Curie Actions \(MSCA\)](#) gateway.



This article is included in the [Atacama Large Aperture Submillimeter Telescope Design Study](#) collection.

**Corresponding author:** Luca Di Mascolo ([luca.di-mascolo@oca.eu](mailto:luca.di-mascolo@oca.eu))

**Author roles:** **Di Mascolo L:** Conceptualization, Formal Analysis, Investigation, Project Administration, Software, Supervision, Visualization, Writing – Original Draft Preparation, Writing – Review & Editing; **Perrott Y:** Formal Analysis, Visualization, Writing – Original Draft Preparation, Writing – Review & Editing; **Mroczkowski T:** Funding Acquisition, Supervision, Visualization, Writing – Original Draft Preparation, Writing – Review & Editing; **Andreon S:** Visualization, Writing – Original Draft Preparation, Writing – Review & Editing; **Ettori S:** Visualization, Writing – Original Draft Preparation, Writing – Review & Editing; **Simionescu A:** Writing – Original Draft Preparation, Writing – Review & Editing; **Raghunathan S:** Formal Analysis, Software, Visualization, Writing – Review & Editing; **van Marrewijk J:** Formal Analysis, Software, Writing – Original Draft Preparation, Writing – Review & Editing; **Cicone C:** Funding Acquisition, Project Administration, Supervision, Writing – Review & Editing; **Lee M:** Project Administration, Supervision, Writing – Review & Editing; **Nelson D:** Investigation, Resources, Software, Visualization, Writing – Review & Editing; **Sommovigo L:** Software, Visualization; **Booth M:** Software, Supervision, Writing – Review & Editing; **Klaassen P:** Conceptualization, Funding Acquisition, Project Administration, Supervision, Writing – Review & Editing; **Andreani P:** Supervision; **Cordiner MA:** Writing – Review & Editing; **Johnstone D:** Writing – Review & Editing; **van Kampen E:** Project Administration, Writing – Review & Editing; **Liu D:** Writing – Review & Editing; **Maccarone TJ:** Writing – Review & Editing; **Morris TW:** Methodology, Software; **Saintonge A:** Writing – Review & Editing; **Smith M:** Writing – Review & Editing; **Thelen AE:** Writing – Review & Editing; **Wedemeyer S:** Writing – Review & Editing

**Competing interests:** No competing interests were disclosed.

**Grant information:** This project has received funding from the European Union's Horizon 2020 research and innovation programme under grant agreement No [951815] (Towards an Atacama Large Aperture Submillimeter Telescope [AtLAST]). L.D.M. is supported by the European Research Council under a Starting Grant, grant agreement No [716762] (Fundamental physics, Cosmology and Astrophysics: Galaxy Clusters at the Cross-roads [ClustersXCosmo]). L.D.M. further acknowledges financial contribution from the agreement ASI-INAF n.2017-14-H.0. This work has been supported by the French government, through the UCAJ.E.D.I. Investments in the Future project managed by the National Research Agency (ANR) with the reference number ANR-15-IDEX-01. Y.P. is supported by a Rutherford Discovery Fellowship ("Realising the potential of galaxy clusters as cosmological probes") and Marsden Fast Start grant ("Turbulence in the Intracluster Medium: toward the robust extraction of physical parameters"). S.A. acknowledges INAF grant "Characterizing the newly discovered clusters of low surface brightness" and PRIN-MIUR 20228B938N grant "Mass and selection biases of galaxy clusters: a multi-probe approach". S.E. acknowledges the financial contribution from the contracts Prin-MUR 2022 supported by Next Generation EU (n.20227RNLY3 The concordance cosmological model: stress-tests with galaxy clusters), ASI-INAF Athena 2019-27-HH.0, "Attività di Studio per la comunità scientifica di Astrofisica delle Alte Energie e Fisica Astroparticellare" (Accordo Attuativo ASI-INAF n. 2017-14-H.0), and from the European Union's Horizon 2020 programme under grant agreement No [871158] (Integrated Activities for the High Energy Astrophysics Domain [AHEAD2020]). M.L. acknowledges support from the European Union's Horizon Europe research and innovation programme under the Marie Skłodowska-Curie grant agreement No 101107795. D.N. acknowledges funding from the Deutsche Forschungsgemeinschaft (DFG) through an Emmy Noether Research Group (grant number NE 2441/1-1). T.Mo. acknowledges the support of L. Page. S.W. acknowledges support by the Research Council of Norway through the EMISSA project (project number 286853) and the Centres of Excellence scheme, project number 262622 ("Rosseland Centre for Solar Physics").

*The funders had no role in study design, data collection and analysis, decision to publish, or preparation of the manuscript.*

**Copyright:** © 2024 Di Mascolo L *et al.* This is an open access article distributed under the terms of the [Creative Commons Attribution License](#), which permits unrestricted use, distribution, and reproduction in any medium, provided the original work is properly cited.

**How to cite this article:** Di Mascolo L, Perrott Y, Mroczkowski T *et al.* **Atacama Large Aperture Submillimeter Telescope (AtLAST) science: Resolving the hot and ionized Universe through the Sunyaev-Zeldovich effect [version 1; peer review: 1 approved with reservations]** Open Research Europe 2024, 4:113 <https://doi.org/10.12688/openreseurope.17449.1>

**First published:** 10 Jun 2024, 4:113 <https://doi.org/10.12688/openreseurope.17449.1>

## 1 Introduction: clusters and the evolution of large scale structure

Clusters of galaxies, groups, and massive galaxies trace the large scale structure of the Universe, and have therefore, since their discovery, served as probes of cosmology (Kravtsov & Borgani, 2012). For example, clusters provided the first tentative hints of dark matter (Zwicky, 1933) as well as early evidence that we live in a universe with a low matter density  $\Omega_M \sim 0.2\text{--}0.3$  (Bahcall & Cen, 1992; White *et al.*, 1993). While the large catalogs compiled by cluster and large scale structure surveys have offered the testbeds of, for example, the growth of structure and cosmic shear, these tests are limited by systematics originating primarily from astrophysical effects—shocks, feedback, non-thermal pressure, and the objects' dynamical and virialization states, to name a few — as well as from contamination due to interlopers and sources within the systems that can bias our measurements and any resulting cosmologically relevant observable (e.g., the cluster mass, a key proxy of structure evolution).

The same sources that can contaminate measurements, primarily radio-loud active galactic nuclei (AGN) and star forming galaxies, or cause departures from thermal equilibrium, such as shocks, are also the main drivers of the physical and thermodynamic evolution of the intracluster medium (ICM). The ICM, in turn, is the large scale environment within which a large fraction of galaxies reside, so the feedback and interactions between the two are important to both cosmology as well as cluster and galaxy evolution. The study of galaxy clusters is thus complex and multifaceted, but the reward to understanding the nature of clusters and large scale structure is that it allows us to test the properties of the ubiquitous dark matter, and to peer into the dark universe itself.

Some of the dominant astrophysical processes occurring in clusters are shown in the cartoon depiction in Figure 1. Studying in greater detail the multi-scale physical processes taking place within the most massive structures in the Universe will ultimately allow us to build a more complete understanding of the thermal history of our universe, how structure grew and evolved, or fundamentally how the Universe came to be the way it is.

Here we seek to motivate deep, multi-band or multichroic high resolution and wide field observations with the Atacama Large Aperture Submillimeter Telescope (AtLAST; Klaassen *et al.*, 2020; Mroczkowski *et al.*, 2023; Mroczkowski *et al.*, 2024; Ramasawmy *et al.*, 2022) that will address questions of cluster astrophysics as well as the contamination that could potentially plague cluster cosmology done at arcminute resolutions. At the same time, the observations discussed here are not simply to aid cosmological studies, but can probe interesting astrophysics and solve important questions about astrophysics in their own right — with the unique potential of providing a link between galaxy evolution, large-scale structure, and cosmological studies. Our primary tool here is the Sunyaev-Zeldovich effect, described below.

## 2 The multi-faceted Sunyaev-Zeldovich effect

The thermal Sunyaev-Zeldovich (SZ) effect (Sunyaev & Zeldovich, 1970; Sunyaev & Zeldovich, 1972) — an up-scattering to higher energies of photons from the cosmic microwave background (CMB) by hot electrons — was proposed theoretically as an alternative way to probe the pressure along the line of sight (l.o.s.) of the hot gas in galaxy clusters. A schematic picture for the scattering due to the thermal SZ effect, which scales as the Compton  $y$  parameter ( $y \propto P_e dl$  for electron pressure  $P_e$  and l.o.s.  $l$ ), is shown in Figure 1. Shortly after the theoretical foundations of the thermal SZ effect, the kinetic SZ effect ( $\propto n_e v_z dl$  for electron density  $n_e$  l.o.s. peculiar velocity  $v_z$ ; see Sunyaev & Zeldovich, 1980) was proposed as a way to measure gas momentum with respect to the CMB, our ultimate and most universal reference frame. The following decade saw developments in the theory regarding relativistic corrections to the thermal SZ and kinetic SZ effects as well as anticipating more exotic SZ effects from non-thermal and ultrarelativistic electron populations (e.g., Enßlin & Kaiser, 2000; Itoh *et al.*, 1998; Nozawa *et al.*, 1998). Observations of the SZ effects, however, took longer to come to the fore, beginning with pioneering measurements such as Birkinshaw *et al.* (1984) and culminating more recently in several thousand measurements or detections from both low-resolution (1-10') SZ surveys (e.g., Carlstrom *et al.*, 2011; Swetz *et al.*, 2011) and dedicated observations, often at higher (subarcminute) resolution (e.g., Adam *et al.*, 2014; Kitayama *et al.*, 2016; Mason *et al.*, 2010; Plagge *et al.*, 2013). For more comprehensive reviews of the various aspects of the SZ effect, see, e.g., Birkinshaw (1999); Carlstrom *et al.* (2002); Kitayama (2014), and Mroczkowski *et al.* (2019).

The proposed millimeter/submillimeter facility, AtLAST, presents novel, unique capabilities that will revolutionize both deep targeted observations aiming for detailed astrophysical studies, as well as wide-field surveys aiming to push SZ observations to much lower mass limits and higher redshifts. Since the epoch of reionization, the majority of baryons have been making their way up to high enough temperatures ( $> 10^5$  K) that their emission is nearly completely undetectable at optical wavelengths (visible and near-IR band), where the majority of telescopes operate. Such a hot phase is an omnipresent feature of the multi-phase cosmic web, representing a relevant contribution to the volume-filling matter budget on multiple scales — from Mpc-scale filaments of intergalactic medium, to the intracluster medium (ICM), and down to the circumgalactic medium (CGM) surrounding individual galaxies up to their virial radius (up to few 100s of kpc). Through the SZ effect, the millimeter/submillimeter wavelength regime offers a view of this important component of galaxies and their surrounding environments (clusters, groups, filaments) — components that are largely invisible to all but X-ray and SZ instruments.

## 3 Proposed science goals

Here we provide a summary of the main applications in the context of SZ studies enabled by AtLAST that will allow us

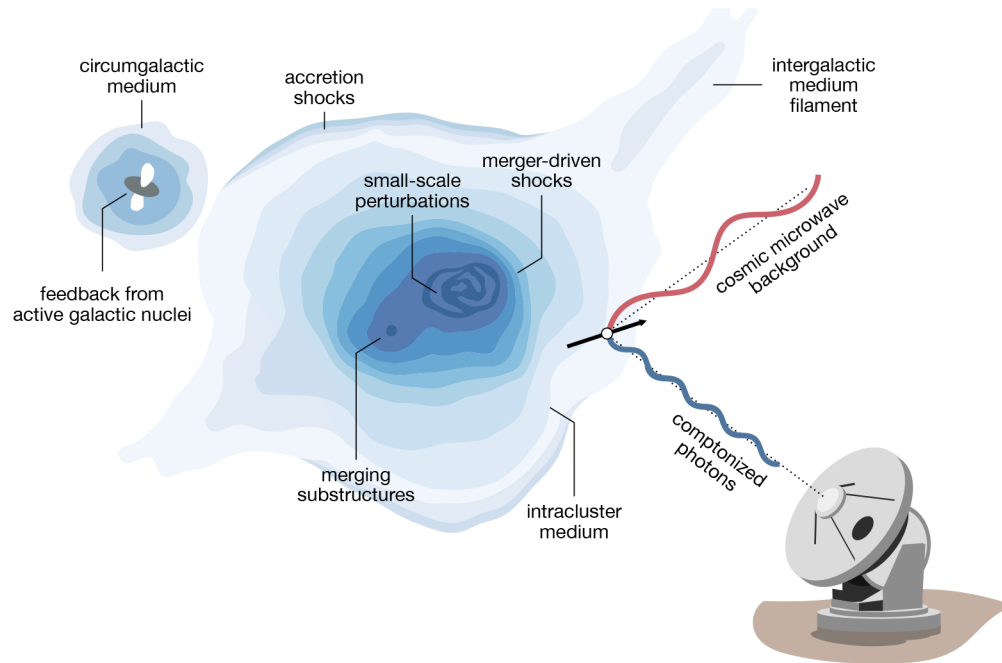


**Figure 1. Expanded diagram highlighting some of the aspects of galaxy clusters and large-scale structures that will be studied through the Sunyaev-Zeldovich (SZ) effect using AtLAST.** The SZ effect is caused by the interaction of photons from the cosmic microwave background (CMB) with reservoirs of energetic electrons within cosmic large-scale structures. Thanks to AtLAST's unparalleled capabilities, it will be possible to fully exploit multiple aspects of the SZ effect to characterize the impact of active galactic nuclei (AGN) on the circumgalactic medium (CGM), and the multi-scale properties of the intracluster medium (ICM) of the large-scale filaments of intergalactic medium (IGM). The figure is an adaptation of the SZ schematic in [Mroczkowski et al. \(2019\)](#), which was based on that from L. van Speybroeck as adapted by J. E. Carlstrom.

to develop a more profound and complete understanding of the thermal history of the Universe, ultimately transforming our understanding of the numerous processes involved in structure formation, evolution, feedback, and the quenching of star formation in overdense environments. We refer to [Lee et al. \(2024\)](#) and [van Kampen et al. \(2024\)](#) for companion AtLAST case studies focused on emission line probes of the cold circumgalactic medium (CGM) of galaxies and on providing a comprehensive survey of high- $z$  galaxies and protoclusters, respectively. Common to all the specific science cases discussed below is the need for a wide field, high angular resolution facility able to optimally probe the full SZ spectrum ([Figure 2](#)). We refer to [Section 4](#) for a more extended discussion of the technical requirements for the proposed science goals.

### 3.1 Thermodynamic properties of the ICM: radial profiles and small-scale perturbations

The morphological and thermodynamic properties of the ICM represent key records of the many physical processes shaping the evolution of galaxy clusters and groups. Non-gravitational processes — e.g., cooling, AGN feedback, different dynamical states and accretion modes ([Battaglia et al., 2012](#); [Ghirardini et al., 2019](#)) — are expected to leave their imprint on the pressure distribution of the ICM in the form of deviations

from the radial models derived under universal and self-similar assumptions for structure formation (see, e.g., [Arnaud et al., 2010](#); [Nagai et al., 2007](#); [Sayers et al., 2023](#)). On cluster scales, shock fronts induced by cluster mergers as well as cosmological accretion deposit their kinetic energy into the ICM, contributing to its overall thermalization ([Ha et al., 2018](#); [Markevitch & Vikhlinin, 2007](#)). On smaller scales, turbulent motion ([Khatri & Gaspari, 2016](#); [Romero et al., 2023](#); [Schuecker et al., 2004](#)) can induce significant non-thermal contributions to the ICM pressure support, in turn hampering the validity of the hydrostatic equilibrium assumption. We thus need robust constraints on the level of turbulence affecting the energy budget of the ICM along with an independent census of the “hydrostatic mass bias” (e.g., [Biffi et al., 2016](#)) via a combination of fluctuations and resolved hydrostatic mass information. This will be crucial for inferring corrections to the hydrostatic mass due to the non-thermalized gas (see, e.g., [Angelinelli et al., 2020](#); [Ettori & Eckert, 2022](#)) and therefore strengthening the role of thermodynamic quantities for cosmological purposes ([Pratt et al., 2019](#)).

The thermal SZ effect provides a direct proxy for the (thermal) pressure due to the free electrons in the ICM and, as such, the optimal tool for gaining a direct calorimetric view

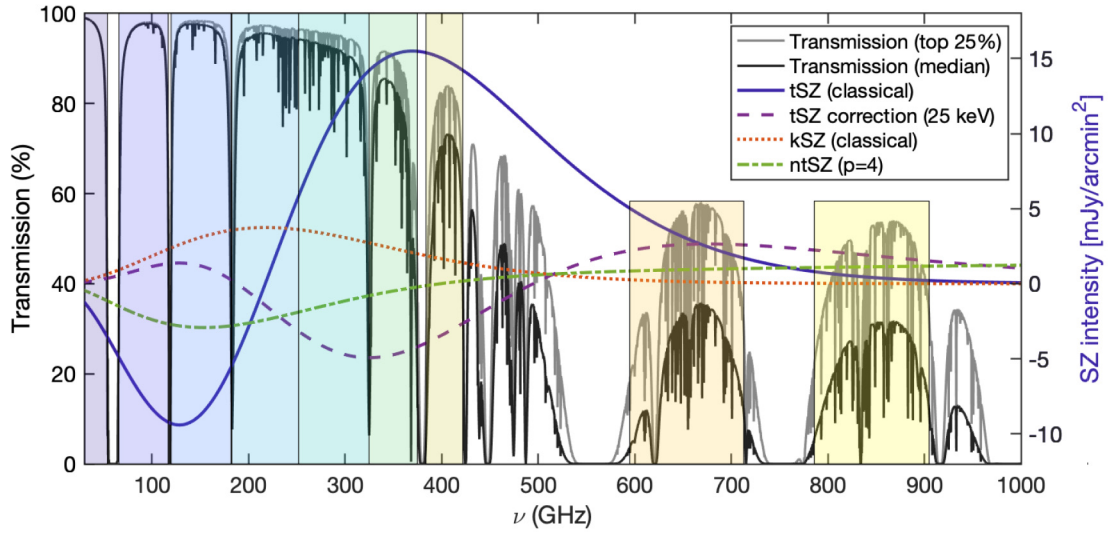


**Figure 2.** Various SZ spectra versus transmission in the top quartile (lighter gray) and median (darker gray) atmospheric transmission conditions available at the Chajnantor Plateau ( $\approx 5000$  meters above sea level). The left y-axis corresponds to transmission, and the right y-axis is appropriate for the SZ intensity for a cluster with  $y = 10^{-4}$ . The kinetic SZ values assume a line of sight velocity component  $v_z = -1000$  km/s (i.e. toward the observer, implying a net blueshift in the CMB toward the cluster) and an electron opacity  $\tau = 0.01$ . Here we used `szpack` to solve for the SZ spectral distortions (Chluba *et al.*, 2012), and the `am` code for atmospheric transmission (Paine, 2019). The optimal continuum bands of the proposed AtLAST SZ observations, reported in Table 1, are shown as background shaded regions.

**Table 1.** Frequencies, sensitivities and beam sizes for an AtLAST type of SZ experiment. The sensitivity levels are computed assuming the standard values for weather condition (2<sup>nd</sup> octile) and elevation ( $\alpha = 45$  deg), but consider the broad-band re-implementation of the AtLAST sensitivity calculator. The specific frequencies of the band edges correspond to the ones that minimizes the output noise RMS level in the corresponding band per given integration time.

band	ref. frequency [GHz]	bandwidth [GHz]	band edges [GHz]	beam [arcsec]	sensitivity [ $\mu\text{Jy beam}^{-1} \text{h}^{1/2}$ ]	survey noise [ $\mu\text{K}_{\text{cmb}} - \text{arcmin h}^{1/2}$ ]
2	42.0	24	30–54	35.34	6.60	2.40
3	91.5	51	66–117	16.22	6.46	1.27
4	151.0	62	120–182	9.83	7.14	1.21
5	217.5	69	183–252	6.82	9.22	1.86
6	288.5	73	252–325	5.14	11.91	3.71
7	350.0	50	325–375	4.24	23.59	12.26
8	403.0	38	384–422	3.68	39.98	34.70
9	654.0	118	595–713	2.27	98.86	$1.67 \times 10^3$
10	845.5	119	786–905	1.76	162.51	$3.70 \times 10^4$

of the gas thermal properties. In fact, observational models for a statistically relevant sample of clusters are currently limited to the indirect determination of resolved pressure models for clusters up to  $z \lesssim 1$  (Arnaud *et al.*, 2010; McDonald *et al.*, 2014; Sayers *et al.*, 2023). Direct constraints of the properties of the ICM within protoclusters and clusters early

in their formation have been obtained for only a handful of extreme systems ( $z > 1$ ; Andreon *et al.*, 2021; Andreon *et al.*, 2023; Brodwin *et al.*, 2016; Di Mascolo *et al.*, 2023; Gobat *et al.*, 2019; Tozzi *et al.*, 2015; van Marrewijk *et al.*, 2023) or limited samples (e.g., Ghirardini *et al.*, 2021b). Despite the significant time investment with the Atacama Large

Millimeter/Submillimeter Array (ALMA; [Wooten & Thompson, 2009](#)) or the 100-meter Green Bank Telescope (GBT; [White et al., 2022](#)), these observations only allow one to perform a characterization of the physical and thermodynamic state of these early systems for a few select systems. Still, these have generally required the combination with ancillary X-ray observations, due to observational limitations including poor

signal to noise or the data being limited to fewer than 5 bands.

In order to gain a radially resolved view of pressure profiles and of their small-scale perturbations for a large variety of clusters (in terms of dynamical state, mass, and redshift; see [Figure 3](#)), it is key to have simultaneous access to

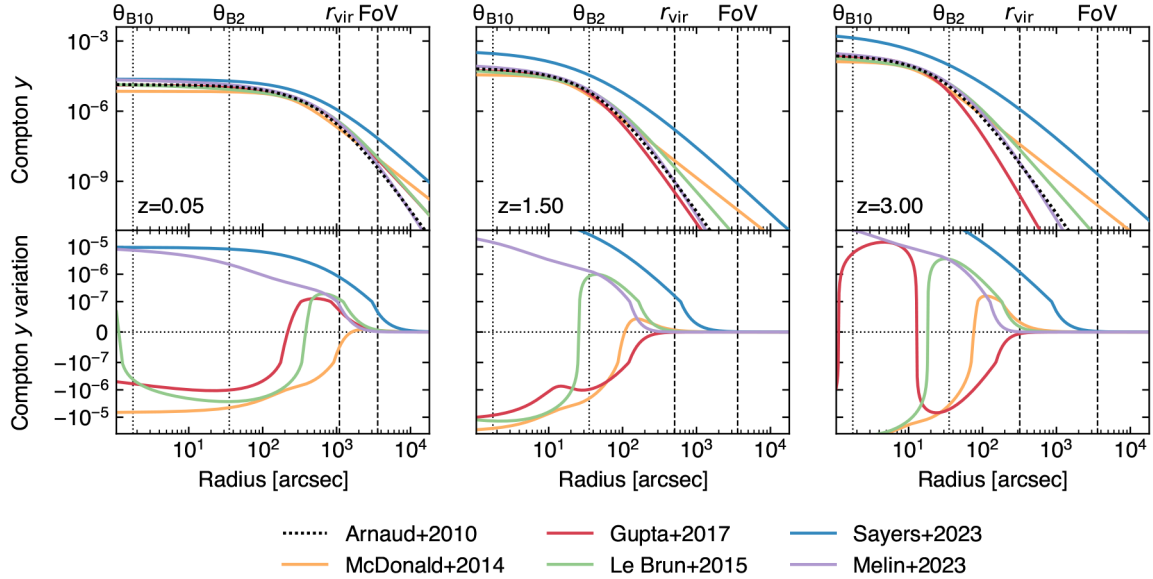


**Figure 3.** Observed Compton  $y$  profiles when considering different fiducial models for the ICM pressure distribution (top panels; [Arnaud et al., 2010](#); [Gupta et al., 2017](#); [Le Brun et al., 2015](#); [McDonald et al., 2014](#); [Melin & Pratt, 2023](#); [Sayers et al., 2023](#)) and respective variations (bottom panels) with respect to the universal pressure profile from [Arnaud et al. \(2010\)](#), commonly adopted as reference model for the inference of cluster masses. In this plot, we consider a cluster with fixed mass ( $M_{500} = 10^{14} M_{\odot}$ ) for an arbitrary set of redshifts ( $z = \{0.05, 1.50, 3.00\}$ ). The different profiles are computed on heterogeneous samples in terms of mass and redshift ranges, and thus encode different biases associated to the intrinsic scatter of pressure profiles, deviations from self-similar evolution and hydrostatic equilibrium. Thanks to AtLAST's sensitivity to Compton  $y$  levels  $\leq 10^{-7}$ , it will be possible to characterize such effects, while providing a model for the evolution of ICM pressure across cosmic history. As reference, we report as dashed vertical lines the virial radius of the model clusters and the instantaneous field of view expected for AtLAST (see [Section 4](#)). We further denote as dotted vertical lines the largest and smallest angular resolution  $\theta$ , achievable with AtLAST, respectively obtained in the proposed Band 2 and Band 10 (see [Section 4.1](#) and [Table 1](#) below).

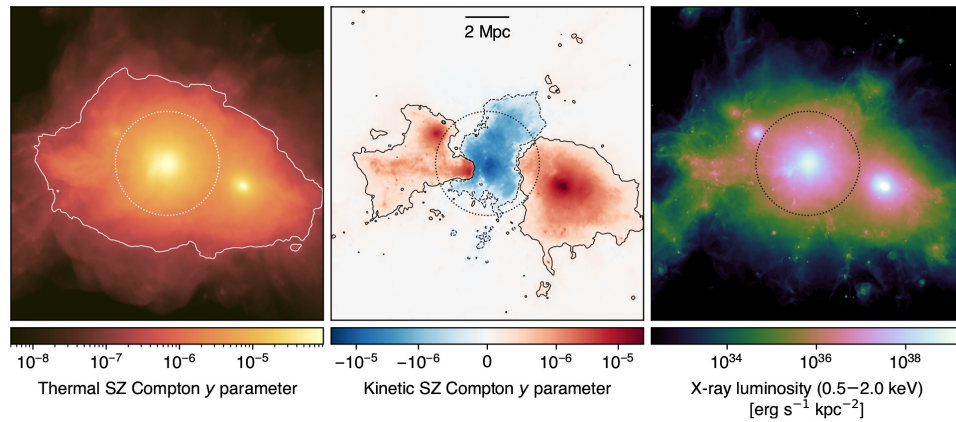


**Figure 4.** Thermal (left) and kinetic (center) SZ effects, and X-ray luminosity (right) from a simulated massive cluster undergoing a major merger ( $M_{200} \simeq 1.5 \times 10^{15} M_{\odot}$ ,  $z = 0$ ) extracted from the TNG-Cluster simulation ([Nelson et al., 2023](#)). The contours in both panels trace a Compton  $y$  level of  $2 \times 10^{-7}$ , roughly corresponding to the reference SZ depth for a deep AtLAST survey ([Section 4.2](#)). As a reference, we mark with a circle the virial radius of the galaxy cluster. This implies that AtLAST will be able to efficiently trace the SZ signal out to the low-density outskirts of clusters.



enhanced sensitivity, high angular resolution, and wide spectral coverage across the millimeter/submillimeter spectrum. These observations are important, as from hydrodynamical simulations the pressure distribution of high- $z$  galaxy clusters are predicted to diverge from the universal pressure models (Battaglia *et al.*, 2012; Gupta *et al.*, 2017), leading to a systematic offset between the mass-to-SZ observable scaling relation for high- $z$  haloes with respect to local ones (Yu *et al.*, 2015). Constraining such deviations is crucial as they carry fundamental information on the complex interplay between all those multi-scale processes — e.g., merger and accretion events, AGN and stellar feedback, turbulent motion — at epochs ( $z > 1$ ) when their impact from galactic to cluster scales are expected to be the strongest. At the same time, tracing the pressure profiles out to the cluster outskirts will be key to pinpoint and characterize virial and accretion shocks (Anbajagane *et al.*, 2022; Anbajagane *et al.*, 2024; Hurier *et al.*, 2019), whose existence is a fundamental prediction of the current paradigm of large-scale structure formation (e.g., Ryu *et al.*, 2003; Zhang *et al.*, 2021). In particular, the location and properties of their SZ features can be exploited to study the mass assembly of galaxy clusters and to place direct constraints on their mass accretion rate (a quantity otherwise difficult to infer observationally; see, e.g., Baxter *et al.*, 2021; Baxter *et al.*, 2024; Molnar *et al.*, 2009; Lau *et al.*, 2015; Towler *et al.*, 2024). And finally, pressure perturbations due to the turbulent motion within the ICM have been measured to result in fluctuations of the Compton  $y$  signal with fractional amplitude  $\lesssim 10^{-1}$  compared to the underlying bulk SZ signal (Khatri & Gaspari, 2016; Romero *et al.*, 2023). The enhanced sensitivity and calibration stability that will be achieved by AtLAST will allow it to easily probe this level of fluctuations, providing important albeit indirect information on the level of non-thermal pressure support in the ICM. More in general, it is only with the unique technical prospects offered by AtLAST that we will be able to probe to thermal SZ signal down to the levels Compton  $y \approx 10^{-7}$  (Section 4.2) required to probe the full extent of the ICM pressure distribution (Figure 3), unparalleled by any of the current or forthcoming submillimeter facilities.

### 3.2 Measuring the ICM temperature via relativistic SZ effect

The classical formulation of the thermal SZ effect relies on a non-relativistic assumption for the velocity distribution of the electron populations responsible for the SZ signal. These can however manifest velocities of the order of a few tens percent of the speed of light. Accounting for any associated special-relativistic effects introduce a temperature-dependent distortion of the SZ spectral model (Figure 2). The resulting relativistic SZ effect thus offers a valuable (yet largely unexplored) opportunity to directly measure the temperature of ICM electrons. This represents a key ingredient for enhancing our physical models of galaxy clusters and improving their utility as cosmological probes via more accurate tuning of mass calibrations and scaling relations (e.g., Lee *et al.*, 2020; Remazeilles & Chluba, 2020). At the same time, having simultaneous access to the full ICM thermodynamics (via temperature  $T_e$ , as well

as pressure  $P_e$  and density  $n_e$  measurements via the combination of the relativistic and purely thermal SZ effects) offers the key chance of building a temporal census of the ICM entropy distribution ( $\propto T_e n_e^{-2/3}$ , or  $\propto T_e^{5/3} P_e^{-2/3}$  when considering thermodynamic quantities directly probed by the SZ effect; Voit, 2005). The many processes affecting cluster evolution — e.g., AGN and stellar feedback, injection of kinetic energy due to merger activity — are observed to modify the entropy profiles throughout the cluster volumes (e.g., Ghirardini *et al.*, 2017; Pratt *et al.*, 2010; Walker *et al.*, 2012), compared to a baseline model that includes only the non-radiative sedimentation of low-entropy gas driven by gravity (Tozzi & Norman, 2001; Voit *et al.*, 2005). As such, the spatially resolved study of the ICM entropy distribution provides a fundamental proxy of the thermal evolution of cosmic structures as well as the specific dynamical state of galaxy clusters.

Currently, estimates of the relativistic corrections to the thermal SZ effect are limited to a few pioneering studies targeting individual systems (Hansen *et al.*, 2002; Prokhorov & Colafrancesco, 2012) or focusing on stacking analyses (Erlor *et al.*, 2018; Hurier, 2016). Still, even in the case of individual clusters with extremely rich observational spectral coverage (see, e.g., Butler *et al.*, 2022 and Zemcov *et al.*, 2012, focusing on the well-known cluster RX J1347.5-1154), SZ-based inferences of the ICM temperature have commonly resulted in constraints with limited significance. Higher angular resolutions, such as those offered by AtLAST, will be an asset for constraining SZ temperatures. First, the higher angular resolution allows spatially-distinct foregrounds such as radio sources, dusty galaxies and the Galactic dust foreground to be accurately modelled and removed. Second, the extraction of resolved pressure and temperature profiles provides the unique opportunity of performing the physical modeling of the ICM relying solely on the SZ effect. This represents a key advantage. Although electron temperatures can be measured using X-ray data, these are roughly density-square-weighted estimates (e.g., Mazzotta *et al.*, 2004) and therefore subject to biases due to clumping (e.g., Simionescu *et al.*, 2011). Further, observations can become prohibitive at large cluster radii, due to the low X-ray emissivity, and at high redshift, due to cosmological dimming. Churazov *et al.* (2015) showed that the self-similar evolution of galaxy clusters would introduce a near independence of redshift of the X-ray luminosity at fixed cluster mass — when this is defined as the mass enclosed in the radius within which the average matter density equals some fiducial cosmic overdensity value (e.g.  $500 \times \rho_{\text{crit}}$ ). Nevertheless, we note that these considerations are valid only under the assumption that the local mass-observable scaling relations are applicable at high redshift. At the same time, both the resolved SZ signal and the respective cluster-integrated flux would still be  $(1+z)^{3/2}$  larger than the X-ray emission from the same system at a given redshift  $z$ .

On the other hand, since the SZ effect is characterized by a surface brightness that is inherently independent of redshift, ICM temperature constraints can in principle be derived

without specific limits on the distance of the target systems. And lastly, the temperatures inferred using data on the same clusters but taken using different X-ray observatories may suffer large systematic variations due to inherent calibration differences (Migkas *et al.*, 2024; Schellenberger *et al.*, 2015). In contrast, the SZ temperature estimate is pressure-weighted and is therefore predicted to be less biased by emission while being easier to constrain at large cluster radius due to the linear (instead of squared) dependence on density. And even in the case of low-mass (i.e., low-SZ surface brightness; see also Section 3.4) clusters for which it will not be possible to extract resolved SZ-based temperature information, the availability of deep, high angular resolution SZ observations for a large sample of systems will still allow for matching resolution with X-ray observations and to extract resolved full thermodynamic properties of the ICM (see Section 3.1 and Section 5.2.4). An exploratory study of AtLAST's expected capabilities to measure temperature via the relativistic SZ effect is presented in Section 4.3. We refer to this for more details on the impact of the specific spectral setup on the reconstruction of the relativistic SZ effect and on the technical requirements for extending such measurements over broad ranges of cluster masses and redshifts.

### 3.3 Kinematic perspective on large scale structures

The kinetic component of the SZ effect represents a valuable tool for revealing the peculiar motion of cosmic structures. Nevertheless, its properties – namely its shape, the fact that the kinetic SZ signal is generally weaker than the thermal SZ effect (Figure 2), and that it traces the integrated line of sight momentum – make the kinetic SZ effect somewhat elusive to measure and interpret. Further, the kinetic SZ spectral distortion is consistent with a Doppler shift of the CMB photons, making it spectrally indistinguishable from small-scale primordial CMB anisotropies.

Past targetted kinetic SZ studies (e.g., Adam *et al.*, 2017; Mroczkowski *et al.*, 2012; Sayers *et al.*, 2013; Sayers *et al.*, 2019; Silich *et al.*, 2023) have already reported direct measurements of the kinetic SZ signal due to the large-scale gas flows associated with merger events. All of these works focused on individual, relatively extreme clusters (either in terms of overall mass, dynamical state, or orientation of the merger direction with respect to the line-of-sight). The broad spectral coverage and the expected sensitivity of AtLAST, in combination with its capability of probing a high dynamic range of angular scales, will instead allow for systematically including the kinetic SZ information in the reconstruction of the thermodynamic characterization of large statistical samples of galaxy clusters and groups.

Statistical measurements of the kinetic SZ effect in disturbed and merging systems represent a crucial ingredient for cosmological studies via direct measurements of the amplitude and the growth rate of cosmological density perturbations (e.g., Bhattacharya & Kosowsky, 2007; Soergel *et al.*, 2018). They can also be used to distinguish  $\Lambda$ CDM from alternative cosmologies with modified gravitational forces (Bianchini & Silvestri, 2016; Kosowsky & Bhattacharya, 2009; Mueller *et al.*, 2015). Further, correlating the velocity structure with

information from facilities at other wavelengths on the baryonic and dark matter content of merging systems will represent a preferential probe of the collisional nature of dark matter (Silich *et al.*, 2023). In the case of relatively relaxed systems (i.e., with velocity fields not manifesting complex morphologies), the joint analysis of the thermal and kinematic SZ effects would naturally complement the inference of the ICM pressure and temperature distributions with information on the bulk peculiar velocity of galaxy clusters and tighter constraints on the ICM density (Mroczkowski *et al.*, 2019).

The detailed spatial mapping of the kinetic SZ effect could also be used to characterize turbulent motions and to identify their driving dissipation scales which are relevant for feedback mechanisms. This can be done, in particular, by computing the velocity structure function (VSF), defined as the average absolute value of the line of sight velocity differences as a function of projected scale separation. The VSF is an effective way of characterizing turbulent motions and identifying their driving and dissipation scales (see, e.g., Ayromlou *et al.*, 2023; Ganguly *et al.*, 2023; Gatuuz *et al.*, 2023; Li *et al.*, 2020). Determining the driving scale of turbulence would constrain the relative importance of gas motions driven by AGN feedback on small scales and mergers on large scales, while the dissipation scale is sensitive to the microphysics of the ICM, such as its effective viscosity (Zhuravleva *et al.*, 2019). In general, constraints on the small-scale properties of the velocity field associated with turbulent motion (Nagai *et al.*, 2003; Sunyaev *et al.*, 2003), coherent rotation of gas within their host dark matter haloes (Altamura *et al.*, 2023; Baldi *et al.*, 2018; Bartalesi *et al.*, 2024; Baxter *et al.*, 2019; Cooray & Chen, 2002), or merger-induced perturbations (Biffi *et al.*, 2022) can complement the reconstruction of ICM thermodynamic fluctuations (Khatri & Gaspari, 2016; Romero *et al.*, 2023) and the potential mitigation of biases due to non-thermal pressure support (e.g., Angelinelli *et al.*, 2020; Ansarifard *et al.*, 2020; Ettori & Eckert, 2022; Shi *et al.*, 2016) discussed in Section 3.1. Perturbations in the kinetic SZ distribution will result in smallscale kinetic SZ fluctuations more than an order of magnitude smaller than the corresponding thermal SZ component (Biffi *et al.*, 2022; Mroczkowski *et al.*, 2019; Sunyaev *et al.*, 2003) even for massive systems. The clear requirement of extremely demanding observations (along with the difficulty in spectrally disentangling the kinetic SZ effect from the underlying CMB signal; Mroczkowski *et al.*, 2019) have so far limited the possibility of directly measuring any small-scale kinetic SZ feature. However, AtLAST will be able to efficiently measure percent-level deviations from the dominant thermal SZ effect (see, e.g., Section 4.3 below for a discussion in the context of relativistic SZ corrections) and to swiftly survey wide sky areas at  $\sim 1.5 - 35$  arcsec resolution, thus opening a novel observational window on ICM velocity substructures.

Finally, AtLAST's simultaneous sensitivity to both small and large spatial scales facilitates studies of the distortions in the CMB across a broad range of spatial scales ( $300 \lesssim \ell \lesssim 20000$ ). Existing and forthcoming CMB experiments cannot probe beyond  $\ell \sim 4000$ , whose power spectrum is dominated by both regular CMB anisotropies and CMB lensing effects. However, at 220 GHz around  $\ell \approx 7000$ , the kinetic SZ effect becomes

the dominant contributor to the angular power spectra (Smith & Ferraro, 2017), thus enabling studies on the kinetic SZ imprint from the epoch of reionization, originating from relativistic electrons within expanding ionizing bubbles (Ferraro & Smith, 2018) – the so-called “patchy kinetic SZ” signal.

### 3.4 Overcoming cluster selection biases

It is becoming generally appreciated that X-ray selected clusters offer a biased view of the cluster population (Andreon *et al.*, 2017; Andreon *et al.*, 2019; Eckert *et al.*, 2011; Maughan *et al.*, 2012; Pcaud *et al.*, 2007; Planck Collaboration, 2011; Planck Collaboration 2012; Stanek *et al.*, 2006). This is because, in a given sample, bright clusters are over-represented (see, e.g., Mantz *et al.*, 2010 for discussion of Malmquist and Eddington biases), whereas those systems fainter-than-average for their mass are underrepresented, if not missing altogether. This bias is difficult to correct because the correction depends on assumptions about the unseen population (Andreon *et al.*, 2017; Vikhlinin *et al.*, 2009). On the other hand, SZ-selected cluster samples are generally thought to offer a less biased view and indeed show a larger variety (e.g., in gas content) than X-ray selected samples (e.g., Planck Collaboration, 2011; Planck Collaboration, 2012). Comparisons of the X-ray properties of SZ-selected systems (see, e.g., CHEX-MATE Collaboration, 2021) have highlighted the fact that ICM-based selection biases can depend on the specific morphology (Campitiello *et al.*, 2022) or the presence of a dynamically relaxed cool core (the so-called “cool-core bias”; Rossetti *et al.*, 2017).

However, the selection of clusters via their galaxies (i.e., based on the identification of cluster members) or via gravitational lensing (i.e., based on the effect of the cluster potential on the images of background sources) can provide an observational perspective that is potentially unbiased with respect to the thermodynamic state of the ICM. Although methods based on galaxies can still suffer from significant biases due to contamination and projection effects (e.g., Donahue *et al.*, 2002; Willis *et al.*, 2021), the fact that they are not dependent on the ICM-specific biases have granted the possibility of unveiling the existence of a variety of clusters at a given mass larger than X-ray or current SZ-based approaches. In particular, the low-surface brightness end of the unveiled new population of clusters is changing our view of galaxy clusters. These are found to introduce significant scatter in many ICM-based mass-observable scaling relations (Andreon *et al.*, 2022), at very the heart of our understanding of cluster physics and broadly used in the context of cluster cosmology. Characterizing such a population of low surface brightness clusters will necessarily require a major leap in the SZ sensitivity with respect to state-of-the-art facilities.

The possibility of performing deep, high angular resolution mapping over wide sky areas offered by AtLAST will allow observers to efficiently detect those clusters that are presently underrepresented in, or entirely missing from, catalogs due to an SZ or X-ray signal inherently fainter than expected from their mass. Indeed, clusters with low X-ray surface brightness tend to have low central values of Compton  $y$ , of the order of

few  $10^{-6}$  (based on Andreon *et al.*, 2022), at the very limit of long pointed observations with current single-dish telescopes, when not beyond their effective detection capabilities. In combination with X-ray, strong and weak-lensing data, this will allow for a thorough characterization of their physical and thermodynamic state, and for discriminating between any variation in the inherent properties of the intracluster gas and observational biases induced by any astrophysical processes more or less associated with the specific evolution and physics of the target clusters — e.g., energetic AGN feedback, recent merger events, low gas fraction, enhanced clustering of millimeter-bright galaxies.

### 3.5 Identification and thermodynamic characterization of high- $z$ clusters and protocluster

Next generation SZ facilities like Simons Observatory (SO; Simons Observatory Collaboration, 2019) and CMB-S4 (Abazajian *et al.*, 2016) will extend our observational window into the high- $z$  and low-mass realm (see, e.g., Raghunathan *et al.*, 2022 and Figure 5) of galaxy clusters and protoclusters. Tracing the earliest phases of their evolution will be crucial for constraining the physical origin of the thermal properties of the large-scale structures observed in the nearby Universe.

Nevertheless, current forecasts estimate that next-generation wide-field surveys (Gardner *et al.*, 2024) will detect less than 20% of the most massive (proto)clusters ( $M_{200} \lesssim 10^{14} M_{\odot}$ ,  $z > 2$ ). This is mostly a consequence of the competing impact of inherently low SZ amplitudes (due to low mass, disturbed state, and severe deviations from full gas thermalization and virialization; Bennett & Sijacki, 2022; Li *et al.*, 2023; Sereno *et al.*, 2021), the low angular resolution of the facilities, and of the increasing contamination level due to, e.g., enhanced star formation and AGN activity, or possibly due to massive CGM gas and dust reservoirs at high redshift (Lee *et al.*, 2024). And as already broadly discussed in Section 3.1, extreme limitations are also faced in the case of high angular resolution measurements. Clearly, having access to deep, high angular resolution and multi-band SZ observations will allow observers to simultaneously tackle all such issues, making AtLAST the optimal telescope that will definitively shape our perspective on high- $z$  (proto)clusters.

The correlation of such constraints with the properties of the galactic populations observed within the (proto)cluster complexes will further allow for directly linking the evolution of the forming intracluster gas to the multi-phase protocluster environment and its only partially understood impact on galaxy formation and evolution (Figure 6). Current multi-wavelength observations have highlighted that the environmental effects might act on Mpc scales and well beyond the more or less virialized regions within these protocluster galaxy overdensities (Alberts & Noble, 2022). These studies however rely on the characterization of environmental processing solely from the perspective of protocluster galaxies (Overzier, 2016). On the other hand, the wide field, the extreme sensitivity and the capability of AtLAST to trace low density regions thanks to the SZ effect will allow for an efficient

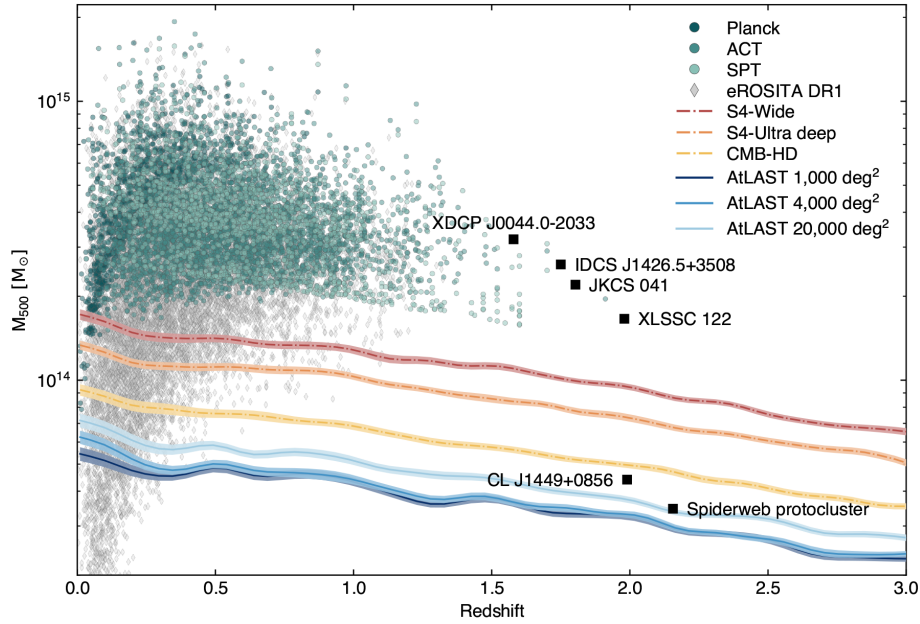


**Figure 5.** Mass vs. redshift detection forecast for AtLAST assuming different survey strategies (covering 1000 deg<sup>2</sup>, 4000 deg<sup>2</sup>, and 20000 deg<sup>2</sup>, respectively, for a fixed survey time of 5 years) in comparison with next-generation wide-field millimeter surveys (Abazajian *et al.*, 2016; Sehgal *et al.*, 2019) and the eROSITA all-sky (X-ray) survey (Bulbul *et al.*, 2024). Poisson realizations of the thermal SZ confusion were simulated in the AtLAST survey case, while the other resolution surveys used Gaussian realizations appropriate in the case where the lower resolution and sensitivity limit the ability to surpass the thermal SZ confusion limit. We refer to Raghunathan (2022) for a more general discussion of the different treatments of the SZ confusion noise. For comparison, we report as green points the clusters from the available SZ survey samples (Bleem *et al.*, 2020; Bleem *et al.*, 2024; Hilton *et al.*, 2021; Planck Collaboration, 2016), as well as relevant high-*z* clusters from the literature: XDCP J0044-2033 (Tozzi *et al.*, 2015), IDCS J1426.5+3508 (Brodwin *et al.*, 2016), JKCS 041 (Andreon *et al.*, 2023), XLSSC 122 (Mantz *et al.*, 2020; van Marrewijk *et al.*, 2023), CL J1449+0856 (Gobat *et al.*, 2019), and the Spiderweb protocluster (Di Mascolo *et al.*, 2023). This figure is adapted from Raghunathan *et al.* (2022).

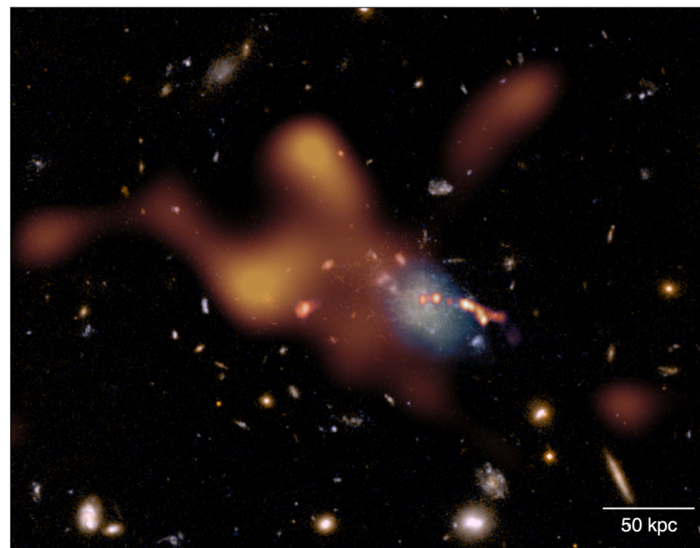


**Figure 6.** Composite Hubble Space Telescope (HST) image based on ACS/WFC F475W and F814W data of the Spiderweb protocluster field. Overlaid (orange) is the thermal SZ signal from the ICM assembling within the protocluster complex as observed by ALMA over a total of more than 12 h of on-source integration time. In a similar amount of time and with the same spectral tuning, AtLAST will achieve a depth comparable to ALMA, however providing a dramatic improvement of  $\sim 10^3$  in field of view and, thus, in overall mapping speed. At the same time, AtLAST will provide a novel perspective on the reservoirs of cold gas (light blue overlay; Emonts *et al.*, 2016) coexisting with the warm/hot phase within protocluster cores (see the CGM science case study by Lee *et al.* (2024) for a discussion). For comparison, we also include the bright jet of radio emission output from the central galaxy as observed by VLA (the linear east-west feature, shown in red; Carilli *et al.*, 2022). The present figure is adapted from Di Mascolo *et al.* (2023) and the corresponding ESO Press Release eso2304.

imaging of the complex galaxy-environment puzzle with a comprehensive glance of the multi-scale and multi-phase nature of high- $z$  (proto)cluster systems.

### 3.6 Impact of AGN feedback and halo heating

Acting in practice as a calorimeter of astrophysical electron populations, the thermal SZ effect can shed light on the interplay of feedback processes and heating of large-scale halos from galactic to cluster scales. This is particularly relevant in the context of AGN studies, in relation to the specific impact of feedback and AGN-driven outflows in contributing to the heating of cosmic haloes (Fabian, 2012). In fact, despite the importance of supermassive black holes (SMBH) in driving the evolution of cosmic structures, we still have a limited understanding of the complex connection between multi-scale physical properties of SMBH and their host galaxies (Gaspari *et al.*, 2020). Current multi-wavelength observations support a rough duality in the feedback framework (Padovani *et al.*, 2017), with the level of radiative efficiency depending on the specific scenario regulating SMBH accretion (Hlavacek-Larrondo *et al.*, 2022; Husemann & Harrison, 2018). From the perspective of the observational properties of the hot ICM/CGM phase, different feedback models would naturally result in different levels of energy injection and, thus, in deviations from the halo thermal budget expected from virial considerations. At the same time, the strong interaction of winds and jets with the surrounding medium introduces a significant amount of non-thermal support to the overall pressure content — in the form, e.g., of turbulent motion, buoyantly rising bubbles of extremely hot plasma ( $\gtrsim 100$  keV) and associated shock-heated gas cocoons (Abdulla *et al.*, 2019; Ehlert *et al.*, 2019; Marchegiani, 2022; Orłowski-Scherer *et al.*, 2022; Pfrommer *et al.*, 2005). All this implies, however, that gaining a detailed view of the thermodynamic properties of the circumgalactic haloes would allow us to obtain better insights into the AGN energetics and improve our feedback models.

Measurements of the integrated thermal SZ signal have already been broadly demonstrated to provide an efficient means for probing the evolution of the imprint of feedback on the thermal energy of cosmic structures (Crichton *et al.*, 2016; Hall *et al.*, 2019; Yang *et al.*, 2022). These are however limited mostly to stacking measurements of arcminute-resolution SZ data, and are thus hampered by the low angular resolution of the wide-field survey data employed. On the other hand, targeted observations at higher angular resolution currently comprise an extremely small set of high- $z$  quasars (Brownson *et al.*, 2019; Jones *et al.*, 2023; Lacy *et al.*, 2019). The overall limited sensitivity as well as interferometric effects such as poor  $uv$ -coverage and the filtering of large scales, however, resulted only in what appear to be low significance detections of the SZ signal in the direction of these systems. While these works have been pioneering for high resolution studies, they so far provide little constraining power on the AGN energetics and feedback scenarios.

On the other hand, the SZ signal from AGN-inflated bubbles has been robustly detected in one, extreme case (MS

0735.6+7421; Abdulla *et al.*, 2019; Orłowski-Scherer *et al.*, 2022). Still, the observations required 10s hours with the current-generation MUSTANG-2 instrument (Dicker *et al.*, 2014), and 100s of hours with the previous-generation CARMA interferometer (Woody *et al.*, 2004), and were limited to single frequency observations. Since the SZ signal scales as the amount of energy displaced, future observations with current instruments to observe additional, less energetic AGN outbursts could require much more time on the source. As such, this singular example serves largely as a proof-of-principle for further, future resolved studies. We note that some progress will be made in this decade with, e.g., TolTEC (Bryan *et al.*, 2018), though the Large Millimeter Telescope Alfonso Serran (LMT; Hughes *et al.*, 2010) was designed to achieve a surface accuracy of  $\sim 50 \mu\text{m}$  (2.5 $\times$  worse than AtLAST), and regardless will be limited by the atmospheric transmission to  $\nu \lesssim 350$  GHz in all but the most exceptional weather (see, e.g., the site comparison in Klaassen *et al.*, 2020). Other single dish facilities delivering similarly high resolution will be limited to even lower frequencies (e.g. Nobeyama, Green Bank Telescope, Sardinia Radio Telescope), while ALMA has difficulty recovering scales larger than 1' in all but its lowest bands (see Section 4).

Recently, multiple studies (e.g., Chakraborty *et al.*, 2023; Grayson *et al.*, 2023; Moser *et al.*, 2022) showed that obtaining high angular resolution observations of the thermal SZ effect (in combination with X-ray observations) would allow for constraining the distinct contribution from different feedback models. First observational studies based on the cross-correlation of the thermal and kinetic SZ signals (e.g., Amodeo *et al.*, 2021; Das *et al.*, 2023; Schaan *et al.*, 2021; Vavagiakis *et al.*, 2021) already showed independent and competitive constraints. Recently, Coulton *et al.* (2024) demonstrated that the so-called “patchy screening” can provide an alternative and highly complementary perspective on feedback mechanisms. Still, the low angular resolution of such measurements is not sufficient to spatially separate first and higher-order halo terms, and are thus hampered by respective systematics. On the other hand, based on numerical predictions for different feedback models (Yang *et al.*, 2022), extending our observational constraints to include a broad range of masses and redshift and distinguishing between different feedback models will be highly impractical with current high angular resolution facilities. Further, it is worth noting that strongly asymmetric outflows from quasars, as well as gas inflows, would result in small-scale distortions of the overall SZ signal due to the localized thermal, kinetic and relativistic SZ contributions (see, e.g., Bennett *et al.*, 2024). Similarly, the inflation of cavities by large-scale jets and the consequent generation of shock fronts and turbulent motion would imprint observable deviations in the global SZ signal in the direction of AGN hosts (Ehlert *et al.*, 2019). Having access to sensitive, multi-frequency observations as provided by AtLAST would thus be crucial, on the one hand, for reducing any biases associated with the missing decomposition of the different SZ components to the measured signal as well as any contamination (due to, e.g., millimeter/submillimeter bright emission from the AGN within

the studied haloes). On the other hand, it will allow for cleanly dissecting the spectral and morphological features characteristic of the different feedback scenarios. Concerning the reconstruction of the thermal properties of the CGM, this will have an impact even beyond the context of the evolution of the physical processes driving the heating of cosmic haloes. In fact, it will be possible to swiftly build a multi-phase picture of the CGM by concurrently tracing its cold phase along with direct constraints on the otherwise elusive warm/hot constituent — comprising  $\approx 80\%$  of the total baryonic material in the CGM overall (e.g., Schimek *et al.*, 2024). This is an unparalleled feature of (sub)millimeter measurements, that necessarily require a combination of high spectral and angular resolution, along with the capability of mapping large-scale diffuse signals. Clearly, AtLAST will be the optimal facility for such a task. For a broader discussion of the importance of multi-phase CGM studies in the context of galaxy formation and evolution, we refer to the companion AtLAST CGM science case study by Lee *et al.* (2024).

### 3.7 Galaxy cluster outskirts and intercluster structures

A significant portion of the baryonic content of the Universe at  $z \lesssim 3$  is expected to lie well beyond the virial boundaries of cosmic structures (Cen & Ostriker, 1999). This diffuse “warm-hot intergalactic medium” (WHIM) is expected to have temperatures  $T_e \approx 10^5 - 10^7$  K, largely invisible at optical wavelengths and generally too low in temperature for all but the deepest X-ray observations, often being limited to line of sight absorption studies (Nicastro *et al.*, 2018). Obtaining a detailed view of the large-scale WHIM is however crucial. Accurately constraining the actual amount of matter constituting the WHIM will provide fundamental information on the “missing baryons” budget associated to this specific phase of the filamentary intergalactic medium (e.g., Shull *et al.*, 2012). This will be connected to the specific mechanisms driving the heating of large-scale structure on cosmological scales: on the one hand, matter inflows and mergers along large-scale filaments driving strong accretion and virialization shocks (Anbajagane *et al.*, 2022; Anbajagane *et al.*, 2024; Baxter *et al.*, 2021 see also Section 3.1); on the other hand, the impact of feedback processes and of the environmental preprocessing of galaxies (e.g., Alberts & Noble, 2022; Fujita, 2004).

To date, the identification and characterization of the physical properties of the filamentary WHIM has been performed mostly through stacked SZ and/or X-ray measurements (e.g., de Graaff *et al.*, 2019; Singari *et al.*, 2020; Tanimura *et al.*, 2019; Tanimura *et al.*, 2020; Tanimura *et al.*, 2022), and is often dominated by the hottest extremes of the range of temperatures expected for the WHIM (see Lokken *et al.*, 2023 for discussion). Recently, direct SZ imaging of a nearby intercluster bridge was presented in Hincks *et al.* (2022), which used the combination of ACT+*Planck* data to reveal details at a much higher spatial dynamic range than the previous results using *Planck* alone. The results are shown in Figure 7. This work, while serving as a valuable pathfinder, highlighting the SZ substructures possible to image at even modestly higher ( $\sim 6\times$ ) resolution, was still limited to nearby ( $z \approx 0.05$ ) massive clusters. Deep maps with AtLAST will allow

improved spatial dynamic range and higher fidelity, enabling such studies for many more clusters going to both higher redshifts and lower mass regimes.

Thanks to its sensitivity and to the possibility of recovering large scales over extremely wide fields, AtLAST will provide the ideal tool for searching for the presence of the SZ effect in accreting and unbound intergalactic gas surrounding the virialized volume of clusters and groups. In particular, this will make it possible to routinely explore intercluster structures in a large number of cluster pairs without the need for time demanding observations. For instance, it will be possible to achieve the same Compton  $y$  (or surface brightness) sensitivity as in the observation of the A399-A401 observations by Hincks *et al.* (2022, see also Figure 7) in less than  $\sim 10$  h of integration, but with better spectral coverage and an order of magnitude improvement in the angular resolution. On the other hand, we can consider as a rough lower limit of the expected amplitude for large-scale filaments the results from previous stacking experiments on intergalactic gas. For instance, de Graaff *et al.* (2019) provide estimates of the average SZ signal to have amplitudes in Compton  $y$  unit of  $\lesssim 10^{-8}$ , corresponding to a maximum amplitude of the thermal SZ signal of  $\gtrsim -64$  nJy beam $^{-1}$  for the decrement, and  $\lesssim 9.5$  nJy beam $^{-1}$  for the increment. Although impractical for performing any direct imaging of WHIM between and around individual galaxies, the extreme observing speed of AtLAST will allow for extending the stacking constraints to higher redshift and resolutions, providing a resolved evolutionary perspective on the hot phase of the cosmic web and the processes driving their thermal properties. Similarly, the broad spectral coverage will allow for reducing contamination from inter-filamentary structures, while providing the means for directly inferring robust temperature constraints (currently representing the main limitation for using the SZ effect for determining the overall contribution of WHIM to the missing baryon budget).

## 4 Technical justification

The field of view of a (sub)millimeter telescope represents a key parameter in the context of SZ science. Current high resolution instruments on large single dish telescopes — e.g., MUSTANG-2 (Dicker *et al.*, 2014), NIKA2 (Adam *et al.*, 2018), TolTEC (Bryan *et al.*, 2018) — lose signals on scales larger than their instantaneous fields of view ( $\approx 4 - 6'$ ; Romero *et al.*, 2020), where much of the most interesting, faint target SZ signals exist. We note that continuum observations using the 12-meter antennas in the ALMA Total Power Array (TPA; Iguchi *et al.*, 2009) suffer even more egregiously from being unable to remove atmospheric contamination due to their limited fields of view. They also suffer from the poor mapping speeds associated with single beam observations, and from relatively small collecting areas. The issue associated with large-scale filtering is arguably more restrictive in the case of interferometric observations, which generally feature maximum recoverable scales that fall within the sub-arcminute regime (e.g., ALMA Bands 4–10; we refer to the ALMA Technical Handbook for further details). So far, instruments with much larger instantaneous fields of view,

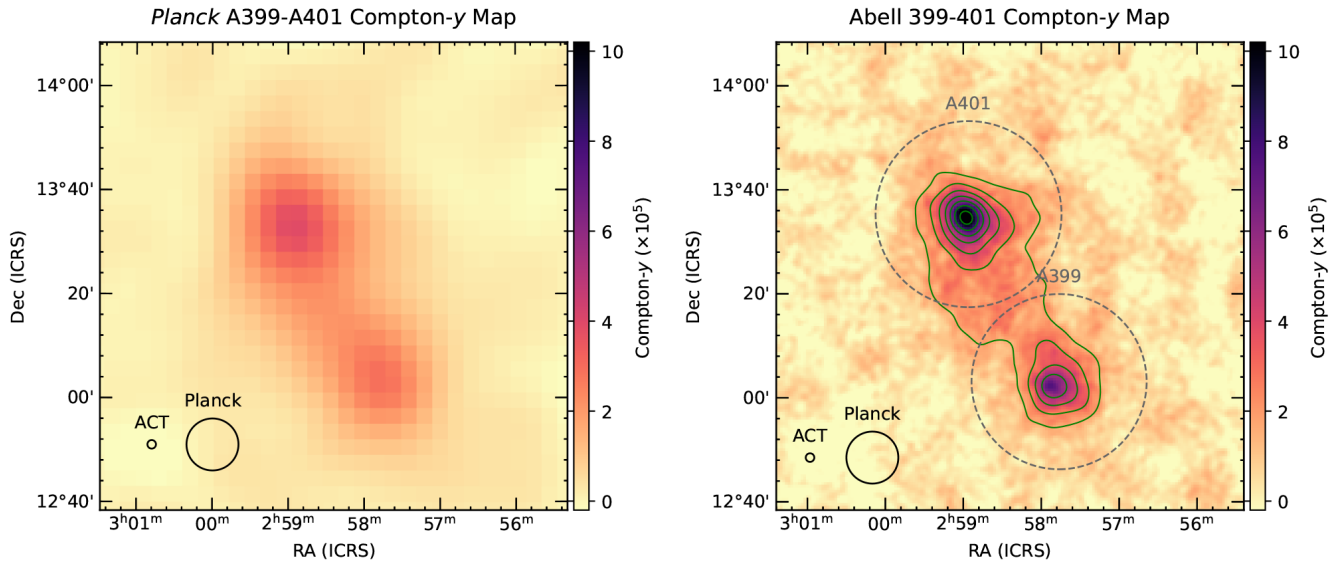


**Figure 7. Comparison of the Compton- $y$  maps produced with *Planck* alone (left, 10' resolution) and ACT (right, 1.7' resolution).** AtLAST will deliver an 8.3 $\times$  improvement in resolution, and 69.4 $\times$  the instantaneous sensitivity per beam, with respect to that of ACT (and other 6-m CMB experiments) for the same observing frequencies, allowing one to image substructures in intercluster bridges and directly identify and remove source contamination. The figure has been reproduced and adapted with permission from [Hincks \*et al.\* \(2022\)](#).

which are therefore better able to recover larger scales, have been employed in the context of CMB/SZ survey experiments like ACT ([Swetz \*et al.\*, 2011](#)), SPT ([Carlstrom \*et al.\*, 2011](#)), SO ([Simons Observatory Collaboration, 2019](#)), CMB-S4 ([Abazajian \*et al.\*, 2016](#)), CCAT-prime (Fred Young submillimeter Telescope or FYST; [CCAT-Prime Collaboration, 2023](#)). Still, these feature small apertures ( $\leq 15$ -m). This results in poor source sensitivity due to their limited collecting areas and in arcminute-level angular resolution, making these telescopes not suitable for imaging the small-scale morphologies of galaxy clusters and protoclusters (except for a few systems in the nearby Universe). In general, larger scales are difficult to recover due to the large, and largely common mode, atmospheric signal which dominates. A field of view of reduced size requires a tailored observational strategy and data reduction pipeline to mitigate signal loss at large scales. Nevertheless, even in such a case, the recovery of astrophysical information beyond the maximum recoverable scales of such facilities would still be severely hampered. This would critically affect many of the proposed science goals, particularly those requiring both wide field of views and extended recoverable scales. Intergalactic filaments are in fact expected to extend over tens of Mpc (e.g., [Galárraga-Espinosa \*et al.\*, 2020](#)) and, thus, extending over degree scales in the case of nearby superclusters ([Ghirardini \*et al.\*, 2021a](#)). Similar physical extents are observed also in the case of high- $z$  protocluster complexes ( $\lesssim 20$  arcmin; see, e.g., [Cantalupo \*et al.\*, 2019](#); [Hill \*et al.\*, 2020](#); [Jin \*et al.\*, 2021](#); [Matsuda \*et al.\*, 2005](#)). And as shown in [Figure 3](#) and [Figure 4](#), effectively probing the distribution of the ICM thermodynamic properties out to the cluster outskirts requires mapping the SZ signal beyond  $\sim 1$  deg in clustercentric distance. Therefore, the capability of gaining instantaneous observations of structures

extending from few arcminutes up to degree scales will represent a crucial benefit of AtLAST compared to state-of-the-art and future telescopes covering the same observational windows.

Multi-band observations are also critical to suppress/mitigate non-SZ signals below the detection threshold, making wide spectral coverage essential for many of the science goals detailed above. Current high resolution facilities on large telescopes have at most three bands, and are limited to relatively low-frequency observations — e.g.  $\leq 350$  GHz for the LMT ([Hughes \*et al.\*, 2010](#)),  $\leq 270$  GHz for the 30-meter Institute for Millimetric Radio Astronomy (IRAM), and  $\leq 115$  GHz for the 100-meterGBT ([White \*et al.\*, 2022](#)), the 64-meter Sardinia Radio Telescope (SRT; [Prandoni \*et al.\*, 2017](#)), or any potential single dish component of the ngVLA ([Selina \*et al.\*, 2018](#)). This implies that any current or next-generation facilities will provide limited constraining power for the relativistic and kinetic SZ, as well as contamination from the cosmic infrared background or diffuse dust contamination.

Most foregrounds should be spatially distinguishable from the SZ signal. However there may be a spatially coincident large-scale dust component originating from within clusters themselves (e.g., [Erler \*et al.\*, 2018](#)) which makes at least two bands in the range 400–900 GHz indispensable to trace the Rayleigh-Jeans tail of the dust spectral energy distribution and to mitigate biases in the SZ spectral modeling. An additional band at  $\approx 1200$  GHz would be even more helpful to resolve degeneracies between dust and SZ signals, but this is precluded by the severe reduction in atmospheric transmission.

To meet the observational requirements for pursuing the proposed scientific goals (Section 2), we perceive the most salient instrumentation requirements to be the ability to achieve high continuum mapping speeds over large areas and in multiple bands. This would convert into the key demand of densely filling the telescope focal plane with a large count of multi-frequency detectors. In this regard, current state-of-the-art continuum cameras (e.g., transition edge sensor bolometers or kinetic inductance detectors) have already demonstrated a high technical readiness level, providing background-limited performance in the (sub)submillimeter the possibility of being read out in large numbers (tens-to-hundreds of thousands, as noted in Klaassen *et al.*, 2020) through frequency multiplexing, allowing the construction of large imaging arrays. We further refer to the AtLAST Memo 4 for details on the expected instrumental specifications for AtLAST.

To illustrate the observational capabilities of the proposed AtLAST continuum setup, we generate mock observations using the *maria* simulation library (van Marrewijk *et al.*, 2024) and consider a simulated galaxy cluster extracted from the Dianoga hydrodynamical cosmological simulations (Bassini *et al.*, 2020; Rasia *et al.*, 2015) as input. The results are shown in Figure 8. For comparison, we include simulated observations performed with MUSTANG-2 and jointly with ALMA and the 7-m Atacama Compact Array (ACA; Iguchi *et al.*, 2009). The clear result is the superior capability of AtLAST in recovering spatial features over a broad range of scales at high significance, while MUSTANG-2 and ACA+ALMA suffer from limited sensitivity and significant large-scale

filtering, respectively. We note that, in this test, we are considering only single-band observations at the same frequency to facilitate the comparison. Although ALMA Band 1 offers an improved sensitivity, spatial dynamic range, and field of view compared to Band 3, it still provides a limited sampling of largescale SZ structures (with a maximum recoverable scale  $MRS \lesssim 1.20'$  when ALMA is in its most compact configuration).

#### 4.1 Optimizing the spectral setup

As mentioned broadly in Section 2 and discussed in the introduction to this section, among the critical aspects for performing a robust reconstruction of the SZ effect is the requirement of cleanly separating the multiple spectral components of the SZ signal from contaminating sources. From a technical point of view, this converts to maximizing the spectral coverage while requesting maximum sensitivity (i.e., lowest noise root-mean-square) for each of the bands. Given the deteriorating atmospheric transmission when moving to higher frequencies, this is not obtained by trivially expanding the effective bandwidth arbitrarily. At the same time, we would like to consider a minimum setup in order not to result in an over-sampling of the target spectral range.

A summary of the selected bands, specifically optimized to minimize the output noise root-mean-square level per given integration time, is provided in Table 1. Our low-frequency set ( $\lesssim 300GHz$ ) extend upon the multi-band set-up proposed for CMB-S4 (Abazajian *et al.*, 2016), shown in forecasts to provide an optimal suppression of the contribution from astrophysical foregrounds and backgrounds (Abazajian *et al.*,

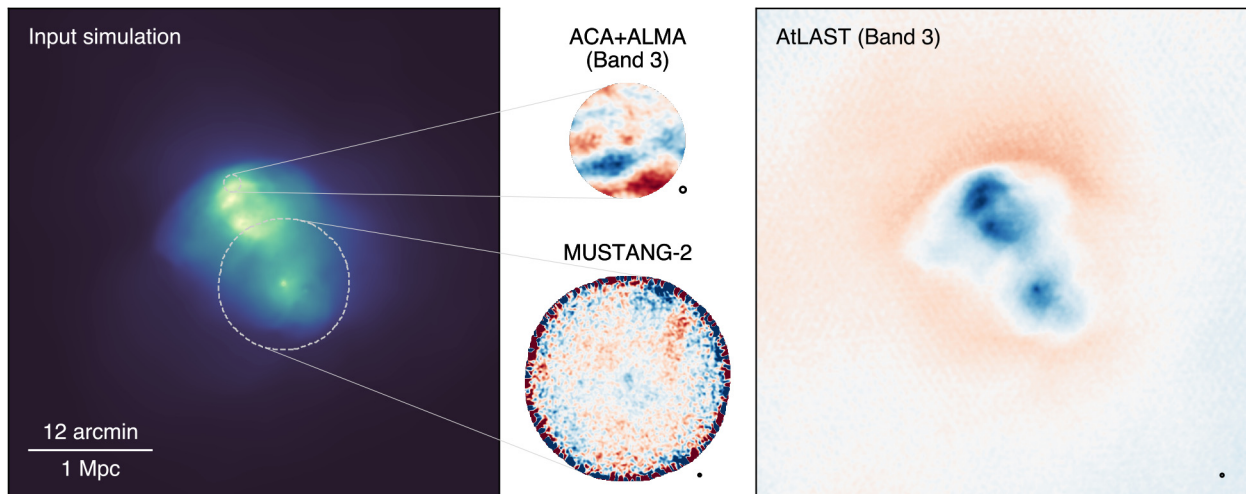


**Figure 8.** A simulated nearby galaxy clusters ( $M_{500} = 1.28 \times 10^{15} M_{\odot}$ ,  $z = 0.0688$ ; left) as observed by ALMA+ACA in Band 3 (top center), MUSTANG-2 (bottom center), and by AtLAST in Band 3 (right). The respective beams are shown in the bottom right corner of each panel. The input simulation is extracted from the Dianoga cosmological simulation suite (Bassini *et al.*, 2020; Rasia *et al.*, 2015). Overlaid as dashed white circles are the ACA+ALMA and MUSTANG-2 footprints. We note that the respective panels on the central column are scaled up arbitrarily with the goal of highlight any observed features, and do not reflect the relative angular sizes of the fields. For all cases, we consider an on-source time of 8 hours. The mock AtLAST and MUSTANG-2 observations are generated using the *maria* simulation tool (see van Marrewijk *et al.*, 2024 for details), assuming an AtLAST setup with the minimal detector counts of 50,000 (Section 4.2). For ACA+ALMA, we employ the *simobserve* task part of the Common Astronomy Software Applications (CASA; CASA Team, 2022).



2019). Nevertheless, motivated by the expected coverage of the  $\lesssim 30$  GHz range by future radio facilities (e.g. SKA, ngVLA), we decide do not include the synchrotron-specific 20 GHz band. On the other hand, given the centrality of the high-frequency ( $\gtrsim 500$  GHz) for maximizing AtLAST's capability of separating different SZ components and the signal from contaminating sources (see Section 4.3), we extend the overall spectral coverage beyond 300 GHz to include four additional bands up to 900 GHz. Compared to FYST's choice of survey bands (CCAT-Prime Collaboration, 2023), our choice will allow one to better sample the high-frequency end of AtLAST's spectral range and, in turn, to gain a better handle on the relativistic SZ effect and on the dust contamination (Figure 9; we further refer to van Kampen *et al.*, 2024 for a direct comparison of the large-scale distribution of submillimeter bright sources observed by the arcminute-resolution ACT and AtLAST). Currently, we are investigating the possibility of integrating an additional band covering the  $\sim 500$  GHz atmospheric window, but the low transmission and limited fractional bandwidth are expected to limit the effectiveness of such an addition in terms of an increase of the overall SZ sensitivity. However, we emphasize that AtLAST coverage of the ALMA Band 8 frequencies up to  $\nu = 492$  GHz would be fundamental for other application in the context of AtLAST science. We refer the interested readers to the companion AtLAST case studies by Lee *et al.* (2024) and Liu *et al.* (2024).

#### 4.2 Survey strategy and detector requirements

To obtain a straightforward estimate of the instrumental performance expected when adopting the proposed spectral setup,

we extend the analysis performed by Raghunathan (2022) to simulate an AtLAST-like facility (we refer to the aforementioned paper for technical details). As broadly discussed in the previous sections, performing a clean and robust separation of the multiple spectral components determining the millimeter/submillimeter sky will represent the major observational challenge to the achievement of the proposed SZ science goals. This will inherently result in more or less severe residual noise, as a combination of any contributions from instrumental noise, galactic foregrounds and extragalactic backgrounds are not properly accounted for the separation. As such, it represents a limiting factor in the detectability of any SZ signal and could be interpreted as the final SZ depth of the proposed observations.

In Figure 10 we present the result of an optimal internal linear combination of simulated multi-frequency AtLAST maps when adopting a wide-field survey strategy over a period of 5 years. The proposed spectral configuration will in particular allow for reaching a lower mass limit almost a factor of  $2\times$  lower than achievable with CMB-HD (Sehgal *et al.*, 2019), a reference next-generation CMB facility in terms of proposed survey depth, and with better angular resolution. This implies that AtLAST will be able to probe the SZ signal to Compton  $y$  levels  $\lesssim 5\times 10^{-7}$  over an extreme dynamic range of spatial scales when considering a deep survey approach ( $< 4000$  deg<sup>2</sup>). Targeted observations will allow us to reach a beam-level Compton  $y$  depth of  $\sim 2\times 10^{-6}$  per hour of integration time. Previous studies (e.g., Dolag *et al.*, 2016; Raghunathan, 2022) have predicted a Compton  $y$  confusion floor of

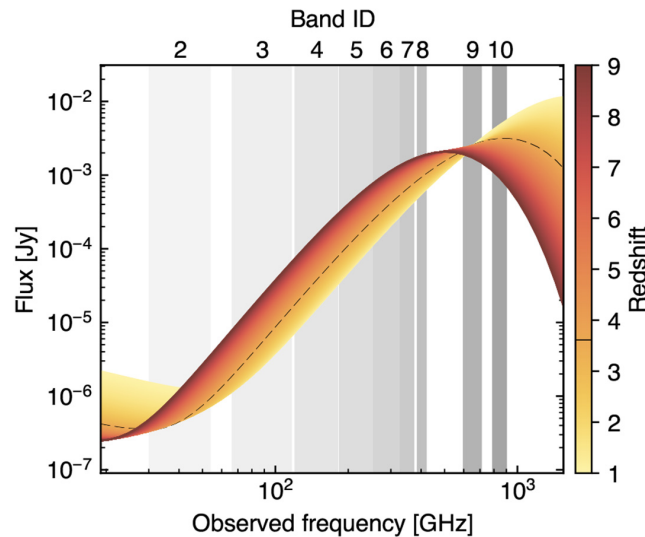


**Figure 9. The high-frequency bands (Band 8–10) will be crucial for optimally sampling the peak of the dust continuum emission from individual high- $z$  background galaxies.** Along with inferring the physical properties of their dust content, this will be crucial for minimizing the contamination of the SZ signal due to cospatial dusty components (see also Section 4.3). As a reference, we show here model emission for star-forming galaxies at varying redshift. Here, the dust contribution is based on the  $z$ -dependent dust temperature model from Sommovigo *et al.* (2022) for a dust mass  $M_d = 10^8 M_\odot$  (consistent with the galaxy REBELS sample; Bouwens *et al.*, 2022). The low-frequency radio component reproduces the radio model from Delvecchio *et al.* (2021), assuming an infrared-to-radio luminosity ratio of  $q_{IR} = 2.646$ . The dashed line denotes the lowest redshift at which the dust emission peak falls within the AtLAST spectral range ( $z \approx 3.60$ ).

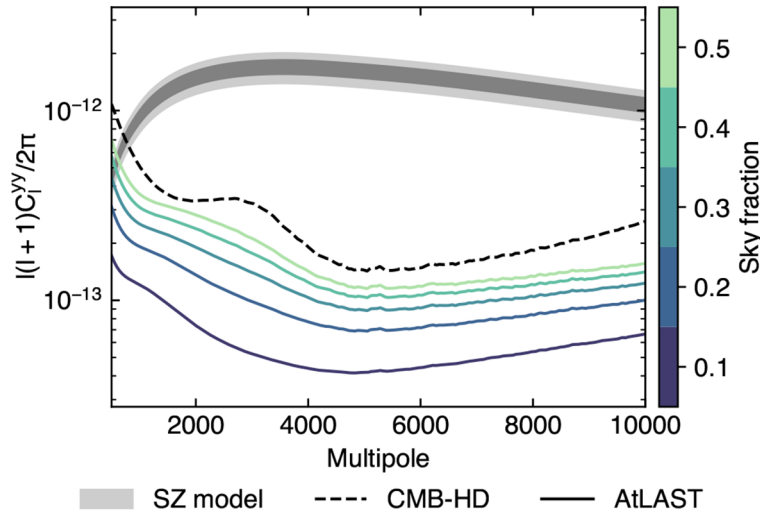


**Figure 10.** Residual Compton- $\gamma$  noise power spectra as a function of the sky coverage ( $f_{\text{sky}}$ ) in the case of a wide-field AtLAST survey (adapted from Raghunathan *et al.*, 2022, which we refer to for details). We include as a reference the residual noise curve expected in the case of the CMB-HD survey (Sehgal *et al.*, 2019). The shaded band denotes the power spectrum for a fiducial thermal SZ sky as extracted from the BAHAMAS simulations (McCarthy *et al.*, 2017), with  $1\sigma$  and  $2\sigma$  credible intervals based on George *et al.* (2015).

$2\text{--}5 \times 10^{-7}$  from  $< 10^{13} M_{\odot}$  haloes (corresponding to predicted detection threshold for AtLAST). As such, the estimated sensitivity imply that AtLAST will obtain SZ confusion limited observations in  $\sim 100$  h with single-pointing strategy. Nevertheless, we note that this sensitivity estimate corresponds to the residual Compton  $\gamma$  root-mean-square noise obtained when applying a constrained internal linear combination procedure to a simple set of mock AtLAST observations. In particular, we generate flat-sky sky realizations at the AtLAST bands including Galactic foregrounds and extragalactic background. The foreground model is based on the `pysm3` models (Thorne *et al.*, 2017), but the code was ported and adapted to extend the stochastic components down to arcsecond scales. The output mock realization comprises the dust (`d11` model), AME (default), free-free (default) and synchrotron (`s6`) from the Milky Way. The background signal is composed by a random CMB realization, as well as infrared and radio background from unresolved sources as extracted from the SIDES (Béthermin *et al.*, 2017) and RadioWeb-Sky simulations (Li *et al.*, 2022), respectively. To reproduce a clean subtraction of any dominant contaminating compact sources, we excluded all the radio and infrared components with fluxes in at least two bands larger than  $3\times$  the corresponding noise root-mean-square. As such, it should be considered as a rough ground reference for the actual depth achievable with future AtLAST measurements. Future forecasting studies will particularly investigate how different observation strategies, source subtraction, and modeling techniques will affect the contamination mitigation and the effective SZ sensitivity.

Still, achieving such frontier capabilities will necessarily demand a considerable mapping speed and, thus, a crucial effort in the optimization of the detector array. To estimate a minimal detector count for filling the focal plane, we

consider the sensitivity estimates reported in Table 1 as target depths for surveys with varying observing period and sky coverage (see Figure 5). The results are reported in Figure 11. A detector count  $n_{\text{det}} \simeq 5 \times 10^4$  is sufficient for achieving the sensitivity goal in the case of a narrow survey configuration ( $1000 \text{ deg}^2$ ) both in Band 2 and Band 3, key for tracing the decrement regime of the thermal SZ signal. For the same bands, the same  $n_{\text{det}}$  constraints would allow to achieve a similar survey sensitivity also in the intermediate  $4000 \text{ deg}^2$  case over  $\sim 4\text{--}5$  years. Nevertheless, extending these considerations to other bands or a wide-field scenario would require a significant increase in  $n_{\text{det}}$ . For instance, in the case of Band 5—crucial for constraining the departures from the thermal SZ effect due to kinetic and relativistic contributions—such a boost would range over almost an order of magnitude.

As broadly highlighted in Section 2, constraining the small-scale fluctuations in the thermal and kinetic SZ effects, while tracing the temperature-dependent relativistic SZ corrections would imply measuring deviations from the global SZ distribution order of magnitudes smaller than the bulk, non-relativistic thermal SZ signal. This would in turn require a significant reduction of any systematic effects hampering the overall calibration accuracy. In this regard, an interesting technical aspect of AtLAST is the plan for closed-loop metrology for tracking the alignment of the primary mirror panels (see, e.g., Mroczkowski *et al.*, 2024; Reichert *et al.* in prep.). By using active, closedloop metrology such as the laser system currently being developed for the Sardinia Radio Telescope (Attoli *et al.*, 2023) or the wavefront sensing system being developed on the Nobeyama Radio Observatory 45-m (Nakano *et al.*, 2022; Tamura *et al.*, 2020) the errors in the beam can be kept down to sub-percent levels, meaning the beam will be diffraction limited and stable throughout observations. This in

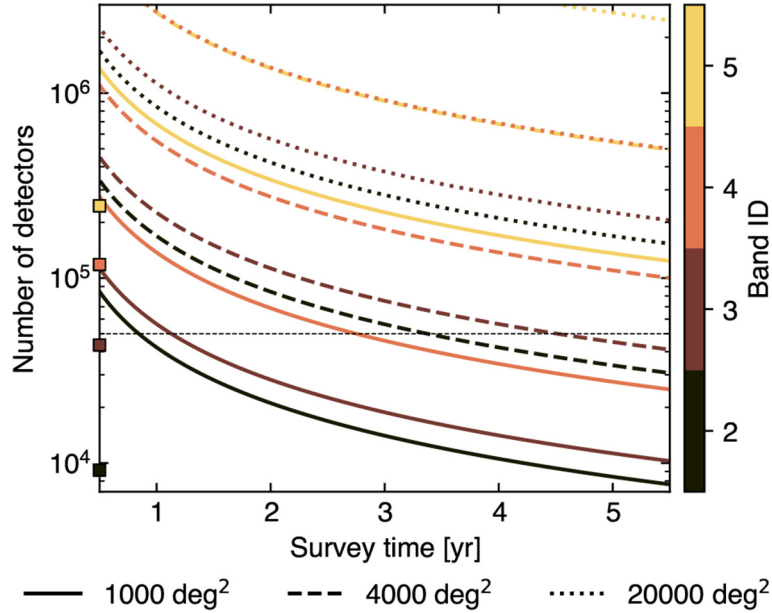


**Figure 11.** Required number of detectors to reach the target sensitivity estimates listed in Table 1 for different bands and considering different survey strategies. For comparison, the squares on the ordinate marks the detector counts required in each band for fully covering a  $1 \text{ deg}^2$  field of view. The horizontal line traces the minimal number of detectors (50,000) identified for reaching the target depth in Band 2 and 3 in the case of  $1000 \text{ deg}^2$  and  $4000 \text{ deg}^2$  surveys. We note that this is consistent with the estimated specifications reported in the *AtLAST Memo 4* for the 1<sup>st</sup> generation instruments.

turn will improve the calibration accuracy and reduce systematics (see, e.g., [Naess et al., 2020](#) for discussion of the diurnal effects on the ACT beams) that have been shown to impact CMB and SZ results at the several percent level in the case of passive optics (3 – 5%; [Hasselfield et al., 2013](#); [Lungu et al., 2022](#)), with the result that the daytime data have generally been excluded from cosmological analyses. Future dedicated forecasts will analyze the benefits of metrology for secondary CMB measurements using AtLAST, including improvements to the calibration, reduction of systematics, and the ability to recover larger angular scales on sky. However, the salient takeaway message is that uncertainties in the beam should no longer be a leading source of systematic error.

#### 4.3 Mock reconstruction of the relativistic SZ effect

The relative amplitude of the relativistic component compared to the thermal and kinetic SZ effects makes this modeling task highly challenging. To test the prospects of using AtLAST measurements for performing a spectral separation and analysis of the SZ effect, we thus perform a mock reconstruction of the intracluster temperature using the relativistic SZ effect.

**4.3.1 SZ-only reconstruction.** As a test case, we consider a galaxy cluster with temperature  $T_{\text{SZ}} = 10 \text{ keV}$  and Compton  $y = 10^{-4}$ . We note that, despite representing relatively extreme (but realistic) values, the setup  $(T_{\text{SZ}}, y) = (10 \text{ keV}, 10^{-4})$  is chosen to facilitate this first study of the AtLAST capabilities of providing spectral constraints on temperature-dependent distortions of the thermal SZ effect. A broader exploration of the parameter

space will be presented in [Section 4.3.3](#). The amplitude of the SZ signal at each of the selected bands in the minimal spectral set is obtained by integrating the relativistically-corrected thermal SZ (rtSZ) spectrum across each band assuming flat bandpasses. We then obtained estimates for the corresponding uncertainties based on the sensitivity estimates from the AtLAST sensitivity calculator. First, we compute the integration time required to achieve a signal-to-noise (SNR) of 50 in Band 8, arbitrarily chosen among the two spectral windows closest to the peak in the rtSZ effect ([Figure 2](#) & [Figure 12](#)). The resulting noise root-mean-square (RMS) is defined as the corresponding uncertainty. The uncertainties  $\delta I$  for each of the remaining bands are thus computed assuming the same integration time as for the Band 8 estimation above, but taking into account both the differing point-source sensitivities and beam sizes across frequency bands,

$$\frac{\delta I(n)}{\delta I(8)} = \frac{\sigma(n)}{\sigma(8)} \times \frac{\Omega(8)}{\Omega(n)}. \quad (1)$$

Here,  $n$  denotes the band index ( $n = \{2, \dots, 10\}$ ), while  $\sigma$  and  $\Omega(\nu)$  are the flux density RMS and the beam size at a given frequency  $\nu$ , respectively. The resulting simulated measurements are shown in [Figure 12](#).

The derived SZ measurements can then be used to perform a simple joint inference of the Compton  $y$  and electron temperature for the target case. If only lower-frequency data points ( $\lesssim 200 \text{ GHz}$ ) are measured, then there is a complete

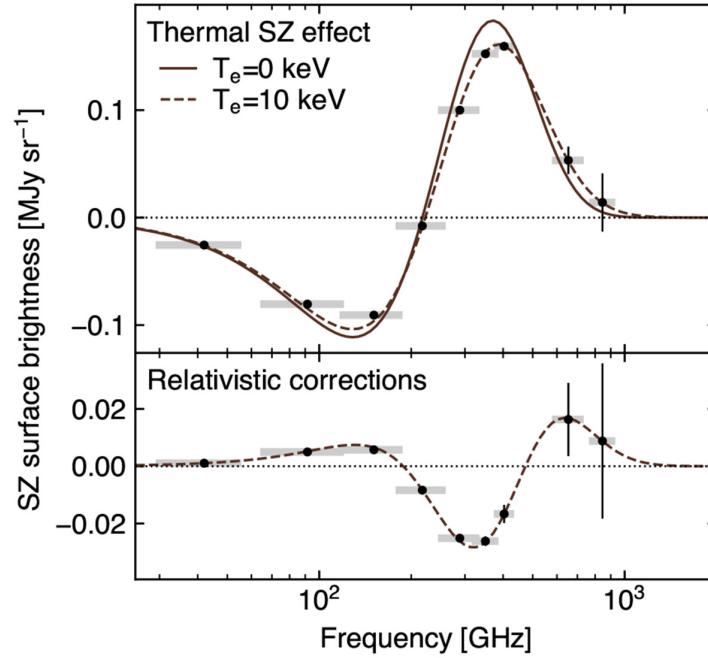


**Figure 12.** Predicted rtSZ measurements for a cluster with a temperature of 10 keV and Compton  $y$  of  $10^{-4}$ , assuming flat bandpasses in the Bands 2–10 (denoted as gray bands; see also Table 1). We assume the same exposure time in each band and account for flux sensitivity and beam size differences, tuned to achieve a SNR = 50 in Band 8. For comparison, the non-relativistic approximation is also shown. The bottom axis shows the difference between the relativistic and non-relativistic spectra.

degeneracy between  $T_e$  and the Compton  $y$  parameter. In this spectral range, in fact, an increase in the electron temperature reduces the signal in a similar manner as decreasing the overall Compton  $y$  amplitude. When higher-frequency points are included, the degeneracy can be minimized as shown in Figure 13. By dropping one band at a time from the fit, we find that Band 6 ( $\approx 240$  GHz) has the greatest influence in breaking the degeneracy since the signal-to-noise on the difference between nearly-degenerate models is greatest in this band.

**4.3.2 SZ+dust reconstruction.** So far, we have assumed that the only signal present is the SZ signal. However, in reality there will of course be other astrophysical foregrounds and backgrounds present along the line of sight, resulting in non-negligible contamination of the overall SZ signal observed in the direction of a galaxy cluster. In this test, we however assume that signals that are not spatially correlated to the SZ effect can be removed by means of component separation methods (see Section 4.2) or targeted forward modeling procedures in the case of unresolved compact sources (e.g., Andreon *et al.*, 2021; Di Mascolo *et al.*, 2019a; K eruzor e *et al.*, 2020; Kitayama *et al.*, 2020; Ruppig *et al.*, 2017). However, previous studies (e.g. Erler *et al.*, 2018) showed that there is a spatially correlated signal within clusters associated with the diffuse dust emission. To understand the impact on the capability of AtLAST in constraining any rtSZ deviation, we repeat the

above test by adding an additional dust-like spectral component (Figure 14). In particular, we assume a modified black body signal given by (Erler *et al.*, 2018)

$$I_{\text{Dust}}(\nu) = A_{\text{dust}}^{857} \left( \frac{\nu}{\nu_0} \right)^{\beta_{\text{Dust}}+3} \frac{\exp\left[ \frac{h\nu_0}{k_B T_{\text{Dust}}} \right] - 1}{\exp\left[ \frac{h\nu}{k_B T_{\text{Dust}}} \right] - 1}, \quad (2)$$

where  $\nu_0 = 857$  GHz is chosen as the reference frequency, and  $A_{\text{dust}}^{857}$  is the amplitude at this frequency. We use the (Erler *et al.*, 2018) parameter fits for  $A_{\text{dust}}^{857}$ ,  $\beta_{\text{Dust}}$  and  $T_{\text{Dust}}$  to generate a dust signal, and add them as free parameters to our fit with uniform priors on all parameters. The uncertainties on the measurements in each band are the same as in the SZ-only fit (Section 4.3.1)

In this case, more bands become necessary to correctly constrain the rtSZ temperature and disentangle the rtSZ and dust spectral components. The best minimal combination comprises Bands 2, 4, 6, 8 and 10, that provide almost identical constraints to the full set of bands on the rtSZ parameters, while achieving a lower precision on the dust parameters (as shown in Figure 15). Most importantly, it is important to note that the broad spectral coverage offered by the proposed setup allows a clean separation of the rtSZ and dust signals with only a marginal impact on the rtSZ constraints compared to the SZ-only case (Section 4.3.1).

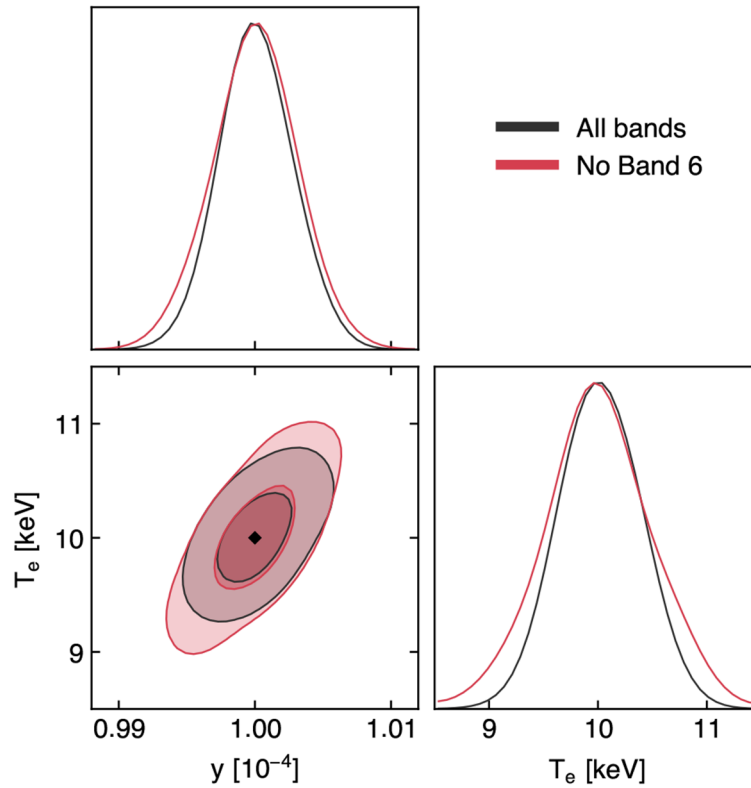


**Figure 13.** Fits to the simulated measurements shown in Figure 12, using all bands (grey) and all except Band 6 (red). Excluding Band 6 increases the  $y$ - $T_e$  degeneracy substantially. The black diamond denotes the input parameters.

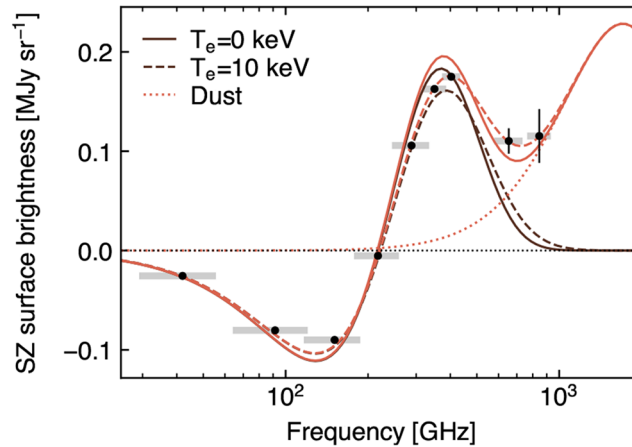


**Figure 14.** Same as Figure 12, but with the addition of a modified black body dust component based on the model from Erler *et al.* (2018). The red dotted line shows the dust signal. The red solid and dashed lines show the total signal from the dust and non-relativistic and relativistic signals respectively.

**4.3.3 Required sensitivity and time forecasts.** The reference SNR of 50 employed above was mainly intended to achieve a general perspective on the spectral constraining power of the proposed setup without being limited by the inherent significance of the test SZ signal. Thus, we now investigate what SNR is required to achieve good temperature constraints

from rSZ measurements. In particular, we run similar fits for different values of the reference SNR and different temperatures.

The impact of the varying SNR on the temperature reconstruction is summarized in Figure 16. If we require, for example, an

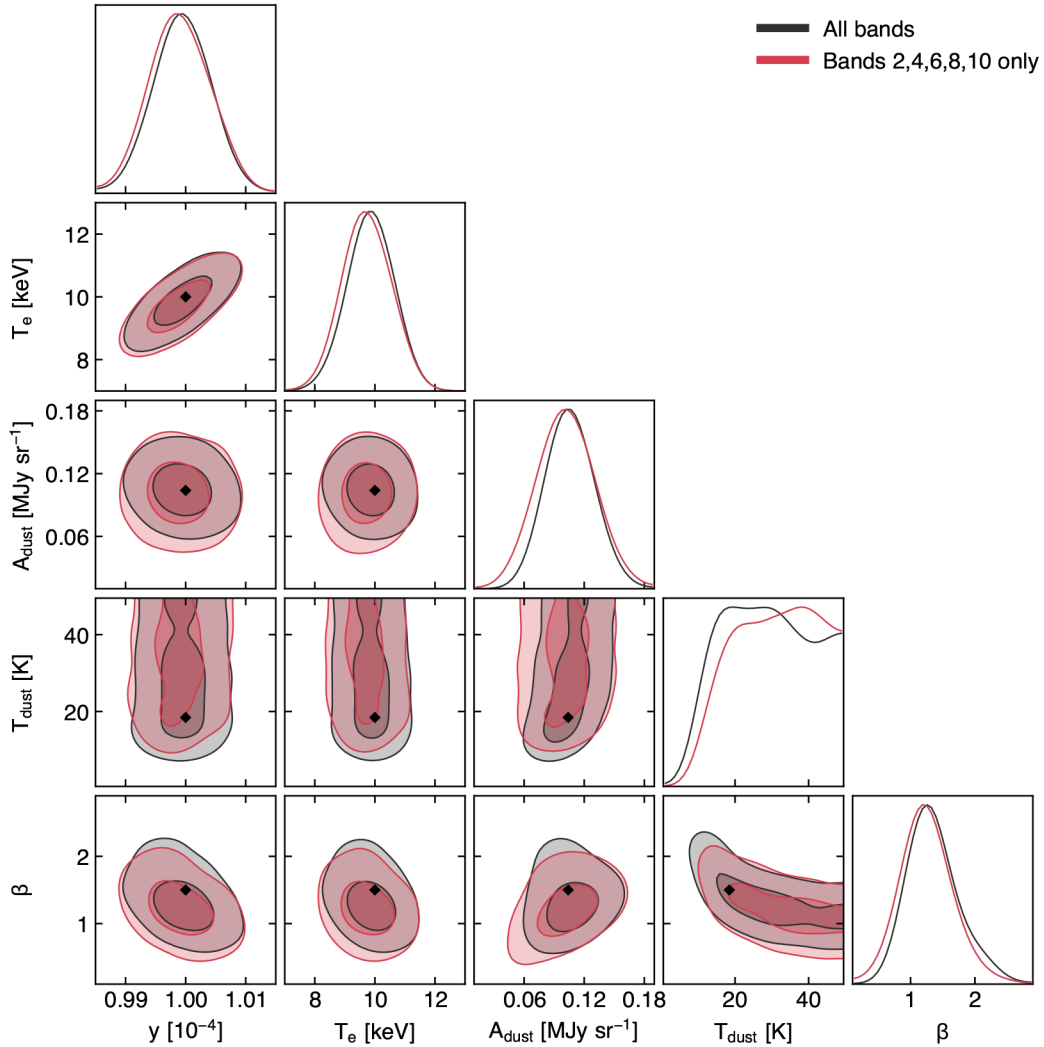


**Figure 15.** Fits to the simulated measurements shown in Figure 14, using all bands (grey) and Bands 2, 4, 6, 8 and 10 only (blue). With this optimal set of five bands, the constraints on the rtSZ parameters are almost equivalent to the constraints with all bands, but we obtain a slightly reduced constraining power on the dust parameters. The dotted diamonds denote the input parameters.

accuracy of 1 keV in temperature, a reference SNR of 40 is sufficient for all the temperatures tested. A reference SNR of 30 is instead sufficient for all except the very hottest clusters when dust is included.

Although AtLAST will be able to observe clusters spanning a broad range in mass and redshift (and, hence, temperature), the example analysis presented in the previous section is aimed only at forecasting AtLAST capabilities of measuring relativistic deviations from the standard thermal SZ and not at testing the expected detection threshold as a function of cluster properties. To take into account the evolution of the rtSZ effect with the mass and redshift of a galaxy cluster, we aim here at estimating the required observing time to reach a target SNR in Band 8, our reference spectral window (Section 4.3.1).

To do so, we construct cluster signal maps for a range of masses and redshifts, using the physical model given in Olamaie *et al.* (2012) and Javid *et al.* (2019). Assuming hydrostatic equilibrium, this model gives us physically consistent pressure and temperature profiles which we use with the SZPACK (Chluba *et al.*, 2012; Chluba *et al.*, 2013) temperature-moment method to predict relativistic SZ effect signal maps, taking into account the spatial variation of the temperature. The resulting observing time predictions for a reference SNR of 30 are shown in Figure 17. For reasonable observing times (< 16 hours) we can get average temperature constraints for most clusters at redshifts up to  $z \approx 0.1$ , and high-mass clusters ( $M_{200} \gtrsim 4 \times 10^{14} M_{\odot}$ ) up to arbitrarily high redshift. It is important to note that the enhanced angular resolution of AtLAST could easily allow one to obtain spatially resolved information

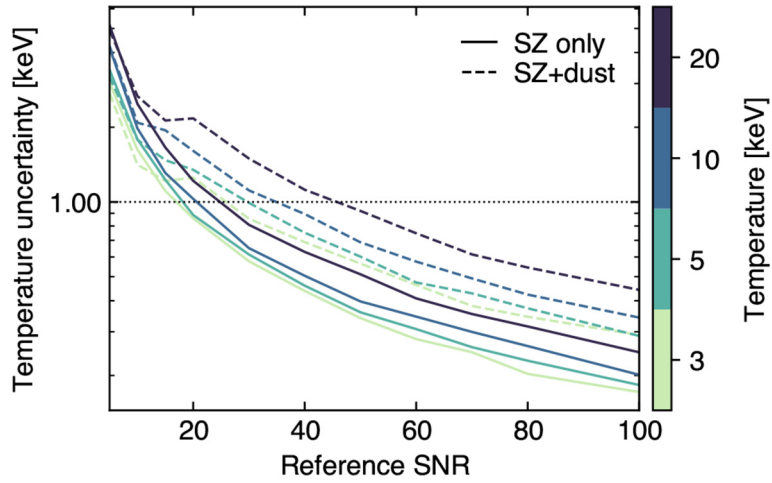


**Figure 16.** Precision achieved on the temperature reconstruction as a function of the SNR in the reference band (384–422 GHz; Band 8) and for a range of ICM temperatures. The horizontal line denotes the target temperature  $T_{\text{SZ}} = 1$  keV discussed in the text.

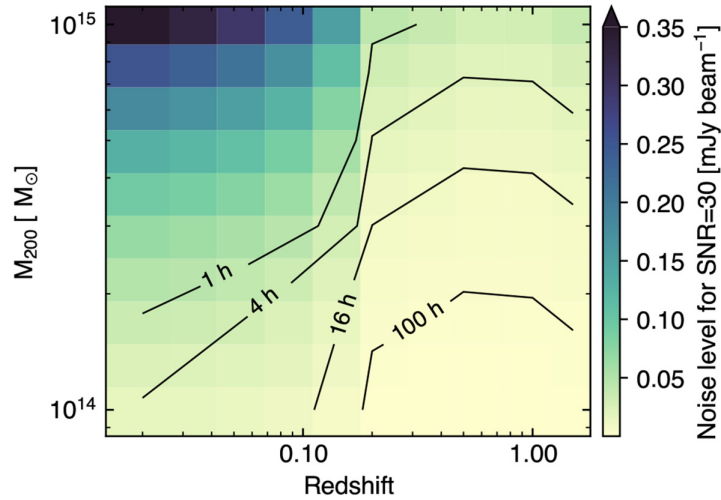


**Figure 17.** Beam-level noise root-mean-square and observing times as a function of cluster redshift and mass  $M_{200}$  required to reach an SNR of 30 in the reference spectral band (384–422 GHz; Band 8), allowing average SZ temperatures to be well constrained.

on the temperature distribution, once the SNR requirements are satisfied for each spatial element considered for the analysis — e.g., radial bins or spectrally homogeneous regions as generally considered in high-resolution X-ray studies (e.g., Sanders, 2006).

### 5 AtLAST SZ studies in a multi-probe context

AtLAST will provide an unprecedented speed and spectral grasp across the (sub)millimeter spectrum. This will make AtLAST inherently relevant beyond just SZ science, and will open up possibilities for fundamental synergies in the a multi-wavelength and multi-probe exploration of the Universe.

### 5.1 AtLAST scientific cross-synergies

Thanks to the novel multi-instrument design (Mroczkowski *et al.*, 2024), AtLAST will be aimed at representing a high-impact (sub)millimeter facility with a broad and varied scientific reach. As such, this will set the ground for a natural cross-synergy across the different scientific applications identified as part of the AtLAST Science Development effort.

In the case of a wide-field continuum survey discussed Section 4.2, the multi-band coverage and the extended temporal span will make the SZ-driven observations extremely

valuable for temporally-dependent studies as for transient surveys (Orlowski-Scherer *et al.* in prep.). Similarly, the multiple bands and likely polarization sensitivity will be useful in the study of Galactic dust and molecular clouds (Klaassen *et al.*, 2024), building on the lower resolution results with, for example, the Simons Observatory (Hensley *et al.*, 2022).

Related to the science goals proposed in this work, the availability of a wide-field spectroscopic survey of the distant Universe (van Kampen *et al.*, 2024) will immediately enhance the validity of the SZ identification and study of high- $z$  clusters and protoclusters by providing accurate redshift information. The broad spectral coverage achieved thanks to the proposed multi-band setup will actually play a crucial role in maximizing the redshift domain. At the same time, as already mentioned in previous sections, having access simultaneously to constraints on the physical properties of large-scale environments via the SZ effect (Section 3.5) and on the associated galaxy populations (via the spectral characterization of their cold molecular gas and the inference of their dust content; see Figure 9) will represent an unprecedented opportunity in the context of galaxy-environment co-evolution studies.

Similarly, the information on the warm/hot component of galactic haloes will be essential for building a comprehensive picture of the diffuse and multi-phase CGM (Lee *et al.*, 2024). A combination of the novel perspective offered by AtLAST on the cold contribution with the tight measurements of the thermal and kinetic properties of such elusive haloes (Section 3.6) will represent the only way for shedding light on the many potential evolutionary routes of the elusive large-scale CGM.

## 5.2 Synergies with other state-of-the-art and forthcoming facilities

In the context of large scale structures, AtLAST's constraints on the multi-faceted SZ effect will be highly complementary to multi-wavelength information on the galaxy motions and distribution, the gravitational potentials of the systems, the X-ray emission, magnetic field structure, and the highly non-thermal and relativistic emission traced by radio emission. Below, we highlight some of the key facilities and experiments that provide the most synergy with AtLAST.

**5.2.1 Radio.** The radio waveband offers information that can complement and enhance many of the science cases outlined above, and next-generation instruments such as the Square Kilometer Array (SKA; Huynh & Lazio, 2013) and the next-generation Very Large Array (ngVLA; Selina *et al.*, 2018) will have the angular resolution and sensitivity required to provide it. On the one hand, getting a clear view of the resolved SZ effect and searching for intrinsic scatter and surface brightness fluctuations requires sensitive detection and removal of contaminating radio sources (e.g., Dicker *et al.*, 2021). While this will already be possible with AtLAST's data itself thanks to its spectral coverage and  $\approx 5''\lambda$  mm<sup>-1</sup> resolution (i.e. 10'' at 2 mm), interferometric observations at lower frequency (SKA-MID) will aid in pinpointing the location and morphology of the radio sources, while also being more

sensitive to fainter sources as most will be brighter at lower frequency.

On the other hand, radio information provides a powerful complementary probe of the astrophysics in the cluster, being sensitive to magnetic fields and populations of non-thermal electrons. The reference surveys proposed for the SKA (Prandoni & Seymour, 2015) predict the detection of  $\sim 1000$ s of radio halos with SKA1-LOW, out to redshifts of at least 0.6 and masses  $M_{500} > 10^{14} M_{\odot}$  (Cassano *et al.*, 2015; Ferrari *et al.*, 2015; see also, e.g., Knowles *et al.*, 2021, Knowles *et al.*, 2022, Duchesne *et al.*, 2024 for preliminary results from SKA precursors), along with potential first detections of the polarization of radio halos (Govoni *et al.*, 2015). This offers the opportunity not only to compare the detailed astrophysics of the thermal and non-thermal components of clusters, shedding light on the turbulent properties currently limiting the accuracy of mass estimation (see Section 3.1), but also to potentially discover new populations of clusters via their radio signals. When also observed by AtLAST, these populations will offer insight into the variation in cluster properties when selecting by different methods (see also Section 3.4). Faraday Rotation Measure observations of polarized sources behind galaxy clusters as well as studies of tailed radio galaxies *in* clusters will enable the study of cluster magnetic fields in unprecedented detail (Bonafede *et al.*, 2015; Johnston-Hollitt *et al.*, 2015a; Johnston-Hollitt *et al.*, 2015b), contributing to our astrophysical understanding and ability to make the realistic simulations crucial for interpreting observations.

Ultimately, the direct correlation of the SZ information with the spatial, spectral, and polarimetric properties of the multitude of radio structures observed in the direction of galaxy clusters will be essential for constraining the detailed mechanisms governing particle (re)acceleration within the ICM (van Weeren *et al.*, 2019). Specifically, there is mounting evidence that the non-thermal plasma observed in the form of (multi-scale) radio halos (e.g., Cuciti *et al.*, 2022; Gitti *et al.*, 2015) as well as intercluster bridges (e.g., Bonafede *et al.*, 2022; Botteon *et al.*, 2020b; Radiconi *et al.*, 2022) originates due to turbulent (re)acceleration (Brunetti & Lazarian, 2007; Brunetti & Jones, 2014; Cassano *et al.*, 2023; Eckert *et al.*, 2017). On the other hand, radio relics are connected to (re)acceleration at shock fronts (Akamatsu & Kawahara, 2013; Botteon *et al.*, 2020a; van Weeren *et al.*, 2017). While it is clear that cluster mergers are driving both processes (turbulence and shocks), our understanding of the physics of (re)acceleration in clusters is limited by two factors: (i) information about the distribution of gas motions in the ICM is currently sparse and usually inferred via indirect methods (for a review, see Simionescu *et al.*, 2019), and (ii) characterizing shocks in the low-density cluster outskirts, where radio relics are usually found, is very challenging. Detailed mapping of the thermal (sensitive to shocks) and kinetic (sensitive to gas motions) SZ signals throughout the volume of a large sample of galaxy clusters (potentially extending out into the cosmic web), and how these signals relate to features observed in the radio band, will be invaluable towards painting a clear picture of the connection



between large-scale structure assembly, magnetic field amplification, and cosmic ray acceleration.

Understanding the impact of AGN feedback, on the other hand, (Section 3.6) requires complementary observations of the AGN themselves. Gitti *et al.* (2015) finds that even with early SKA1 (50% sensitivity), all AGN with luminosity  $> 10^{23} \text{ W Hz}^{-1}$  can be detected up to  $z \leq 1$  with subarcsecond resolution, and the radio lobes thought to be responsible for carving out the X-ray cavities should be detectable in any medium – large mass cluster at any redshift in the SKA1-MID deep tier surveys. Moreover, SKA1-MID is predicted to detect intercluster filaments at around  $2.5 - 6\sigma$  (Giovannini *et al.*, 2015), providing information on their magnetic fields as a complement to the SZ information on their thermodynamic properties (Section 3.7).

At the top of the SKA frequency range, it will be possible to directly access thermal SZ information. Future extensions to the SKA-MID Phase 1 setup (with the integration of the high-frequency Band 6; we refer to the SKA Memo 20-01 for details) and the ones envisioned for SKA Phase 2 (2030+) will allow SKA to probe the low-frequency ( $\lesssim 24 \text{ GHz}$ ) domain of the SZ spectrum, less affected by kinetic and relativistic deviations than the range probed by AtLAST. In fact, Grainge *et al.* (2015) find that 1 hour of integration is sufficient for obtaining a  $14\sigma$  detection of the SZ effect from a  $M_{200} = 4 \times 10^{14} M_{\odot}$  cluster at  $z > 1$ . On the other hand, the clean perspective offered by AtLAST on the multiple SZ components will provide the means, e.g., for cleanly disentangling the SZ footprint of galaxy clusters from the faint, diffuse signal from mini- to cluster-scale radio haloes, large-scale relics, and back-/foreground and intracluster radio galaxies, enhancing their joint study.

**5.2.2 Millimeter/submillimeter.** Millimetric/submillimetric survey experiments like SO (Simons Observatory Collaboration, 2019) and its upgrades, CCAT-prime/FYST (CCAT-Prime Collaboration, 2023), upgrades to the South Pole Telescope (Anderson *et al.*, 2022), and ultimately CMB-S4 (Abazajian *et al.*, 2016) will cover roughly half the sky over the next few years to a decade, predominantly in the Southern sky. Along with past and current facilities, these however have  $\sim$  arcmin resolution, well-matched to the typical angular size of clusters in order to optimize their detection but not optimal for peering inside clusters to explore astrophysical effects (aside from few nearby exceptional clusters). Nevertheless, while limited to resolutions approximately  $8.33\times$  lower than AtLAST at the same frequencies, their data will provide robust constraints at large scales, lending itself naturally to joint map-making and data combination, as well as valuable source finders for deep AtLAST follow-up. On the other hand, AtLAST will be able to resolve any structures probed by these wide-field surveys, defining a natural and intrinsic synergy.

At still higher resolutions, ALMA will undergo a number of upgrades improving its bandwidth and sensitivity over the next decade. These upgrades are called the Wideband Sensitivity Upgrade (WSU; Carpenter *et al.*, 2023), which in the context of SZ science could deliver  $2 - 4\times$  ALMA's current

bandwidth. Wide field mapping capabilities are however not part of the key goals for the WSU, and it is unlikely ALMA will ever map more than a few tens of square arcminutes. Nevertheless, the improved sensitivity and bandwidth could allow for exploiting ALMA to complement AtLAST observations with a high spatial resolution view of astrophysics through detailed follow-up studies. At the same time, such observations will require AtLAST to recover more extended scales (see Section 4). The necessity of such a combination will however allow us to fully leverage the synergistic strengths of single-dish and interferometric facilities for gaining an unprecedented view of the hot baryonic content of the Universe, along with its multi-phase counterparts.

**5.2.3 Optical/infrared.** The *Euclid* mission (Euclid Collaboration *et al.*, 2022; Laureijs *et al.*, 2011) has recently started surveying the optical/infrared sky, and is expected to result in the identification of  $\gtrsim 10^5$  galaxy clusters and protoclusters across the entire cluster era ( $0 \lesssim z \lesssim 2$ ; Euclid Collaboration, 2019). Complemented with data from the Legacy Survey of Space and Time (LSST) survey by the forthcoming Vera C. Rubin Observatory (Ivezić *et al.*, 2019), these will represent a wealth of complementary constraints on the cluster and protocluster populations that will be essential for enhancing the scientific throughput of AtLAST in the context of SZ studies. The characterization of the weak lensing footprint of galaxy clusters and groups jointly with resolved information on the thermodynamics of their ICM will enable a thorough exploration of the many processes biasing our cluster mass estimates (Section 3.1). At the same time, the detailed characterization of the SZ signal from the vast number of weak-lensing selected systems (and, thus, with different selection effects than surveys relying on ICM properties) will allow for studying in detail the origin of the under-luminous clusters (Section 3.4). Similarly, AtLAST will provide an unprecedented view on the ICM forming within the wealth of high- $z$  galaxy overdensities that will be identified by *Euclid*/LSST, in turn providing an unbiased means for constraining the physical processes driving the thermalization of protoclusters complexes into the massive clusters we observe at  $z \lesssim 2$ .

More in general, the access to a rich set of imaging and spectroscopic measurements by wide-field surveys — *Euclid*, Rubin Observatory, and the next generation Nancy Grace Roman Space Telescope (Spergel *et al.*, 2015), SPHEREx (Doré *et al.*, 2014) — along with deep, targeted observation from high-resolution facilities — e.g., JWST (Gardner *et al.*, 2006), or the upcoming Extremely Large Telescope — will be greatly complemented by the resolved, wide perspective of AtLAST on the SZ Universe. Tracing the faint warm/hot backbone of large-scale structure (Section 3.7), as well as tightly correlating resolved thermodynamic constraints for the large-scale cluster environment with the physical properties of the galaxies embedded within them (Alberts & Noble, 2022; Boselli *et al.*, 2022) and the distribution of the more elusive intracluster light (Contini *et al.*, 2014), will be essential to shed light on their complex and dynamical co-evolution.

In addition, to facilitate precision cosmology studies with *Euclid*/LSST, it is imperative to gain a better understanding

of the impact of galactic processes on the redistribution of baryons over large scales. Different prescriptions of feedback employed in various cosmological simulations alter the predicted amplitude and scale dependence of the matter power spectra at separations under 10 Mpc on a level that is considerably larger than the statistical uncertainty expected from upcoming cosmology experiments (Chisari *et al.*, 2019; van Daalen *et al.*, 2020). Mapping the gaseous contents in the low-density outskirts of galaxy groups and WHIM filaments through sensitive AtLAST measurements will thus provide invaluable observational priors necessary to model baryonic feedback for survey cosmology.

**5.2.4 X-ray.** On the X-ray side, *Chandra* and *XMM-Newton*, launched in 1999 with CCDs capable of 0.5 – 5" spatial resolution, are still providing a reasonable thermodynamic mapping of the brightest regions of the collapsed structures up to redshift  $\sim 1.2$ . The *eROSITA* telescope (launched in 2019) has recently delivered the first release of its X-ray all-sky surveys (Merloni *et al.*, 2024) and new catalogs of cluster candidates up to redshift  $z \approx 1.3$  (Bulbul *et al.*, 2024). Still, the large point spread function ( $\sim 15''$ ) and the limited sensitivity does not allow for resolving the temperature structure of the ICM and any derived quantities (e.g., pressure, entropy, mass) with the exception of nearby and bright galaxy clusters (e.g., Ijcenkarevic *et al.*, 2022; Liu *et al.*, 2023; Sanders *et al.*, 2022; Whelan *et al.*, 2022).

The 5 eV spectral resolution of the *Resolve* microcalorimeter onboard *XRISM*, launched in September 2023, will soon enable the first systematic investigation of the gas kinematics in hot, X-ray bright galaxy clusters. However, these studies will be limited by the low ( $\sim 1.3'$ ) angular resolution, small field of view and effective area, especially at soft X-ray energies. This particularly hinders the study of less massive haloes (galaxy groups and CGM) and the mapping of extended cluster outskirts and WHIM filaments. Forthcoming space missions are expected to improve all these performances through the development of next-generation instruments with higher both spectral and spatial resolutions over a wider field of view and with a larger collecting area: *Athena* (expected to be adopted as a L-mission by ESA in 2027 for a launch in 2037) will outperform the current satellites thanks to the larger effective area by an order of magnitude with a spatial resolution better than 10 arcsecs; *LEM* (a proposed US Probe mission; Patnaude *et al.*, 2023) is designed to effectively map the thermodynamics and kinematics of the low-density CGM and WHIM using spectral imaging of soft X-ray line emission; *AXIS* (another US Probe proposal) will extend and enhance the science of sensitive, high angular resolution X-ray imaging.

The complementarity of SZ and X-ray measurements of the warm/hot content of cosmic large-scale structures has long represented a valuable asset for a cross-enhancement of the respective astrophysical information. The different dependence of these tracers on the physical properties of the ionized gas has been broadly exploited — from, e.g. obtaining tighter constraints on the thermodynamics of the hot gas in distant

clusters and cluster outskirts (e.g., Andreon *et al.*, 2021; Castagna & Andreon, 2020; Ghirardini *et al.*, 2019; Ghirardini *et al.*, 2021b; Lepore *et al.*, 2024; Ruppin *et al.*, 2021) and large-scale filaments (e.g., Akamatsu *et al.*, 2017; Hincks *et al.*, 2022; Planck Collaboration, 2013), to studying local deviations from particle and thermal equilibrium (e.g., Basu *et al.*, 2016; Di Mascolo *et al.*, 2019b; Sayers *et al.*, 2021), deriving detailed morphological models of the three-dimensional distribution of ionized gas (e.g., De Filippis *et al.*, 2005; Kim *et al.*, 2023; Limousin *et al.*, 2013; Sereno *et al.*, 2018; Umetsu *et al.*, 2015), or obtaining measurements of the Hubble–Lemaître parameter independently of more standard probes (e.g., Bonamente *et al.*, 2006; Kozmanyán *et al.*, 2019; Wan *et al.*, 2021).

The enhanced sensitivity, spatial resolution, and mapping speed of AtLAST for various flavors of the SZ effect, combined with the capabilities of next-generation X-ray facilities, will undoubtedly take these already existing synergies one leap further. On the other hand, the novel high spectral resolution imaging capabilities in the soft X-ray band (expected to become available in the next decade with, e.g., *LEM* and *Athena*) will give rise to new opportunities for complementary measurements with the SZ band. Namely, X-ray observations are primarily expected to map the line emission or absorption signals from *metals* in the diffuse, warm-hot gas permeating large-scale structure WHIM filaments or the low-mass haloes of individual  $L^*$  galaxies. The X-ray continuum emission from these targets will be swamped by the foreground continuum from our own Milky Way, and extremely difficult to probe (see, for instance, Kraft *et al.*, 2022). The ideal path to obtaining a full picture of the physical properties of this diffuse gas component of the cosmic web, therefore, is to combine diagnostics about the metal content (from X-ray line intensities), metal dynamics (from X-ray line widths and shifts), temperature (from X-ray line ratios and relativistic SZ terms) with the gas pressure cleanly measured through the thermal SZ signal. We can then solve for the gas density (knowing the pressure and temperature), and the gas metallicity (knowing the metal content and gas density). Taking this one step even further, by detecting the kinetic SZ signal from the same gas, it will be possible to compare the velocities of metal-poor (primordial) gas from the kinetic SZ measurements which may be different than the velocities of metals probed from the X-ray lines. This will provide truly groundbreaking information about the circulation of gas and metals in and out of galaxies, by offering the opportunity to map, for instance, metal-rich outflows driven by feedback, and metal-poor inflows driven by accretion from the cosmic web, leading to a revolution in our understanding of galaxy evolution.

## 6 Summary and conclusions

AtLAST will provide a transformational perspective on the SZ effect from the warm/hot gas in the Universe. The high angular resolution enabled by the 50-meter aperture, the extensive spectral coverage, and the extreme sensitivity swiftly achievable over wide areas of the (sub)millimeter sky will provide the unprecedented opportunity to measure the SZ signal over

an instantaneous high dynamic range of spatial scales (from few arcsecond to degree scales) and with an enhanced sensitivity ( $\lesssim 5 \times 10^{-7}$  Compton  $y$ ).

Such a combination of technical advances will allow us to constrain simultaneously the thermal, kinematic, and relativistic contribution to the SZ effect for a vast number of individual systems, ultimately opening a novel perspective on the evolution and thermodynamics of cosmic structures. Such an unmatched capability will provide the means for exploring key astrophysical issues in the context of cluster and galaxy evolution.

- By resolving the multi-faceted SZ footprint of galaxy clusters, low-mass groups, and protoclusters, it will be possible to trace the temporal evolution of their thermodynamic properties across (and beyond) the entire cluster era ( $z \lesssim 2$ ), over an unprecedented range in mass. The complementary information on the full spectrum of small-scale ICM perturbations that will be accessed thanks to AtLAST's superior resolution and sensitivity will thus allow us to build a complete picture of the many intertwined processes that make galaxy clusters deviate from the otherwise hydrostatic equilibrium and self-similar evolution. At the same time, we will be able to get a complete census of the cluster population, circumventing the inherent biases associated with current cluster selection strategies. Overall, such studies will allow AtLAST to be pivotal in firming the role of galaxy clusters as key cosmological probes.
- The possibility offered by AtLAST of accessing the low-surface brightness regime will open an SZ window on the low-density warm/hot gas within the cosmic large-scale structure — ranging from the characterization of the mostly unexplored properties of the assembling ICM seeds within protocluster overdensities to the barely bound outskirts of galaxy clusters. These represent the environments where the same process of virialization begins. As such, they are ideal for studying how deviations from thermalization, gas accretion, and strong dynamical processes impact the thermal history of galaxy clusters.
- By tracing the imprint on the thermodynamics properties of circumgalactic medium surrounding galaxies and of the cluster cores, AtLAST will allow to constraint energetics and physical details of AGN feedback. This will provide the means for moving a fundamental step forward in our understanding of the crucial impact of AGN on the evolution of the warm/hot component of cosmic structures over a wide range of spatial scales and across cosmic history.

To achieve these ambitious goals, it will be essential to satisfy the following technical requirements:

- **Degree-scale field of view.** The superior angular resolution achievable thanks to the 50-meter aperture planned for AtLAST will need to be complemented by the capability of effectively recovering degree-level large

scales. Such a requirement is motivated by the aim of mapping the SZ signal from at low or intermediate redshift astrophysical sources that are inherently extended on large scales (e.g., intercluster filaments) and with diffuse signals (e.g., protocluster overdensities). At the same time, we aim at performing a deep ( $\sim 10^{-7}$  Compton  $y$ ) and wide-field ( $> 1000 \text{ deg}^2$ ) SZ survey, key for effectively probing a varied sample of SZ sources. In turn, our requirement consists of an instantaneous field of view covering  $> 1 \text{ deg}^2$ . Clearly, combining wide-field capabilities with enhanced sensitivity will be highly demanding in terms of minimal detector counts. To reach the target sensitivities reported in Table 1, we forecast that the focal plane array should be filled by  $\gtrsim 50,000$  detectors.

- **Wide frequency coverage.** To perform a spectral inference of the multiple SZ components, along with their clean separation from foreground and background astrophysical contamination, it will be crucial to probe the spectral regime from 30 GHz up to 905 GHz with multi-band continuum observations. We specifically identify an overall set of nine spectral bands (centered at 42.0, 91.5, 151.0, 217.5, 288.5, 350.0, 403.0, 654.0, and 845.5 GHz), specifically selected to maximize the in-band sensitivity at fixed integration time. By testing this spectral configuration in the context of a mock spectral component separation, we demonstrated that such a choice allows for achieving a clean separation of multiple SZ components, as well as of the signal from dominant contamination sources.
- **Sub-percent beam accuracy.** An accurate calibration will be essential for reducing potential systematics in the small-amplitude fluctuations of the SZ signal associated with local pressure and velocity perturbations, or to relativistic distortions. As such, we require a sub-percent level control of the beam stability.

## Ethics and consent

Ethical approval and consent were not required.

## Data availability

No data are associated with this article.

## Software availability

The calculations used to derive integration times for this paper were done using the AtLAST sensitivity calculator (Klaassen, 2024), a deliverable of Horizon 2020 research project “Towards AtLAST”, and available from [this link](#).

## Acknowledgements

We thank William Coulton for useful insights on the CMB systematics and recovery of larger scales, and Matthieu Béthermin for the support with the analysis and processing of the SIDES simulations. We further thank Adam D. Hincks and the ACT collaboration for sharing the *Planck* and ACT SZ data for Abell 399–401.

## References

- Abazajian K, Addison G, Adshead P, et al.: **CMB-S4 science case, reference design, and project plan.** *arXiv e-prints*. 2019; arXiv:1907.04473.  
[Publisher Full Text](#)
- Abazajian KN, Adshead P, Ahmed Z, et al.: **CMB-S4 science book, first edition.** *arXiv e-prints*. 2016; arXiv:1610.02743.  
[Publisher Full Text](#)
- Abdulla Z, Carlstrom JE, Mantz AB, et al.: **Constraints on the thermal contents of the X-ray cavities of cluster MS 0735.6+7421 with Sunyaev-Zeldovich effect observations.** *Astron Astrophys J*. 2019; **871**(2): 195.  
[Publisher Full Text](#)
- Adam R, Adane A, Ade PAR, et al.: **The NIKA2 large-field-of-view millimetre continuum camera for the 30 m IRAM telescope.** *Astron Astrophys*. 2018; **609**: A115.  
[Publisher Full Text](#)
- Adam R, Bartalucci I, Pratt GW, et al.: **Mapping the kinetic Sunyaev-Zeldovich effect toward MACS J0717.5+3745 with NIKA.** *Astron Astrophys*. 2017; **598**: A115.  
[Publisher Full Text](#)
- Adam R, Comis B, Macías-Pérez JF, et al.: **First observation of the thermal Sunyaev-Zeldovich effect with Kinetic Inductance Detectors.** *Astron Astrophys*. 2014; **569**: A66.  
[Publisher Full Text](#)
- Akamatsu H, Fujita Y, Akahori T, et al.: **Properties of the cosmological filament between two clusters: a possible detection of a large-scale accretion shock by Suzaku.** *Astron Astrophys*. 2017; **606**: A1.  
[Publisher Full Text](#)
- Akamatsu H, Kawahara H: **Systematic X-ray analysis of radio relic clusters with Suzaku.** *Publ Astron Soc Jpn*. 2013; **65**(1): 16.  
[Publisher Full Text](#)
- Alberts S, Noble A: **From clusters to proto-clusters: the infrared perspective on environmental galaxy evolution.** *Universe*. 2022; **8**(11): 554.  
[Publisher Full Text](#)
- Altamura E, Kay ST, Chluba J, et al.: **Galaxy cluster rotation revealed in the MACSIS simulations with the kinetic Sunyaev-Zeldovich effect.** *Mon Not R Astron Soc*. 2023; **524**(2): 2262–2289.  
[Publisher Full Text](#)
- Amodeo S, Battaglia N, Schaaf E, et al.: **Atacama cosmology telescope: modeling the gas thermodynamics in BOSS CMASS galaxies from kinematic and thermal Sunyaev-Zeldovich measurements.** *Phys Rev D*. 2021; **103**(6): 063514.  
[Publisher Full Text](#)
- Anbajagane D, Chang C, Baxter EJ, et al.: **Cosmological shocks around galaxy clusters: a coherent investigation with DES, SPT, and ACT.** *Mon Not R Astron Soc*. 2024; **527**(3): 9378–9404.  
[Publisher Full Text](#)
- Anbajagane D, Chang C, Jain B, et al.: **Shocks in the stacked Sunyaev-Zeldovich profiles of clusters II: measurements from SPT-SZ + Planck Compton- $\gamma$  map.** *Mon Not R Astron Soc*. 2022; **514**(2): 1645–1663.  
[Publisher Full Text](#)
- Anderson AJ, Barry P, Bender AN, et al.: **SPT-3G+: mapping the high-frequency cosmic microwave background using Kinetic Inductance Detectors.** In: *Millimeter, Submillimeter, and Far-Infrared Detectors and Instrumentation for Astronomy XI*. 2022; **12190**: 1219003.  
[Publisher Full Text](#)
- Andreon S, Moretti A, Trinchieri G, et al.: **Why are some galaxy clusters underluminous? The very low concentration of the CL2015 mass profile.** *Astron Astrophys*. 2019; **630**: A78.  
[Publisher Full Text](#)
- Andreon S, Romero C, Aussel H, et al.: **Witnessing the Intracluster medium assembly at the cosmic noon in JKCS 041.** *Mon Not R Astron Soc*. 2023; **522**(3): 4301–4309.  
[Publisher Full Text](#)
- Andreon S, Romero C, Castagna F, et al.: **Thermodynamic evolution of the  $z = 1.75$  galaxy cluster IDCS J1426.5+3508.** *Mon Not R Astron Soc*. 2021; **505**(4): 5896–5909.  
[Publisher Full Text](#)
- Andreon S, Trinchieri G, Moretti A: **Low X-ray surface brightness clusters: implications on the scatter of the  $M-T$  and  $L-T$  relations.** *Mon Not R Astron Soc*. 2022; **511**(4): 4991–4998.  
[Publisher Full Text](#)
- Andreon S, Wang J, Trinchieri G, et al.: **Variagate galaxy cluster gas content: mean fraction, scatter, selection effects, and covariance with X-ray luminosity.** *Astron Astrophys*. 2017; **606**: A24.  
[Publisher Full Text](#)
- Angelinelli M, Vazza F, Giocoli C, et al.: **Turbulent pressure support and hydrostatic mass bias in the Intracluster Medium.** *Mon Not R Astron Soc*. 2020; **495**(1): 864–885.  
[Publisher Full Text](#)
- Ansarifard S, Rasia E, Biffi V, et al.: **The Three Hundred Project: correcting for the hydrostatic-equilibrium mass bias in X-ray and SZ surveys.** *Astron Astrophys*. 2020; **634**: A113.  
[Publisher Full Text](#)
- Arnaud M, Pratt GW, Piffaretti R, et al.: **The universal galaxy cluster pressure profile from a representative sample of nearby systems (REXCESS) and the  $Y_{5z} - M_{500}$  relation.** *Astron Astrophys*. 2010; **517**: A92.  
[Publisher Full Text](#)
- Attoli A, Poppi S, Buffa F, et al.: **The Sardinia Radio Telescope metrology system.** In: *2023 XXXVth General Assembly and Scientific Symposium of the International Union of Radio Science (URSI GASS)*. 2023; 135.  
[Publisher Full Text](#)
- Ayromlou M, Nelson D, Pillepich A, et al.: **An atlas of gas motions in the TNG-Cluster simulation: from cluster cores to the outskirts.** *arXiv e-prints*. 2023; arXiv:2311.06339.  
[Publisher Full Text](#)
- Bahcall NA, Cen R: **Galaxy clusters and Cold Dark Matter: a low-density unbiased universe?** *Astrophys J Lett*. 1992; **398**: L81.  
[Publisher Full Text](#)
- Baldi AS, De Petris M, Sembolini F, et al.: **Kinetic Sunyaev-Zeldovich effect in rotating galaxy clusters from MUSIC simulations.** *Mon Not R Astron Soc*. 2018; **479**(3): 4028–4040.  
[Publisher Full Text](#)
- Bartalesi T, Ettori S, Nipoti C: **Gas rotation and Dark Matter halo shape in cool-core clusters of galaxies.** *Astron Astrophys*. 2024; **682**: A31.  
[Publisher Full Text](#)
- Bassini L, Rasia E, Borgani S, et al.: **The DIANOGA simulations of galaxy clusters: characterising star formation in protoclusters.** *Astron Astrophys*. 2020; **642**: A37.  
[Publisher Full Text](#)
- Basu K, Sommer M, Emler J, et al.: **ALMA-SZ detection of a galaxy cluster merger shock at half the age of the universe.** *Astrophys J Lett*. 2016; **829**(2): L23.  
[Publisher Full Text](#)
- Battaglia N, Bond JR, Pfrommer C, et al.: **On the cluster physics of Sunyaev-Zeldovich and X-Ray surveys. I. The influence of feedback, non-thermal pressure, and cluster shapes on  $Y-M$  scaling relations.** *Astrophys J*. 2012; **758**(2): 74.  
[Publisher Full Text](#)
- Baxter EJ, Adhikari S, Vega-Ferrero J, et al.: **Shocks in the stacked Sunyaev-Zeldovich profiles of clusters – I. Analysis with the Three Hundred simulations.** *Mon Not R Astron Soc*. 2021; **508**(2): 1777–1787.  
[Publisher Full Text](#)
- Baxter EJ, Pandey S, Adhikari S, et al.: **The impact of halo concentration on the Sunyaev Zeldovich effect signal from massive galaxy clusters.** *Mon Not R Astron Soc*. 2024; **527**(3): 7847–7860.  
[Publisher Full Text](#)
- Baxter EJ, Sherwin BD, Raghunathan S: **Constraining the rotational kinematic Sunyaev-Zeldovich effect in massive galaxy clusters.** *J Cosmology Astropart Phys*. 2019; **2019**: 001.  
[Publisher Full Text](#)
- Bennett JS, Sijacki D: **A disturbing FABLE of mergers, feedback, turbulence, and mass biases in simulated galaxy clusters.** *Mon Not R Astron Soc*. 2022; **514**(1): 313–328.  
[Publisher Full Text](#)
- Bennett JS, Sijacki D, Costa T, et al.: **The growth of the gargantuan black holes powering high-redshift quasars and their impact on the formation of early galaxies and protoclusters.** *Mon Not R Astron Soc*. 2024; **527**(1): 1033–1054.  
[Publisher Full Text](#)
- Béthermin M, Wu HY, Lagache G, et al.: **The impact of clustering and angular resolution on far-infrared and millimeter continuum observations.** *Astron Astrophys*. 2017; **607**: A89.  
[Publisher Full Text](#)
- Bhattacharya S, Kosowsky A: **Cosmological constraints from galaxy cluster velocity statistics.** *Astrophys J*. 2007; **659**(2): L83.  
[Publisher Full Text](#)
- Bianchini F, Silvestri A: **Kinetic Sunyaev-Zeldovich effect in modified gravity.** *Phys Rev D*. 2016; **93**(6): 064026.  
[Publisher Full Text](#)
- Biffi V, Borgani S, Murante G, et al.: **On the nature of hydrostatic equilibrium in galaxy clusters.** *Astrophys J*. 2016; **827**(2): 112.  
[Publisher Full Text](#)
- Biffi V, Zuhone JA, Mroczkowski T, et al.: **The velocity structure of the intracluster medium during a major merger: simulated microcalorimeter observations.** *Astron Astrophys*. 2022; **663**: A76.  
[Publisher Full Text](#)
- Birkinshaw M: **The Sunyaev-Zeldovich effect.** *Phys Rep*. 1999; **310**(2–3): 97–195.  
[Publisher Full Text](#)
- Birkinshaw M, Gull SF, Hardebeck H: **The Sunyaev-Zeldovich effect towards three clusters of galaxies.** *Nature*. 1984; **309**: 34–35.  
[Publisher Full Text](#)
- Bleem LE, Bocquet S, Stalder B, et al.: **The SPTpol Extended Cluster Survey.**

- Astrophys J Suppl Ser.* 2020; **247**(1): 25.  
[Publisher Full Text](#)
- Bleem LE, Klein M, Abbott TMC, *et al.*: **Galaxy clusters discovered via the thermal Sunyaev-Zel'dovich effect in the 500-square-degree SPTpol survey.** *Open J Astrophys.* arXiv: 2311.07512. 2024; **7**.  
[Publisher Full Text](#)
- Bonafede A, Brunetti G, Rudnick L, *et al.*: **The Coma cluster at LOFAR frequencies. II. The halo, relic, and a new accretion relic.** *Astrophys J.* 2022; **933**(2): 218.  
[Publisher Full Text](#)
- Bonafede A, Vazza F, Brügger M, *et al.*: **Unravelling the origin of large-scale magnetic fields in galaxy clusters and beyond through Faraday Rotation Measures with the SKA.** In: *Advancing Astrophysics with the Square Kilometre Array (AASKA14)*. 2015; 95.  
[Publisher Full Text](#)
- Bonamente M, Joy MK, LaRoque SJ, *et al.*: **Determination of the cosmic distance scale from Sunyaev-Zel'dovich Effect and Chandra X-Ray measurements of high-redshift galaxy clusters.** *Astrophys J.* 2006; **647**(1): 25.  
[Publisher Full Text](#)
- Boselli A, Fossati M, Sun M: **Ram pressure stripping in high-density environments.** *Astron Astrophys Rev.* 2022; **30**(1): 3.  
[Publisher Full Text](#)
- Botteon A, Brunetti G, Ryu D, *et al.*: **Shock acceleration efficiency in radio relics.** *Astron Astrophys.* 2020a; **634**: A64.  
[Publisher Full Text](#)
- Botteon A, van Weeren RJ, Brunetti G, *et al.*: **A giant radio bridge connecting two galaxy clusters in Abell 1758.** *Mon Not R Astron Soc.* 2020b; **499**(1): L11–L15.  
[Publisher Full Text](#)
- Bouwens RJ, Smit R, Schouws S, *et al.*: **Reionization Era Bright Emission Line Survey: selection and characterization of luminous Interstellar Medium reservoirs in the  $z > 6.5$  universe.** *Astrophys J.* 2022; **931**(2): 160.  
[Publisher Full Text](#)
- Brodwin M, McDonald M, Gonzalez AH, *et al.*: **IDCS J1426.5+3508: the most massive galaxy cluster AT  $z > 1.5$ .** *Astrophys J.* 2016; **817**(2): 122.  
[Publisher Full Text](#)
- Brownson S, Maiolino R, Tazzari M, *et al.*: **Detecting the halo heating from AGN feedback with ALMA.** *Mon Not R Astron Soc.* 2019; **490**(4): 5134–5146.  
[Publisher Full Text](#)
- Brunetti G, Jones TW: **Cosmic rays in galaxy clusters and their nonthermal emission.** *Int J Mod Phys D.* 2014; **23**(4): 1430007.  
[Publisher Full Text](#)
- Brunetti G, Lazarian A: **Compressible turbulence in galaxy clusters: physics and stochastic particle re-acceleration.** *Mon Not R Astron Soc.* 2007; **378**(1): 245–275.  
[Publisher Full Text](#)
- Bryan S, Austermann J, Ferrusa D, *et al.*: **Optical design of the ToITeC millimeter-wave camera.** In: *Millimeter, Submillimeter, and Far-Infrared Detectors and Instrumentation for Astronomy IX*. 2018; **107080J**.  
[Publisher Full Text](#)
- Bulbul E, Liu A, Kluge M, *et al.*: **The SRG/eROSITA all-sky survey: the first catalog of galaxy clusters and groups in the western Galactic hemisphere.** arXiv: 2402.08452. 2024.  
[Publisher Full Text](#)
- Butler VL, Feder RM, Daylan T, *et al.*: **Measurement of the relativistic Sunyaev-Zeldovich correction in RX J1347. 5-1145.** *Astrophys J.* 2022; **932**(1): 55.  
[Publisher Full Text](#)
- Campitiello MG, Ettori S, Lovisari L, *et al.*: **CHEX-MATE: morphological analysis of the sample.** *Astron Astrophys.* 2022; **665**: A117.  
[Publisher Full Text](#)
- Cantalupo S, Pezzulli G, Lilly SJ, *et al.*: **The large- and small-scale properties of the intergalactic gas in the Slug Ly $\alpha$  nebula revealed by MUSE He II emission observations.** *Mon Not R Astron Soc.* 2019; **483**(4): 5188–5204.  
[Publisher Full Text](#)
- Carilli CL, Anderson CS, Tozzi P, *et al.*: **X-Ray emission from the jets and lobes of the Spiderweb.** *Astrophys J.* 2022; **928**(1): 59.  
[Publisher Full Text](#)
- Carlstrom JE, Ade PAR, Aird KA, *et al.*: **The 10 meter South Pole Telescope.** *Publ Astron Soc Pac.* 2011; **123**(903): 568.  
[Publisher Full Text](#)
- Carlstrom JE, Holder GP, Reese ED: **Cosmology with the Sunyaev-Zel'dovich Effect.** *Annu Rev Astron Astrophys.* 2002; **40**: 643.  
[Publisher Full Text](#)
- Carpenter J, Brogan C, Iono D, *et al.*: **The ALMA Wideband Sensitivity Upgrade.** In: *Dynamics and Chemistry of Star Formation: The Dynamical ISM Across Time and Spatial Scales*. 2023; 304.  
[Publisher Full Text](#)
- CASA Team: **CASA, the Common Astronomy Software Applications for radio astronomy.** *Publ Astron Soc Pac.* 2022; **134**(1041): 114501.  
[Publisher Full Text](#)
- Cassano R, Bernardi G, Brunetti G, *et al.*: **Cluster radio halos at the crossroads between astrophysics and cosmology in the SKA era.** In: *Advancing Astrophysics with the Square Kilometre Array (AASKA14)*. 2015; **73**.  
[Publisher Full Text](#)
- Cassano R, Cuciti V, Brunetti G, *et al.*: **The Planck clusters in the LOFAR sky: IV. LoTSS-DR2: Statistics of radio haloes and re-acceleration models.** *Astron Astrophys.* 2023; **672**: A43.  
[Publisher Full Text](#)
- Castagna F, Andreon S: **JoXSZ: joint X-SZ fitting code for galaxy clusters.** *Astron Astrophys.* 2020; **639**: A73.  
[Publisher Full Text](#)
- CCAT-Prime Collaboration: **CCAT-prime collaboration: science goals and forecasts with Prime-Cam on the Fred Young Submillimeter Telescope.** *Astrophys J Suppl Ser.* 2023; **264**(1): 7.  
[Publisher Full Text](#)
- Cen R, Ostriker JP: **Where are the baryons?** *Astrophys J.* 1999; **514**(1): 1.  
[Publisher Full Text](#)
- Chakraborty A, Chatterjee S, Lacy M, *et al.*: **Cosmological simulations of galaxy groups and clusters. III. Constraining quasar feedback models with the Atacama Large Millimeter Array.** *Astrophys J.* 2023; **954**(1): 8.  
[Publisher Full Text](#)
- CHEX-MATE Collaboration: **The Cluster HERitage project with XMM-Newton: mass assembly and thermodynamics at the endpoint of structure formation: I. Programme overview.** *Astron Astrophys.* 2021; **650**: A104.  
[Publisher Full Text](#)
- Chisari NE, Mead AJ, Joudaki S, *et al.*: **Modelling baryonic feedback for survey cosmology.** *Open J Astrophys.* 2019; **2**(1): 4.  
[Publisher Full Text](#)
- Chluba J, Nagai D, Sazonov S, *et al.*: **A fast and accurate method for computing the Sunyaev-Zel'dovich signal of hot galaxy clusters.** *Mon Not R Astron Soc.* 2012; **426**(1): 510–530.  
[Publisher Full Text](#)
- Chluba J, Switzer E, Nelson K, *et al.*: **Sunyaev-Zeldovich signal processing and temperature-velocity moment method for individual clusters.** *Mon Not R Astron Soc.* 2013; **430**(4): 3054–3069.  
[Publisher Full Text](#)
- Churazov E, Vikhlinin A, Sunyaev R: **(No) dimming of X-ray clusters beyond  $z \sim 1$  at fixed mass: crude redshifts and masses from raw X-ray and SZ data.** *Mon Not R Astron Soc.* 2015; **450**(2): 1984–1989.  
[Publisher Full Text](#)
- Contini E, De Lucia G, Villalobos Á, *et al.*: **On the formation and physical properties of the intracluster light in hierarchical galaxy formation models.** *Mon Not R Astron Soc.* 2014; **437**(4): 3787–3802.  
[Publisher Full Text](#)
- Cooray A, Chen X: **Kinetic Sunyaev-Zeldovich effect from halo rotation.** *Astrophys J.* 2002; **573**(1): 43.  
[Publisher Full Text](#)
- Coulton WR, Schutt T, Maniyar AS, *et al.*: **The Atacama Cosmology Telescope: detection of patchy screening of the cosmic microwave background.** arXiv: 2401.13033. 2024.  
[Publisher Full Text](#)
- Crichton D, Gralla MB, Hall K, *et al.*: **Evidence for the thermal Sunyaev-Zel'dovich effect associated with quasar feedback.** *Mon Not R Astron Soc.* 2016; **458**(2): 1478–1492.  
[Publisher Full Text](#)
- Cuciti V, de Gasperin F, Brügger M, *et al.*: **Galaxy clusters enveloped by vast volumes of relativistic electrons.** *Nature.* 2022; **609**(7929): 911–914.  
[PubMed Abstract](#) | [Publisher Full Text](#) | [Free Full Text](#)
- Das S, Chiang YK, Mathur S: **Detection of thermal Sunyaev-Zel'dovich effect in the circumgalactic medium of lowmass galaxies—a surprising pattern in self-similarity and baryon sufficiency.** *Astrophys J.* 2023; **951**(2): 125.  
[Publisher Full Text](#)
- De Filippis E, Sereno M, Bautz MW, *et al.*: **Measuring the three-dimensional structure of galaxy clusters. I. Application to a sample of 25 clusters.** *Astrophys J.* 2005; **625**(1): 108.  
[Publisher Full Text](#)
- de Graaff A, Cai YC, Heymans C, *et al.*: **Probing the missing baryons with the Sunyaev-Zel'dovich effect from filaments.** *Astron Astrophys.* 2019; **624**: A48.  
[Publisher Full Text](#)
- Delvecchio I, Daddi E, Sargent MT, *et al.*: **The infrared-radio correlation of Star-Forming Galaxies is strongly  $M_*$ -dependent but nearly redshift-invariant since  $z \sim 4$ .** *Astron Astrophys.* 2021; **647**: A123.  
[Publisher Full Text](#)
- Di Mascolo L, Churazov E, Mroczkowski T: **A joint ALMA-Bolocam-Planck SZ study of the pressure distribution in RX J1347.5–1145.** *Mon Not R Astron Soc.* 2019a; **487**(3): 4037–4056.  
[Publisher Full Text](#)
- Di Mascolo L, Mroczkowski T, Churazov E, *et al.*: **An ALMA+ACA measurement of the shock in the bullet cluster.** *Astron Astrophys.* 2019b; **628**: A100.  
[Publisher Full Text](#)
- Di Mascolo L, Saro A, Mroczkowski T, *et al.*: **Forming intracluster gas in a galaxy protocluster at a redshift of 2.16.** *Nature.* 2023; **615**(7954): 809–812.  
[PubMed Abstract](#) | [Publisher Full Text](#) | [Free Full Text](#)
- Dicker SR, Ade PAR, Aguirre J, *et al.*: **MUSTANG 2: a large focal plane array for the 100 m Green Bank telescope.** *J Low Temp Phys.* 2014; **176**: 808–814.  
[Publisher Full Text](#)

- Dicker SR, Battistelli ES, Bhandarkar T, *et al.*: **Observations of compact sources in galaxy clusters using MUSTANG2.** *Mon Not R Astron Soc.* 2021; **508**(2): 2600–2612.  
[Publisher Full Text](#)
- Dolag K, Komatsu E, Sunyaev R: **SZ effects in the magnetic pathfinder simulation: comparison with the Planck, SPT, and ACT results.** *Mon Not R Astron Soc.* 2016; **463**(2): 1797–1811.  
[Publisher Full Text](#)
- Donahue M, Scharf CA, Mack J, *et al.*: **Distant cluster hunting. II. A comparison of X-Ray and optical cluster detection techniques and catalogs from the ROSAT optical X-Ray survey.** *Astrophys J.* 2002; **569**(2): 689.  
[Publisher Full Text](#)
- Doré O, Bock J, Ashby M, *et al.*: **Cosmology with the SPHEREX all-sky spectral survey.** *arXiv e-prints.* arXiv: 1412.4872. 2014.  
[Publisher Full Text](#)
- Duchesne SW, Botteon A, Koribalski BS, *et al.*: **Evolutionary Map of the Universe (EMU): a pilot search for diffuse, non-thermal radio emission in galaxy clusters with the Australian SKA pathfinder.** *arXiv e-prints.* arXiv: 2402.06192. 2024.  
[Publisher Full Text](#)
- Eckert D, Gaspari M, Vazza F, *et al.*: **On the connection between turbulent motions and particle acceleration in galaxy clusters.** *Astrophys J Lett.* 2017; **843**(2): L29.  
[Publisher Full Text](#)
- Eckert D, Molendi S, Paltani S: **The cool-core bias in X-ray galaxy cluster samples I. Method and application to HIFLUGCS.** *Astron Astrophys.* 2011; **526**: A79.  
[Publisher Full Text](#)
- Ehlert K, Pfrommer C, Weinberger R, *et al.*: **The Sunyaev-Zel'dovich effect of simulated jet-inflated bubbles in clusters.** *Astrophys J.* 2019; **872**(1): L8.  
[PubMed Abstract](#) | [Publisher Full Text](#)
- Emonts BHC, Lehnert MD, Villar-Martín M, *et al.*: **Molecular gas in the halo fuels the growth of a massive cluster galaxy at high redshift.** *Science.* 2016; **354**(6316): 1128–1130.  
[Publisher Full Text](#)
- Enßlin TA, Kaiser CR: **Comptonization of the cosmic microwave background by relativistic plasma.** *Astron Astrophys.* 2000; **360**: 417–430.  
[Publisher Full Text](#)
- Erlér J, Basu K, Chluba J, *et al.*: **Planck's view on the spectrum of the Sunyaev-Zel'dovich effect.** *Mon Not R Astron Soc.* 2018; **476**(3): 3360–3381.  
[Publisher Full Text](#)
- Ettori S, Eckert D: **Tracing the non-thermal pressure and hydrostatic bias in galaxy clusters.** *Astron Astrophys.* 2022; **657**: L1.  
[Publisher Full Text](#)
- Euclid Collaboration: **Euclid preparation: III. Galaxy cluster detection in the wide photometric survey, performance and algorithm selection.** *Astron Astrophys.* 2019; **627**: A23.  
[Publisher Full Text](#)
- Euclid Collaboration, Scaramella R, Amiaux J, *et al.*: **Euclid preparation: I. The Euclid Wide Survey.** *Astron Astrophys.* 2022; **662**: A112.  
[Publisher Full Text](#)
- Fabian AC: **Observational evidence of Active Galactic Nuclei feedback.** *Annu Rev Astron Astrophys.* 2012; **50**: 455–489.  
[Publisher Full Text](#)
- Ferrari C, Dabbech A, Smirnov O, *et al.*: **Non-thermal emission from galaxy clusters: feasibility study with SKA.** In: *Advancing Astrophysics with the Square Kilometre Array (AASKA14).* 2015; 75.  
[Publisher Full Text](#)
- Ferraro S, Smith KM: **Characterizing the epoch of reionization with the small-scale CMB: constraints on the optical depth and duration.** *Phys Rev D.* 2018; **98**(12): 123519.  
[Publisher Full Text](#)
- Fujita Y: **Pre-processing of galaxies before entering a cluster.** *Publ Astron Soc Jpn.* 2004; **56**(1): 29–43.  
[Publisher Full Text](#)
- Galárraga-Espinosa D, Aghanim N, Langer M, *et al.*: **Populations of filaments from the distribution of galaxies in numerical simulations.** *Astron Astrophys.* 2020; **641**: A173.  
[Publisher Full Text](#)
- Ganguly S, Li Y, Olivares V, *et al.*: **The nature of the motions of multiphase filaments in the centers of galaxy clusters.** *Front Astron Space Sci.* 2023; **10**: 1138613.  
[Publisher Full Text](#)
- Gardner A, Baxter E, Raghunathan S, *et al.*: **Prospects for studying the mass and gas in protoclusters with future CMB observations.** *The Open Journal of Astrophysics.* 2024; **7**: 2.  
[Publisher Full Text](#)
- Gardner JP, Mather JC, Clampin M, *et al.*: **The James Webb Space Telescope.** *Space Sci Rev.* 2006; **123**(4): 485–606.  
[Publisher Full Text](#)
- Gaspari M, Tombesi F, Cappi M: **Linking macro-, meso- and microscales in multiphase AGN feeding and feedback.** *Nat Astron.* 2020; **4**: 10–13.  
[Publisher Full Text](#)
- Gatuzz E, Mohapatra R, Federrath C, *et al.*: **Measuring the hot ICM velocity structure function using XMM-Newton observations.** *Mon Not R Astron Soc.* 2023; **524**(2): 2945–2953.  
[Publisher Full Text](#)
- George EM, Reichardt CL, Aird KA, *et al.*: **A Measurement of secondary Cosmic Microwave Background anisotropies from the 2500 square-degree SPT-SZ survey.** *Astrophys J.* 2015; **799**(2): 177.  
[Publisher Full Text](#)
- Ghirardini V, Bulbul E, Hoang DN, *et al.*: **Discovery of a supercluster in the eROSITA Final Equatorial Depth Survey: X-ray properties, radio halo, and double relics.** *Astron Astrophys.* 2021a; **647**: A4.  
[Publisher Full Text](#)
- Ghirardini V, Bulbul E, Kraft R, *et al.*: **Evolution of the thermodynamic properties of clusters of galaxies out to redshift of 1.8.** *Astrophys J.* 2021b; **910**(1): 14.  
[Publisher Full Text](#)
- Ghirardini V, Eckert D, Ettori S, *et al.*: **Universal thermodynamic properties of the Intracluster Medium over two decades in radius in the X-COP sample.** *Astron Astrophys.* 2019; **621**: A41.  
[Publisher Full Text](#)
- Ghirardini V, Ettori S, Amodeo S, *et al.*: **On the evolution of the entropy and pressure profiles in X-ray luminous galaxy clusters at  $z > 0.4$ .** *Astron Astrophys.* 2017; **604**: A100.  
[Publisher Full Text](#)
- Giovannini G, Bonafede A, Brown S, *et al.*: **Mega-parsec scale magnetic fields in low density regions in the SKA era: filaments connecting galaxy clusters and groups.** In: *Advancing Astrophysics with the Square Kilometre Array (AASKA14).* 2015; 104.  
[Publisher Full Text](#)
- Gitti M, Tozzi P, Brunetti G, *et al.*: **The SKA view of cool-core clusters: evolution of radio mini-halos and AGN feedback.** In: *Advancing Astrophysics with the Square Kilometre Array (AASKA14).* 2015; 76.  
[Publisher Full Text](#)
- Gobat R, Daddi E, Coogan RT, *et al.*: **Sunyaev-Zel'dovich detection of the galaxy cluster Cl J1449+0856 at  $z = 1.99$ : the pressure profile in  $uv$  space.** *Astron Astrophys.* 2019; **629**: A104.  
[Publisher Full Text](#)
- Govoni F, Murgia M, Xu H, *et al.*: **Cluster magnetic fields through the study of polarized radio halos in the SKA era.** In: *Advancing Astrophysics with the Square Kilometre Array (AASKA14).* 2015; 105.  
[Publisher Full Text](#)
- Grainge K, Borgani S, Colafrancesco S, *et al.*: **The SKA and galaxy cluster science with the Sunyaev-Zel'dovich effect.** In: *Advancing Astrophysics with the Square Kilometre Array (AASKA14).* 2015; 170.  
[Publisher Full Text](#)
- Grayson S, Scannapieco E, Davé R: **Distinguishing Active Galactic Nuclei feedback models with the Thermal Sunyaev-Zel'dovich effect.** *Astrophys J.* 2023; **957**(1): 17.  
[Publisher Full Text](#)
- Gupta N, Saro A, Mohr JJ, *et al.*: **SZE observables, pressure profiles and centre offsets in Magneticum simulation galaxy clusters.** *Mon Not R Astron Soc.* 2017; **469**(3): 3069–3087.  
[Publisher Full Text](#)
- Ha JH, Ryu D, Kang H: **Properties of merger shocks in merging galaxy clusters.** *Astrophys J.* 2018; **857**(1): 26.  
[Publisher Full Text](#)
- Hall KR, Zakamska NL, Addison GE, *et al.*: **Quantifying the thermal Sunyaev-Zel'dovich effect and excess millimetre emission in quasar environments.** *Mon Not R Astron Soc.* 2019; **490**(2): 2315–2335.  
[Publisher Full Text](#)
- Hansen SH, Pastor S, Semikoz DV: **First measurement of cluster temperature using the thermal Sunyaev-Zel'dovich effect.** *Astrophys J.* 2002; **573**(2): L69–L71.  
[Publisher Full Text](#)
- Hasselfield M, Moodley K, Bond JR, *et al.*: **The Atacama Cosmology Telescope: beam measurements and the microwave brightness temperatures of Uranus and Saturn.** *Astrophys J Suppl.* 2013; **209**(1): 17.  
[Publisher Full Text](#)
- Hensley BS, Clark SE, Fanfani V, *et al.*: **The Simons Observatory: galactic science goals and forecasts.** *Astrophys J.* 2022; **929**(2): 166.  
[Publisher Full Text](#)
- Hill R, Chapman S, Scott D, *et al.*: **Megaparsec-scale structure around the protocluster core SPT2349-56 at  $z = 4.3$ .** *Mon Not R Astron Soc.* 2020; **495**(3): 3124–3159.  
[Publisher Full Text](#)
- Hilton M, Sifón C, Naess S, *et al.*: **The Atacama Cosmology Telescope: a catalog of >4000 Sunyaev-Zel'dovich galaxy clusters.** *Astrophys J Suppl Ser.* 2021; **253**(1): 3.  
[Publisher Full Text](#)
- Hincks AD, Radiconi F, Romero C, *et al.*: **A high-resolution view of the filament of gas between Abell 399 and Abell 401 from the Atacama Cosmology Telescope and MUSTANG-2.** *Mon Not R Astron Soc.* 2022; **510**(3): 3335–3355.  
[Publisher Full Text](#)

- Hlavacek-Larrondo J, Li Y, Churazov E: **AGN Feedback in groups and clusters of galaxies.** In: *Handbook of X-ray and Gamma-ray Astrophysics*. 2022; 5. [Publisher Full Text](#)
- Hughes DH, Jáuregui Correa JC, Schloerb FP, et al.: **The Large Millimeter Telescope.** In: *Ground-based and Airborne Telescopes III*. 2010; **773312**: 773312. [Publisher Full Text](#)
- Hurier G: **High significance detection of the tSZ effect relativistic corrections.** *Astron Astrophys*. 2016; **596**: A61. [Publisher Full Text](#)
- Hurier G, Adam R, Keshet U: **First detection of a virial shock with SZ data: implication for the mass accretion rate of Abell 2319.** *Astron Astrophys*. 2019; **622**: A136. [Publisher Full Text](#)
- Husemann B, Harrison CM: **Reality and myths of AGN feedback.** *Nat Astron*. 2018; **2**: 196–197. [Publisher Full Text](#)
- Huynh M, Lazio J: **An overview of the Square Kilometre Array.** *arXiv*. 2013; 1311.4288. [Publisher Full Text](#)
- Iguchi S, Morita KI, Sugimoto M, et al.: **The Atacama Compact Array (ACA).** *Publ Astron Soc Jpn*. 2009; **61**(1): 1–12. [Publisher Full Text](#)
- Iljenkarevic J, Reiprich TH, Pacaud F, et al.: **eROSITA spectro-imaging analysis of the Abell 3408 galaxy cluster.** *Astron Astrophys*. 2022; **661**: A26. [Publisher Full Text](#)
- Itoh N, Kohyama Y, Nozawa S: **Relativistic corrections to the Sunyaev-Zeldovich effect for clusters of galaxies.** *Astrophys J*. 1998; **502**(1): 7–15. [Publisher Full Text](#)
- Ivezić Ž, Kahn SM, Tyson JA, et al.: **LSST: from science drivers to reference design and anticipated data products.** *Astrophys J*. 2019; **873**(2): 111. [Publisher Full Text](#)
- Javid K, Perrott YC, Rumsey C, et al.: **Physical modelling of galaxy cluster Sunyaev-Zel'dovich data using Einasto dark matter profiles.** *Mon Not R Astron Soc*. 2019; **489**(3): 3135–3148. [Publisher Full Text](#)
- Jin S, Dannerbauer H, Emonts B, et al.: **COALAS. I. ATCA CO(1-0) survey and luminosity function in the Spiderweb protocluster at  $z = 2.16$ .** *Astron Astrophys*. 2021; **652**: A11. [Publisher Full Text](#)
- Johnston-Hollitt M, Dehghan S, Pratley L: **Using tailed radio galaxies to probe the environment and magnetic field of galaxy clusters in the SKA era.** In: *Advancing Astrophysics with the Square Kilometre Array (AASKA14)*. 2015a; 101. [Publisher Full Text](#)
- Johnston-Hollitt M, Govoni F, Beck R, et al.: **Using SKA rotation measures to reveal the mysteries of the magnetised Universe.** In: *Advancing Astrophysics with the Square Kilometre Array (AASKA14)*. 2015b; 92. [Publisher Full Text](#)
- Jones GC, Maiolino R, Carniani S, et al.: **An investigation of the circumgalactic medium around  $z \sim 2.2$  AGN with ACA and ALMA.** *Mon Not R Astron Soc*. 2023; **522**(1): 275–291. [Publisher Full Text](#)
- Kéruzoré F, Mayet F, Pratt GW, et al.: **Exploiting NIKA2/XMM-Newton imaging synergy for intermediate-mass high- $z$  galaxy clusters within the NIKA2 SZ large program: observations of ACT-CL J0215.4+0030 at  $z \sim 0.9$ .** *Astron Astrophys*. 2020; **644**: A93. [Publisher Full Text](#)
- Khatiri R, Gaspari M: **Thermal SZ fluctuations in the ICM: probing turbulence and thermodynamics in Coma cluster with Planck.** *Mon Not R Astron Soc*. 2016; **463**(1): 655–669. [Publisher Full Text](#)
- Kim J, Sayers J, Sereno M, et al.: **CHEX-MATE: CLuster Multi-Probes in three dimensions (CLUMP-3D). I. Gas analysis method using X-ray and Sunyaev-Zel'dovich effect data.** *arXiv e-prints*. arXiv: 2307.04794. 2023. [Publisher Full Text](#)
- Kitayama T: **Cosmological and astrophysical implications of the Sunyaev-Zel'dovich effect.** *Prog Theor Exp Phys*. 2014; **2014**(6): 06B111. [Publisher Full Text](#)
- Kitayama T, Ueda S, Akahori T, et al.: **Deeply cooled core of the Phoenix galaxy cluster imaged by ALMA with the Sunyaev-Zel'dovich effect.** *Publ Astron Soc Jpn*. 2020; **72**(2): 33. [Publisher Full Text](#)
- Kitayama T, Ueda S, Takakuwa S, et al.: **The Sunyaev-Zel'dovich effect at 5": RX J1347.5–1145 imaged by ALMA.** *Publ Astron Soc Jpn*. 2016; **68**(5): 88. [Publisher Full Text](#)
- Klaassen P: **AtLAST Sensitivity Calculator and Telescope Simulation Notebook.** *figshare*. 2024. <http://www.doi.org/10.6084/m9.figshare.23506962.v1>
- Klaassen PD, Mroczkowski TK, Cicone C, et al.: **The Atacama Large Aperture Submillimeter Telescope (AtLAST).** In: *Ground-based and Telescopes*. 2020; **8**: 114452F. [Publisher Full Text](#)
- Klaassen P, Traficante A, Beltrán MT, et al.: **Atacama Large Aperture Submillimeter Telescope (AtLAST) science: our galaxy.** *arXiv e-prints*. arXiv: 2403.00917. 2024. [Publisher Full Text](#)
- Knowles K, Cotton WD, Rudnick L, et al.: **The MeerKAT galaxy cluster legacy survey.** *Astron Astrophys*. 2022; **657**: A56. [Publisher Full Text](#)
- Knowles K, Pillay DS, Amodeo S, et al.: **MERGHES pilot: MeerKAT discovery of diffuse emission in nine massive Sunyaev-Zel'dovich-selected galaxy clusters from ACT.** *Mon Not R Astron Soc*. 2021; **504**(2): 1749–1758. [Publisher Full Text](#)
- Kosowsky A, Bhattacharya S: **A future test of gravitation using galaxy cluster velocities.** *Phys Rev D*. 2009; **80**: 062003. [Publisher Full Text](#)
- Kozmalyan A, Bourdin H, Mazzotta P, et al.: **Deriving the hubble constant using Planck and XMM-Newton observations of galaxy clusters.** *Astron Astrophys*. 2019; **621**: A34. [Publisher Full Text](#)
- Kraft R, Markevitch M, Kilbourne C, et al.: **Line Emission Mapper (LEM): probing the physics of cosmic ecosystems.** *arXiv e-prints*. arXiv: 2211.09827. 2022. [Publisher Full Text](#)
- Kravtsov AV, Borgani S: **Formation of galaxy clusters.** *Annu Rev Astron Astrophys*. 2012; **50**(1): 353–409. [Publisher Full Text](#)
- Lacy M, Mason B, Sarazin C, et al.: **Direct detection of quasar feedback via the Sunyaev-Zeldovich effect.** *Mon Not R Astron Soc*. 2019; **483**(1): L22–L27. [Publisher Full Text](#)
- Lau ET, Nagai D, Avestruz C, et al.: **Mass accretion and its effects on the self-similarity of gas profiles in the outskirts of galaxy clusters.** *Astrophys J*. 2015; **806**(1): 68. [Publisher Full Text](#)
- Laureijs R, Amiaux J, Arduini S, et al.: **Euclid definition study report.** *arXiv eprints*. arXiv: 1110.3193. 2011. [Publisher Full Text](#)
- Le Brun AMC, McCarthy IG, Melin JB: **Testing Sunyaev-Zel'dovich measurements of the hot gas content of dark matter haloes using synthetic skies.** *Mon Not R Astron Soc*. 2015; **451**(4): 3868–3881. [Publisher Full Text](#)
- Lee E, Chluba J, Kay ST, et al.: **Relativistic SZ temperature scaling relations of groups and clusters derived from the BAHAMAS and MACSIS simulations.** *Mon Not R Astron Soc*. 2020; **493**(3): 3274–3292. [Publisher Full Text](#)
- Lee MM, Schimek A, Cicone C, et al.: **Atacama Large Aperture Submillimeter Telescope (AtLAST) science: the hidden circumgalactic medium.** *arXiv eprints*. arXiv: 2403.00924. 2024. [Reference Source](#)
- Lepore M, Di Mascolo L, Tozzi P, et al.: **Feeding and feedback processes in the Spiderweb proto-Intracluster Medium.** *Astron Astrophys*. 2024; **682**: A186. [Publisher Full Text](#)
- Li Q, Cui W, Yang X, et al.: **THE THREE HUNDRED Project: the evolution of physical baryon profiles.** *Mon Not R Astron Soc*. 2023; **523**(1): 1228–1246. [Publisher Full Text](#)
- Li Y, Gendron-Marsolais ML, Zhuravleva I, et al.: **Direct detection of black hole-driven turbulence in the centers of galaxy clusters.** *Astrophys J Lett*. 2020; **889**(1): L1. [Publisher Full Text](#)
- Li Z, Puglisi G, Madhavacheril MS, et al.: **Simulated catalogs and maps of radio galaxies at millimeter wavelengths in Websky.** *J Cosmology Astropart Phys*. 2022; **2022**(08): 029. [Publisher Full Text](#)
- Limousin M, Morandi A, Sereno M, et al.: **The three-dimensional shapes of galaxy clusters.** *Space Sci Rev*. 2013; **177**(1–4): 155–194. [Publisher Full Text](#)
- Liu A, Bulbul E, Ramos-Ceja ME, et al.: **X-ray analysis of JWST's first galaxy cluster lens SMACS J0723.3–7327.** *Astron Astrophys*. 2023; **670**: A96. [Publisher Full Text](#)
- Liu D, Saintonge A, Bot C, et al.: **Atacama Large Aperture Submillimeter Telescope (AtLAST) science: gas and dust in nearby galaxies.** *arXiv e-prints*. arXiv: 2403.01202. 2024. [Publisher Full Text](#)
- Lokken M, Cui W, Bond JR, et al.: **Boundless baryons: how diffuse gas contributes to anisotropic tSZ signal around simulated Three Hundred clusters.** *Mon Not R Astron Soc*. 2023; **523**(1): 1346–1363. [Publisher Full Text](#)
- Lungu M, Storer ER, Hasselfield M, et al.: **The atacama cosmology telescope: measurement and analysis of 1D beams for DR4.** *J Cosmology Astropart Phys*. 2022; **2022**: 044. [Publisher Full Text](#)
- Mantz A, Allen SW, Ebeling H, et al.: **The observed growth of massive galaxy clusters - II. X-ray scaling relations.** *Mon Not R Astron Soc*. 2010; **406**(3): 1773–1795. [Publisher Full Text](#)

- Mantz AB, Allen SW, Morris RG, *et al.*: **Deep XMM-Newton observations of the most distant SPT-SZ galaxy cluster.** *Mon Not R Astron Soc.* 2020; **496**(2): 1554–1564.  
[Publisher Full Text](#)
- Marchegiani P: **EPJ Sunyaev Zel'dovich effect in galaxy clusters cavities: Thermal or non-thermal origin?** In: *mm Universe @ NIKA2 - Observing the mm Universe with the NIKA2 Camera.* 2022; **257**: 00030.  
[Reference Source](#)
- Markevitch M, Vikhlinin A: **Shocks and cold fronts in galaxy clusters.** *Phys Rep.* 2007; **443**(1): 1–153.  
[Publisher Full Text](#)
- Mason BS, Dicker SR, Korngut PM, *et al.*: **Implications of a high angular resolution image of the Sunyaev-Zel'Dovich Effect in RXJ1347-1145.** *Astrophys J.* 2010; **716**(1): 739–745.  
[Publisher Full Text](#)
- Matsuda Y, Yamada T, Hayashino T, *et al.*: **Large-scale filamentary structure around the protocluster at redshift  $z = 3.1$ .** *Astrophys J.* 2005; **634**(2): L125.  
[Publisher Full Text](#)
- Maughan BJ, Giles PA, Randall SW, *et al.*: **Self-similar scaling and evolution in the galaxy cluster X-ray luminosity-temperature relation.** *Mon Not R Astron Soc.* 2012; **421**(2): 1583–1602.  
[Publisher Full Text](#)
- Mazzotta P, Rasia E, Moscardini L, *et al.*: **Comparing the temperatures of galaxy clusters from hydrodynamical N-body simulations to Chandra and XMM-Newton observations.** *Mon Not R Astron Soc.* 2004; **354**(1): 10–24.  
[Publisher Full Text](#)
- McCarthy IG, Schaye J, Bird S, *et al.*: **The BAHAMAS project: calibrated hydrodynamical simulations for Large-Scale Structure cosmology.** *Mon Not R Astron Soc.* 2017; **465**(3): 2936–2965.  
[Publisher Full Text](#)
- McDonald M, Benson BA, Vikhlinin A, *et al.*: **The redshift evolution of the mean temperature, pressure, and entropy profiles in 80 spt-selected galaxy clusters.** *Astrophys J.* 2014; **794**(1): 67.  
[Publisher Full Text](#)
- Melin JB, Pratt GW: **Joint measurement of the galaxy cluster pressure profile with Planck and SPT-SZ.** *Astron Astrophys.* 2023; **678**: A197.  
[Publisher Full Text](#)
- Merloni A, Lamer G, Liu T, *et al.*: **The SRG/eROSITA all-sky survey. First X-ray catalogues and data release of the western Galactic hemisphere.** *Astron Astrophys.* 2024; **682**: A34.  
[Publisher Full Text](#)
- Migkas K, Kox D, Schellenberger G, *et al.*: **The SRG/eROSITA all-sky survey: SRG/eROSITA cross-calibration with chandra and XMM-Newton using galaxy cluster gas temperatures.** *arXiv e-prints.* arXiv: 2401.17297. 2024.  
[Publisher Full Text](#)
- Molnar SM, Hearn N, Haiman Z, *et al.*: **Accretion shocks in clusters of galaxies and their SZ signature from cosmological simulations.** *Astrophys J.* 2009; **696**(2): 1640–1656.  
[Publisher Full Text](#)
- Moser E, Battaglia N, Nagai D, *et al.*: **The Circumgalactic Medium from the CAMELS simulations: forecasting constraints on feedback processes from future Sunyaev-Zeldovich observations.** *Astrophys J.* 2022; **933**(2): 133.  
[Publisher Full Text](#)
- Mroczkowski T, Cicone C, Reichert M, *et al.*: **Progress in the design of the Atacama Large Aperture Submillimeter Telescope.** In: *2023 XXXVth General Assembly and Scientific Symposium of the International Union of Radio Science (URSI GASS).* 2023; 174.  
[Publisher Full Text](#)
- Mroczkowski T, Dicker S, Sayers J, *et al.*: **A multi-wavelength study of the Sunyaev-Zel'dovich Effect in the triple-merger cluster macs J0717.5+3745 with MUSTANG and Bolocam.** *Astrophys J.* 2012; **761**(1): 47.  
[Publisher Full Text](#)
- Mroczkowski T, Gallardo PA, Timpe M, *et al.*: **Design of the 50-meter Atacama Large Aperture Submm Telescope.** *arXiv e-prints.* arXiv: 2402.18645. 2024.  
[Publisher Full Text](#)
- Mroczkowski T, Nagai D, Basu K, *et al.*: **Astrophysics with the spatially and spectrally resolved Sunyaev-Zeldovich effects. a millimetre/submillimetre probe of the warm and hot Universe.** *Space Sci Rev.* 2019; **215**(1): 17.  
[Publisher Full Text](#)
- Mueller EM, de Bernardis F, Bean R, *et al.*: **Constraints on gravity and dark energy from the pairwise kinematic Sunyaev-Zel'dovich effect.** *Astrophys J.* 2015; **808**(1): 47.  
[Publisher Full Text](#)
- Naess S, Aiola S, Austermann JE, *et al.*: **The Atacama Cosmology Telescope: arcminute-resolution maps of 18 000 square degrees of the microwave sky from ACT 2008-2018 data combined with Planck.** *J Cosmology Astropart Phys.* 2020; **2020**(12): 046.  
[Publisher Full Text](#)
- Nagai D, Kravtsov AV, Kosowsky A: **Effect of internal flows on Sunyaev-Zeldovich measurements of cluster peculiar velocities.** *Astrophys J.* 2003; **587**(2): 524–532.  
[Publisher Full Text](#)
- Nagai D, Kravtsov AV, Vikhlinin A: **Effects of galaxy formation on thermodynamics of the Intracluster Medium.** *Astrophys J.* 2007; **668**(1): 1–14.  
[Publisher Full Text](#)
- Nakano S, Tamura Y, Taniguchi A, *et al.*: **Characterization of sensitivity and responses of a 2-element prototype wavefront sensor for millimeter-wave adaptive optics attached to the Nobeyama 45m Telescope.** In: *Adaptive Optics Systems VIII.* 2022; **12185**.  
[Publisher Full Text](#)
- Nelson D, Pillepich A, Ayromlou M, *et al.*: **Introducing the TNG-Cluster simulation: overview and physical properties of the gaseous Intracluster Medium.** *arXiv e-prints.* arXiv: 2311.06338. 2023.  
[Publisher Full Text](#)
- Nicastro F, Kaastra J, Krongold Y, *et al.*: **Observations of the missing baryons in the warm-hot intergalactic medium.** *Nature.* 2018; **558**(7710): 406–409.  
[PubMed Abstract](#) | [Publisher Full Text](#)
- Nozawa S, Itoh N, Kohyama Y: **Relativistic corrections to the Sunyaev-Zeldovich effect for clusters of galaxies.** *Astrophys J.* 1998; **508**(1): 7–15.  
[Publisher Full Text](#)
- Olamaie M, Hobson MP, Grainge KJB: **A simple parametric model for spherical galaxy clusters.** *Mon Not R Astron Soc.* 2012; **423**: 1534–1543.  
[Publisher Full Text](#)
- Orlowski-Scherer J, Haridas SK, Di Mascio L, *et al.*: **GBT/MUSTANG-2 9" resolution imaging of the SZ effect in MS0735.6+7421. Confirmation of the SZ cavities through direct imaging.** *Astron Astrophys.* 2022; **667**: L6.  
[Publisher Full Text](#)
- Overzier RA: **The realm of the galaxy protoclusters. A review.** *Astron Astrophys Rev.* 2016; **24**(1): 14.  
[Publisher Full Text](#)
- Pacaud F, Pierre M, Adami C, *et al.*: **The XMM-LSS survey: the class 1 cluster sample over the initial 5 deg<sup>2</sup> and its cosmological modelling.** *Mon Not R Astron Soc.* 2007; **382**(3): 1289–1308.  
[Publisher Full Text](#)
- Padovani P, Alexander DM, Assef RJ, *et al.*: **Active Galactic Nuclei: what's in a name?** *Astron Astrophys Rev.* 2017; **25**(1): 2.  
[Publisher Full Text](#)
- Paine S: **The am atmospheric model.** *Zenodo.* 2019.  
[Publisher Full Text](#)
- Patnaude DJ, Kraft RP, Kilbourne C, *et al.*: **Line Emission Mapper: an X-ray probe mission concept to study the cosmic ecosystems and the physics of galaxy formation.** *J Astron Telesc Instrum Syst.* 2023; **9**: 041008.  
[Publisher Full Text](#)
- Pfrommer C, Enßlin TA, Sarazin CL: **Unveiling the composition of radio plasma bubbles in galaxy clusters with the Sunyaev-Zel'dovich effect.** *Astron Astrophys.* 2005; **430**: 799–810.  
[Publisher Full Text](#)
- Plagge TJ, Marrone DP, Abdulla Z, *et al.*: **CARMA measurements of the Sunyaev-Zel'dovich effect in RX J1347.5-1145.** *Astrophys J.* 2013; **770**(2): 112.  
[Publisher Full Text](#)
- Planck Collaboration: **Planck early results. IX. XMM-Newton follow-up for validation of Planck cluster candidates.** *Astron Astrophys.* 2011; **536**: A9.  
[Publisher Full Text](#)
- Planck Collaboration: **Planck intermediate results. I. Further validation of new Planck clusters with XMM-Newton.** *Astron Astrophys.* 2012; **543**: A102.  
[Publisher Full Text](#)
- Planck Collaboration: **Planck intermediate results. VIII. Filaments between interacting clusters.** *Astron Astrophys.* 2013; **550**: A134.  
[Publisher Full Text](#)
- Planck Collaboration: **Planck 2015 results. XXVII. The second Planck catalogue of Sunyaev-Zeldovich sources.** *Astron Astrophys.* 2016; **594**: A27.  
[Publisher Full Text](#)
- Prandoni I, Murgia M, Tarchi A, *et al.*: **The Sardinia Radio Telescope. from a technological project to a radio observatory.** *Astron Astrophys.* 2017; **608**: A40.  
[Publisher Full Text](#)
- Prandoni I, Seymour N: **Revealing the physics and evolution of galaxies and galaxy clusters with SKA continuum surveys.** In: *Advancing Astrophysics with the Square Kilometre Array (AASKA14).* 2015; 67.  
[Publisher Full Text](#)
- Pratt GW, Arnaud M, Biviano A, *et al.*: **The galaxy cluster mass scale and its impact on cosmological constraints from the cluster population.** *Space Sci Rev.* 2019; **215**(2): 25.  
[Publisher Full Text](#)
- Pratt GW, Arnaud M, Piffaretti R, *et al.*: **Gas entropy in a representative sample of nearby X-ray galaxy clusters (REXCESS): relationship to gas mass fraction.** *Astron Astrophys.* 2010; **511**: A85.  
[Publisher Full Text](#)
- Prokhorov DA, Colafrancesco S: **The first measurement of temperature standard deviation along the line of sight in galaxy clusters.** *Mon Not R Astron Soc.* 2012; **424**(1): L49–L53.  
[Publisher Full Text](#)
- Radiconi F, Vacca V, Battistelli E, *et al.*: **The thermal and non-thermal components within and between galaxy clusters Abell 399 and Abell 401.** *Mon Not R Astron Soc.* 2022; **517**(4): 5232–5246.  
[Publisher Full Text](#)



- Raghunathan S: **Assessing the importance of noise from Thermal Sunyaev-Zel'dovich signals for CMB cluster surveys and cluster cosmology.** *Astrophys J.* 2022; **928**(1): 16.  
[Publisher Full Text](#)
- Raghunathan S, Whitehorn N, Alvarez MA, et al.: **Constraining cluster virialization mechanism and cosmology using Thermal-SZ-selected clusters from future CMB surveys.** *Astrophys J.* 2022; **926**(2): 172.  
[Publisher Full Text](#)
- Ramasawmy J, Klaassen PD, Cicone C, et al.: **The Atacama Large Aperture Submillimetre Telescope: key science drivers.** In: *Millimeter, Submillimeter, and Far-Infrared Detectors and Instrumentation for Astronomy XI.* 2022; **12190**: 1219007.  
[Publisher Full Text](#)
- Rasia E, Borgani S, Murante G, et al.: **Cool Core clusters from cosmological simulations.** *Astrophys J.* 2015; **813**(1): L17.  
[Publisher Full Text](#)
- Remazeilles M, Chluba J: **Mapping the relativistic electron gas temperature across the sky.** *Mon Not R Astron Soc.* 2020; **494**(4): 5734–5750.  
[Publisher Full Text](#)
- Romero CE, Gaspari M, Schellenberger G, et al.: **Inferences from surface brightness fluctuations of Zwicky 3146 via the Sunyaev-Zel'dovich effect and X-ray observations.** *Astrophys J.* 2023; **951**(1): 41.  
[Publisher Full Text](#)
- Romero CE, Sievers J, Ghirardini V, et al.: **Pressure profiles and mass estimates using high-resolution Sunyaev-Zel'dovich effect observations of Zwicky 3146 with MUSTANG-2.** *Astrophys J.* 2020; **891**(1): 90.  
[Publisher Full Text](#)
- Rossetti M, Gastaldello F, Eckert D, et al.: **The cool-core state of Planck SZ-selected clusters versus X-ray-selected samples: evidence for cool-core bias.** *Mon Not R Astron Soc.* 2017; **468**(2): 1917–1930.  
[Publisher Full Text](#)
- Ruppin F, Adam R, Comis B, et al.: **Non-parametric deprojection of NIKA SZ observations: pressure distribution in the Planck-discovered cluster PSZ1 G045.85+57.71.** *Astron Astrophys.* 2017; **597**: A110.  
[Publisher Full Text](#)
- Ruppin F, McDonald M, Bleem LE, et al.: **Stability of cool cores during galaxy cluster growth: a joint Chandra/SPT analysis of 67 galaxy clusters along a common evolutionary track spanning 9 Gyr.** *Astrophys J.* 2021; **918**(2): 43.  
[Publisher Full Text](#)
- Ryu D, Kang H, Hallman E, et al.: **Cosmological shock waves and their role in the large-scale structure of the universe.** *Astrophys J.* 2003; **593**(2): 599–610.  
[Publisher Full Text](#)
- Sanders JS: **Contour binning: a new technique for spatially resolved X-ray spectroscopy applied to cassiopeia A.** *Mon Not R Astron Soc.* 2006; **371**(2): 829–842.  
[Publisher Full Text](#)
- Sanders JS, Biffi V, Brüggem M, et al.: **Studying the merging cluster Abell 3266 with eROSITA.** *Astron Astrophys.* 2022; **661**: A36.  
[Publisher Full Text](#)
- Sayers J, Mantz AB, Rasia E, et al.: **The evolution and mass dependence of galaxy cluster pressure profiles at  $0.05 \leq z \leq 0.60$  and  $4 \times 10^{14} M_{\odot} \leq M_{500} \leq 30 \times 10^{14} M_{\odot}$ .** *Astrophys J.* 2023; **944**(2): 221.  
[Publisher Full Text](#)
- Sayers J, Montaña A, Mroczkowski T, et al.: **Imaging the thermal and kinematic Sunyaev-Zel'dovich effect signals in a sample of 10 massive galaxy clusters: constraints on internal velocity structures and bulk velocities.** *Astrophys J.* 2019; **880**(1): 45.  
[Publisher Full Text](#)
- Sayers J, Mroczkowski T, Zemcov M, et al.: **A measurement of the kinetic Sunyaev-Zel'dovich signal toward macs J0717.5+3745.** *Astrophys J.* 2013; **778**(1): 52.  
[Publisher Full Text](#)
- Sayers J, Sereno M, Ettori S, et al.: **CLUMP-3D: the lack of non-thermal motions in galaxy cluster cores.** *Mon Not R Astron Soc.* 2021; **505**(3): 4338–4344.  
[Publisher Full Text](#)
- Schaan E, Ferraro S, Amodeo S, et al.: **Atacama Cosmology Telescope: combined kinematic and thermal Sunyaev-Zel'dovich measurements from BOSS CMASS and LOWZ halos.** *Phys Rev D.* 2021; **103**(6): 063513.  
[Publisher Full Text](#)
- Schellenberger G, Reiprich TH, Lovisari L, et al.: **XMM-Newton and Chandra cross-calibration using HIFLUGCS galaxy clusters. Systematic temperature differences and cosmological impact.** *Astron Astrophys.* 2015; **575**: A30.  
[Publisher Full Text](#)
- Schimek A, Decataldo D, Shen S, et al.: **High resolution modelling of [CII], [CI], [OIII], and CO line emission from the interstellar medium and circumgalactic medium of a star-forming galaxy at  $z \sim 6.5$ .** *Astron Astrophys.* 2024; **682**: A98.  
[Publisher Full Text](#)
- Schuecker P, Finoguenov A, Miniati F, et al.: **Probing turbulence in the Coma galaxy cluster.** *Astron Astrophys.* 2004; **426**(2): 387–397.  
[Publisher Full Text](#)
- Sehgal N, Aiola S, Akrami Y, et al.: **CMB-HD: an Ultra-Deep, high-resolution millimeter-wave survey over half the sky.** *Bulletin of the American Astronomical Society.* 2019; **51**(7): 6.  
[Publisher Full Text](#)
- Selina RJ, Murphy EJ, McKinnon M, et al.: **The next-generation Very Large Array: a technical overview.** *Ground-based and Airborne Telescopes VII.* 2018; **10700**: 1070010.  
[Publisher Full Text](#)
- Sereno M, Lovisari L, Cui W, et al.: **The thermalization of massive galaxy clusters.** *Mon Not R Astron Soc.* 2021; **507**(4): 5214–5223.  
[Publisher Full Text](#)
- Sereno M, Umetsu K, Ettori S, et al.: **CLUMP-3D: testing  $\Lambda$ CDM with galaxy cluster shapes.** *Astrophys J.* 2018; **860**(1): L4.  
[Publisher Full Text](#)
- Shi X, Komatsu E, Nagai D, et al.: **Analytical model for non-thermal pressure in galaxy clusters - III. Removing the hydrostatic mass bias.** *Mon Not R Astron Soc.* 2016; **455**(3): 2936–2944.  
[Publisher Full Text](#)
- Shull JM, Smith BD, Danforth CW: **The baryon census in a multiphase intergalactic medium: 30% of the baryons may still be missing.** *Astrophys J.* 2012; **759**(1): 23.  
[Publisher Full Text](#)
- Silich EM, Bellomi E, Sayers J, et al.: **ICM-SHOX. paper I: methodology overview and discovery of a gas–dark matter velocity decoupling in the MACS J0018.5+1626 merger.** *arXiv eprints.* 2023; arXiv: 2309.12533.  
[Publisher Full Text](#)
- Simionescu A, Allen SW, Mantz A, et al.: **Baryons at the edge of the X-ray-brightest galaxy cluster.** *Science.* 2011; **331**(6024): 1576.  
[Publisher Full Text](#)
- Simionescu A, Zuhone J, Zhuravleva I, et al.: **Constraining gas motions in the Intra-Cluster Medium.** *Space Sci Rev.* 2019; **215**(2): 24.  
[Publisher Full Text](#)
- Simons Observatory Collaboration: **The simons observatory: science goals and forecasts.** *J Cosmology Astropart Phys.* 2019; **2019**: 056.  
[Publisher Full Text](#)
- Singari B, Ghosh T, Khatri R: **Detection of WHIM in the Planck data using Stack First approach.** *J Cosmology Astropart Phys.* 2020; **2020**(8): 028.  
[Publisher Full Text](#)
- Smith KM, Ferraro S: **Detecting patchy reionization in the Cosmic Microwave Background.** *Phys Rev Lett.* 2017; **119**(2): 021301.  
[Publisher Full Text](#)
- Soergel B, Saro A, Giannantonio T, et al.: **Cosmology with the pairwise kinematic SZ effect: calibration and validation using hydrodynamical simulations.** *Mon Not R Astron Soc.* 2018; **478**(4): 5320–5335.  
[Publisher Full Text](#)
- Sommovigo L, Ferrara A, Pallottini A, et al.: **The ALMA REBELS survey: cosmic dust temperature evolution out to  $z \sim 7$ .** *Mon Not R Astron Soc.* 2022; **513**(3): 3122–3135.  
[Publisher Full Text](#)
- Spergel D, Gehrels N, Baltay C, et al.: **Wide-Field Infrared Survey Telescope-astrophysics focused telescope assets WFIRST-AFTA 2015 report.** *arXiv eprints.* 2015; arXiv: 1503.03757.  
[Publisher Full Text](#)
- Stanev R, Evrard AE, Böhringer H, et al.: **The X-ray luminosity-mass relation for local clusters of galaxies.** *Astrophys J.* 2006; **648**(2): 956–968.  
[Publisher Full Text](#)
- Sunyaev RA, Norman ML, Bryan GL: **On the detectability of turbulence and bulk flows in X-ray clusters.** *Astron Lett.* 2003; **29**: 783–790.  
[Publisher Full Text](#)
- Sunyaev RA, Zeldovich YB: **Small-scale fluctuations of relic radiation.** *Astrophys Space Sci.* 1970; **7**(1): 3–19.  
[Publisher Full Text](#)
- Sunyaev RA, Zeldovich YB: **The observations of relic radiation as a test of the nature of X-Ray radiation from the clusters of galaxies.** *Comments on Astrophysics and Space Physics.* 1972; **4**: 173.  
[Reference Source](#)
- Sunyaev RA, Zeldovich YB: **The velocity of clusters of galaxies relative to the microwave background - the possibility of its measurement.** *Mon Not R Astron Soc.* 1980; **190**(3): 413–420.  
[Publisher Full Text](#)
- Swetz DS, Ade PAR, Amiri M, et al.: **Overview of the Atacama Cosmology Telescope: receiver, instrumentation, and telescope systems.** *Astrophys J Suppl Ser.* 2011; **194**(2): 41.  
[Publisher Full Text](#)
- Tamura Y, Kawabe R, Fukasaku Y, et al.: **Wavefront sensor for millimeter/submillimeter-wave adaptive optics based on aperture-plane interferometry.** In: *Ground-based and Airborne Telescopes VIII.* 2020; **11445**: 114451N.  
[Publisher Full Text](#)
- Tanimura H, Aghanim N, Douspis M, et al.: **X-ray emission from cosmic web filaments in SRG/eROSITA data.** *Astron Astrophys.* 2022; **667**: A161.  
[Publisher Full Text](#)
- Tanimura H, Aghanim N, Kolodzig A, et al.: **First detection of stacked X-ray emission from cosmic web filaments.** *Astron Astrophys.* 2020; **643**: L2.  
[Publisher Full Text](#)

- Tanimura H, Hinshaw G, McCarthy IG, *et al.*: **A search for warm/hot gas filaments between Pairs of SDSS Luminous Red Galaxies.** *Mon Not R Astron Soc.* 2019; **483**(1): 223–234.  
[Publisher Full Text](#)
- Thorne B, Dunkley J, Alonso D, *et al.*: **The python sky model: software for simulating the Galactic microwave sky.** *Mon Not R Astron Soc.* 2017; **469**(3): 2821–2833.  
[Publisher Full Text](#)
- Towler I, Kay ST, Schaye J, *et al.*: **Inferring the dark matter splashback radius from cluster gas and observable profiles in the FLAMINGO simulations.** *Mon Not R Astron Soc.* 2024; **529**(3): 2017–2031.  
[Publisher Full Text](#)
- Tozzi P, Norman C: **The evolution of X-Ray clusters and the entropy of the Intracluster Medium.** *Astrophys J.* 2001; **546**(1): 63–84.  
[Publisher Full Text](#)
- Tozzi P, Santos JS, Jee MJ, *et al.*: **Chandra deep observation of xdcp j0044.0-2033, a massive galaxy cluster AT  $z > 1.5$ .** *Astrophys J.* 2015; **799**(1): 93.  
[Publisher Full Text](#)
- Umetsu K, Sereno M, Medezinski E, *et al.*: **Three-dimensional multi-probe analysis of the galaxy cluster A1689.** *Astrophys J.* 2015; **806**(2): 207.  
[Publisher Full Text](#)
- van Daalen MP, McCarthy IG, Schaye J: **Exploring the effects of galaxy formation on matter clustering through a library of simulation power spectra.** *Mon Not R Astron Soc.* 2020; **491**(2): 2424–2446.  
[Publisher Full Text](#)
- van Kampen E, Bakx T, De Breuck C, *et al.*: **Atacama Large Aperture Submillimeter Telescope (AtLAST) science: surveying the distant Universe.** *arXiv e-prints.* 2024; arXiv: 2403.02806.  
[Publisher Full Text](#)
- van Marrewijk J, Di Mascolo L, Gill AS, *et al.*: **XLSSC 122 caught in the act of growing up: Spatially resolved SZ observations of a  $z = 1.98$  galaxy cluster.** *arXiv e-prints.* 2023; arXiv: 2310.06120.  
[Publisher Full Text](#)
- van Marrewijk J, Morris TW, Mroczkowski T, *et al.*: **Maria: a novel simulator for forecasting (sub-)mm observations.** *arXiv e-prints.* arXiv: 2402.10731. 2024.  
[Publisher Full Text](#)
- van Weeren RJ, Andrade-Santos F, Dawson WA, *et al.*: **The case for electron re-acceleration at galaxy cluster shocks.** *Nat Astron.* 2017; **1**: 0005.  
[Publisher Full Text](#)
- van Weeren RJ, de Gasperin F, Akamatsu H, *et al.*: **Diffuse radio emission from galaxy clusters.** *Space Sci Rev.* 2019; **215**(1): 16.  
[Publisher Full Text](#)
- Vavagiakis EM, Gallardo PA, Calafut V, *et al.*: **The Atacama Cosmology Telescope: probing the baryon content of SDSS DR15 galaxies with the thermal and kinematic Sunyaev-Zel'dovich effects.** *Phys Rev D.* 2021; **104**(4): 043503.  
[Publisher Full Text](#)
- Vikhlinin A, Burenin RA, Ebeling H, *et al.*: **Chandra cluster cosmology project. II. Samples and X-ray data reduction.** *Astrophys J.* 2009; **692**(2): 1033–1059.  
[Publisher Full Text](#)
- Voit GM: **Tracing cosmic evolution with clusters of galaxies.** *Rev Mod Phys.* 2005; **77**(1): 207–258.  
[Publisher Full Text](#)
- Voit GM, Kay ST, Bryan GL: **The baseline intracluster entropy profile from gravitational structure formation.** *Mon Not R Astron Soc.* 2005; **364**(3): 909–916.  
[Publisher Full Text](#)
- Walker SA, Fabian AC, Sanders JS, *et al.*: **Galaxy cluster outskirts: a universal entropy profile for relaxed clusters?** *Mon Not R Astron Soc.* 2012; **427**(1): L45–L49.  
[Publisher Full Text](#)
- Wan JT, Mantz AB, Sayers J, *et al.*: **Measuring  $H_0$  using X-ray and SZ effect observations of dynamically relaxed galaxy clusters.** *Mon Not R Astron Soc.* 2021; **504**(1): 1062–1076.  
[Publisher Full Text](#)
- Whelan B, Veronica A, Pacaud F, *et al.*: **X-ray studies of the Abell 3158 galaxy cluster with eROSITA.** *Astron Astrophys.* 2022; **663**: A171.  
[Publisher Full Text](#)
- White SDM, Efstathiou G, Frenk CS: **The amplitude of mass fluctuations in the universe.** *Mon Not R Astron Soc.* 1993; **262**(4): 1023–1028.  
[Publisher Full Text](#)
- White E, Ghigo FD, Prestage RM, *et al.*: **Green Bank Telescope: overview and analysis of metrology systems and pointing performance.** *Astron Astrophys.* 2022; **659**: A113.  
[Publisher Full Text](#)
- Willis JP, Oguri M, Ramos-Ceja, ME, *et al.*: **Understanding X-ray and optical selection of galaxy clusters: a comparison of the XXL and CAMIRA cluster catalogues obtained in the common XXL-HSC SSP area.** *Mon Not R Astron Soc.* 2021; **503**(4): 5624–5637.  
[Publisher Full Text](#)
- Woody DP, Beasley AJ, Bolatto AD, *et al.*: **CARMA: a new heterogeneous millimeter-wave interferometer.** In: *Z-Spec: A Broadband Millimeter-Wave Grating Spectrometer: Design, Construction, and First Cryogenic Measurements.* 2004; **5498**: 30–41.  
[Publisher Full Text](#)
- Wootten A, Thompson AR: **The Atacama Large Millimeter/Submillimeter Array.** *IEEE Proceedings.* 2009; **97**(8): 1463–1471.  
[Publisher Full Text](#)
- Yang T, Cai YC, Cui W, *et al.*: **Understanding the relation between thermal Sunyaev-Zeldovich decrement and halo mass using the SIMBA and TNG simulations.** *Mon Not R Astron Soc.* 2022; **516**(3): 4084–4096.  
[Publisher Full Text](#)
- Yu L, Nelson K, Nagai D: **The influence of mergers on scatter and evolution in Sunyaev-Zel'dovich Effect scaling relations.** *Astrophys J.* 2015; **807**(1): 12.  
[Publisher Full Text](#)
- Zemcov M, Aguirre J, Bock J, *et al.*: **High spectral resolution measurement of the Sunyaev-Zel'dovich effect null with Z-Spec.** *Astrophys J.* 2012; **749**(2): 114.  
[Publisher Full Text](#)
- Zhang C, Zhuravleva I, Kravtsov A, *et al.*: **Evolution of splashback boundaries and gaseous outskirts: insights from mergers of self-similar galaxy clusters.** *Mon Not R Astron Soc.* 2021; **506**(1): 839–863.  
[Publisher Full Text](#)
- Zhuravleva I, Churazov E, Schekochihin AA, *et al.*: **Suppressed effective viscosity in the bulk intergalactic plasma.** *Nat Astron.* 2019; **3**: 832–837.  
[Publisher Full Text](#)
- Zwicky F: **Die rotverschiebung von extragalaktischen Nebeln.** *Helv Phys Acta.* 1933; **6**: 110–127.  
[Publisher Full Text](#)

# Open Peer Review

Current Peer Review Status: ?

---

## Version 1

Reviewer Report 27 September 2024

<https://doi.org/10.21956/openreseurope.18856.r43967>

© 2024 Désert F. This is an open access peer review report distributed under the terms of the [Creative Commons Attribution License](#), which permits unrestricted use, distribution, and reproduction in any medium, provided the original work is properly cited.



**François-Xavier Désert**

Institut de Planétologie et d'Astrophysique de Grenoble, Univ. Grenoble Alpes, CNRS, IPAG, Grenoble, France

The paper discusses the fantastic scientific capabilities of Atlast (50m, 2deg FOV) with the SZ toolbox. It describes in detail all aspects of the physics of clusters, where Atlast would give a huge gain. This is not like CMB cosmology, where the gain is measured with a few parameters. Here, the vast astrophysics of the large-scale structure of the Universe would see a giant leap in many ways thanks to Atlast.

The paper is well written and detailed enough to give us a good idea of the effort involved. Many citations are given in order to grasp all the ideas, which are numerous and very rich. This paper is also a step forward in designing the best survey strategy (wide or deep surveys). Nevertheless, I think that there are some unsubstantiated claims about this telescope that must at least be acknowledged: the ability to recover large scales thanks to the large field of view, and the ability to recover very small scales at high frequencies. For large scales, we would need some sky noise simulations to show that 1-2 degree scales can be recovered (but I admit this is beyond the scope of this paper). For small scales, this is a technical issue: how to build a telescope with sufficient surface accuracy on a 50m surface and with sufficient pointing accuracy (also beyond this paper).

The paper can be accepted if the following comments are addressed.

**Major comment:** Sensitivity problem: For point sources, a 50m telescope is fantastic, as we gain something like the square of the diameter. For extended sources, the sensitivity brightness does not depend on the size of the telescope, but if we look at a given angular size, the gain is like the diameter of the telescope. Atlast can compete with Alma for point sources although it loses by a factor of about 3 in collecting area. Atlast can outperform other telescopes because of its superior diameter, but the gain in surface brightness sensitivity goes only like the diameter (so not a huge factor). I would rather emphasise mapping speed and angular resolution as the definitive winning parameters.

You need a reference for the Atlast sensitivity calculator. Finally, I don't understand the last two columns of table 1. It seems that this is a telescope that is 10-100 times better for point sources

than existing telescopes. For example, an rms of 0.600 mJy in one second at 1mm is unheard of! If I convert page 17, the one hour sensitivity in  $\gamma$  per beam of  $2E-6$ , I get less than 1 mJy in one second, which is also a very optimistic sensitivity. To get  $\gamma$  to  $5E-7$  you need 16 hours per FOV, so 64000 hours for  $4000 \text{ deg}^2$ . At 9000 hours per year that is seven years without any overhead!

**Minor comments:** Fig. 2 describe ntSZ( $p=4$ )

Tab. 1 : Can you give the  $\gamma$  sensitivity per  $\sqrt{\text{hour}}$ , and the mapping speed (I see some indications in page 17 only). The caption is cryptic to me "*but consider the broad-band re-implementation of the AtLAST sensitivity calculator. The specific frequencies of the band edges correspond to the ones that minimizes the output noise RMS level in the corresponding band per given integration time.*"? What is survey noise?

There is a claim that large scales can be recovered, say up to the scales of the field-of-view of Atlast. Is that claim based on simulations of the sky noise? Does it depend on the frequencies (I would expect higher frequencies are more difficult to deal with)?

Fig. 3 : use of theta B10 and B2 is not the best illustration for SZ effect as the sensitivity will mostly be at 2-1mm. Also, for a radius in abscissae, shouldn't we use  $\theta/2$  ? Finally, SZ effect is independent of redshift, if the cluster is resolved (which it is with Atlast). There are clearly some inconsistencies in that figure.

Fig. 4 : kSZ  $\gamma$  parameter is a misnomer. It is not a tSZ distortion. We should rather use something like  $b=\beta \cdot \tau$  where  $b$  is the adimensional distortion parameter (like  $\Delta T/T$ ),  $\beta=v/c$  and  $\tau$  is the cluster line-of-sight opacity.

Fig. 8: what is shown in the left panel? What is the colour scale on the right panel?

Fig 10. What is the kSZ power spectrum? Isn't that a goal to measure it? To be fair, you address the issue qualitatively at the end of 3.3. Can you extend the figure to 20000 in  $l$  (claimed on page 10)?

rtSZ, by measuring the cluster temperature (without X-rays) will give a brand-new avenue in cluster physics. But it will provide results only for the hottest clusters (how many are there) which are the most massive ones.

**Is the background of the case's history and progression described in sufficient detail?**

Yes

**Is the work clearly and accurately presented and does it cite the current literature?**

Yes

**If applicable, is the statistical analysis and its interpretation appropriate?**

Yes

**Are all the source data underlying the results available to ensure full reproducibility?**

Yes

**Are the conclusions drawn adequately supported by the results?**

Partly

**Is the case presented with sufficient detail to be useful for teaching or other practitioners?**

Yes

***Competing Interests:*** No competing interests were disclosed.

***Reviewer Expertise:*** Clusters of galaxies, CMB, ISM

**I confirm that I have read this submission and believe that I have an appropriate level of expertise to confirm that it is of an acceptable scientific standard, however I have significant reservations, as outlined above.**

---